Dissertation
submitted to the
Combined Faculties for the Natural Sciences and for Mathematics
of the Ruperto-Carola University of Heidelberg, Germany
for the degree of
Doctor of Natural Sciences

presented by
Master of Science-Physics: Khamphee Karwan
born in: Bangkok, Thailand
Oral examination: 14.02.2006

Fluctuations in a Quintessence Universe

Referees: Prof. Dr. Christof Wetterich
Prof. Dr. Matthias Bartelmann

Fluktuationen in einem Quintessenz-Universum
Zusammenfassung

Wir diskutieren die Entwicklung und Effekte von Quintessenzfluktuationen in einem FRW und inflationärem Universum. Nachdem wir die Prinzipien der kosmologischen Störungstheorie eingeführt haben, geben wir Entwicklungsgleichungen für metrische, Materie- und Quintessenzfluktuationen an. Wir verwenden diese Gleichungen, um die Entwicklung von Quintessenzfluktuationen in einem FRW Universum zu studieren. Die Fluktuationen in einem Exponentialpotentialmodell mit nicht-kanonischem kinetischen Term können das CMB Leistungsspektrum bei niedrigen Multipolen sowohl erhöhen als auch erniedrigen, vorausgesetzt das Quintessenzfeld bleibt bis heute eingefroren. In unserer Analyse benötigen wir keinen Mechanismus zur Verstärkung der Feldfluktuationen. Um zu überprüfen, ob das Quintessenzfeld bis heute eingefroren sein kann, betrachten wir dessen Entwicklung während der Inflation. Während der Inflation wird der Erwartungswert des Quintessenzfeldes zu grösseren Werten hin verschoben. Dadurch ist der Erwartungswert zu Beginn der Strahlungsdominierten Phase gross genug, um die Quintessenz bis heute eingefroren zu lassen. Schliesslich studieren wir Einschränkungen an die Entwicklung der Dunklen Energie durch Beobachtungsdaten. Wir verwenden hierzu eine Parametrisierung, welche von Wetterich vorgeschlagen wurde.

Fluctuations in a Quintessence Universe
Abstract

In this thesis, we discuss the evolution and effects of quintessence fluctuations in a FRW and inflationary universe. After introducing the fundamental ideas of cosmological perturbation theory, we give the evolution equations for metric, matter and quintessence fluctuations. We use these equations to study the evolution and effects of quintessence fluctuations in a FRW universe. The fluctuations in an exponential quintessence model with non-canonical kinetic term can suppress or enhance the CMB power spectrum at low multipoles, if the quintessence field is frozen until the present epoch. In our analysis, we do not need any mechanism for amplifying the field fluctuations. To check whether the quintessence field can be frozen until the present epoch, we consider its evolution during inflation. During inflation, the mean value of the quintessence field is driven towards a large value by its quantum fluctuations. As a result, the value of the quintessence field at the beginning of radiation domination is large enough to keep the quintessence field frozen until the present epoch. Finally, we study observational constraints on the dark energy evolution using a parameterization proposed by Wetterich.

Contents

Chapter 1

Introduction

Before the 17th century, attempts to understand the universe were based on philosophical point of view. The scientific perceptions of the universe have started after Newton proposed the law of gravity. Because of the limits of observational informations, those perceptions were not quite right. At the beginning of the 20th century, Einstein used the theory of general relativity to construct the model of the universe. Since people believed that the universe is static, Einstein introduced the cosmological constant to balance the gravitational attractive force due to the matter in the universe. In 1929, Hubble measured distance-redshift relation of galaxies and found that the redshift of light emitted from galaxies increases with their distance so the universe is expanding. Thus, the cosmological constant was not necessary because the Einstein equations can give rise to the expanding universe. Many theories for the expanding universe were proposed but some of them have been falsified by current observations. Recently the instruments and techniques for observing the universe have been improved and the picture of our universe is more clear than 20 years ago. Cosmology now is in the stage of "Modern Cosmology". In this chapter, we will give a brief overview of cosmology.

Observations currently suggest that the expansion of the universe is accelerating at the present epoch [1]. Since the cosmological constant can give rise to the accelerating universe, it plays a crucial role in modern cosmology. However, the origin of the cosmological constant is mysterious because its magnitude is extremely small compared with the energy scale at the time when it should originate. This is the cosmological constant problem [2, 3]. Because of the cosmological constant problem, a mysterious form of energy, called dark energy, has been suggested [4]-[12] for explaining the accelerated expansion of the universe. The evolving scalar field, i.e., quintessence, is a possible candidate for dark energy. The cosmological model is called Lambda Cold Dark Matter Model (ΛCDM model) if the cosmological constant drives the accelerated expansion of the universe, and called Quintessence Cold Dark Matter Model (QCDM model) if quintessence drives the accelerated expansion. The

recent observational data cannot be used to distinguish the cosmological constant from the evolving dark energy [13]-[15]. Moreover, many high energy physics models of dark energy cannot be ruled out by the current observations. At the present epoch, dark energy constitutes about $60\% - 70\%$ of the total energy in the universe [16] while the remainder is mainly contributed by dark matter. Dark matter is also a mysterious object in the universe. It has been introduced for explaining the rotation of galaxies [17]. In the simplest case, we expect that the circular velocity v of matter, which orbits around the center of a galaxy, should follow Kepler's law $v \propto r^{-1/2}$, where r is the distance from the center of galaxy. The surprising result from measurements of galaxy rotation curve is that the velocity does not follow the $r^{-1/2}$ law, but stays constant. This implies that the mass of galaxies are larger than we can observe. This missing mass is non-luminous. Thus, it is called dark matter. There are many candidates for dark matter, for example, axions, axinos, massive neutrinos, etc, but the massive neutrinos candidate has been ruled out by observations [18].

In section 1.1, we consider the dynamics of the Friedmann-Robertson-Walker (FRW) universe. We give a brief overview of the standard cosmological model in section 1.2. We summarize some observational constraints on cosmological models in section 1.3.

1.1 FRW Universe

In the theory of general relativity, gravity is viewed as a manifestation of spacetime curvature. The action of gravity on matter is described by the Einstein equation [19]

$$G_{\mu\nu} = R_{\mu\nu} - \frac{1}{2} R g_{\mu\nu} = 8\pi G T_{\mu\nu}, \tag{1.1}$$

where $G_{\mu\nu}$ is the Einstein tensor, $g_{\mu\nu}$ is the metric tensor and G is Newton's constant. The Ricci scalar R and Ricci tensor $R_{\mu\nu}$ correspond to the curvature of spacetime, while the energy momentum tensor $T_{\mu\nu}$ describes the energy and momentum of the matter in the spacetime. According to the observations, the universe looks rather homogeneous and isotropic on large scales. One might think at first sight that the homogeneous universe should be isotropic, but it is not really true when we apply these notions to the spacetime of the universe. Because the universe evolves in time, the universe is homogeneous and isotropic in space, but not in time. A space manifold, such as $R \times S^2$, can be homogeneous but nowhere isotropic, while a cone is isotropic around its vertex but not necessarily homogeneous. If the universe is isotropic around one point and also homogeneous, it will be isotropic around every point. This means that there is no special point in the universe, i.e. the universe looks the same around every point. Hence, we assume both homogeneity

and isotropy. This is the cosmological principle. The homogeneity and isotropy of the space imply that the space must be maximally symmetric [19]. Using this fact, one can derive the metric tensor for the spacetime of the universe. The line element can be written as

$$ds^2 = -dt^2 + a^2(t)\left[\frac{dr^2}{1-\mathcal{K}r^2} + r^2(d\theta^2 + \sin^2\theta\, d\phi^2)\right], \tag{1.2}$$

where a is the scale factor, and r, θ and ϕ are the comoving coordinates. This is the **Friedmann-Robertson-Walker metric**. The parameter $\mathcal{K}$ denotes the curvature on spatial hypersurfaces. The cases $\mathcal{K} < 0, \mathcal{K} = 0$, and $\mathcal{K} > 0$ correspond to constant negative, no, and positive curvature on spatial hypersurfaces, respectively. Usually, these cases are called open for $\mathcal{K} < 0$, flat for $\mathcal{K} = 0$, and close for $\mathcal{K} > 0$. For the flat case, the metric is

$$ds^2 = -dt^2 + a^2\left(dr^2 + r^2 d\theta^2 + r^2\sin^2\theta\, d\phi^2\right) = -dt^2 + a^2\left(dx^2 + dy^2 + dz^2\right). \tag{1.3}$$

The spatial part is simply flat Euclidean space. We will see that the flat case is suggested by observations. The Ricci scalar and Ricci tensor can be computed using the metric given by eq. (1.2).

We next consider the possible forms of energy and matter in the universe. The energy and matter in the universe can be treated as a perfect fluid which is defined as a fluid that is isotropic in its rest frame [19, 20]. Since a perfect fluid is at rest in comoving coordinates, its 4 velocity is $u^\mu = (1, 0, 0, 0)$. Using the definition of the energy momentum tensor in eq. (2.7), we obtain

$$T_{\mu\nu} = \begin{pmatrix} \rho & 0 \\ 0 & g_{ij}p \end{pmatrix}, \tag{1.4}$$

here ρ is the energy density and p is the pressure of the fluid. In this equation we have neglected the anisotropic stress tensor because the background universe is isotropic. From the zero component of the conservation of energy equation, i.e., $\nabla_\mu T^\mu{}_0 = 0$, we obtain

$$\rho' = -3\mathcal{H}(1+w)\rho, \tag{1.5}$$

where a prime denotes the derivative with respect to conformal time, $w = p/\rho$ is the equation of state parameter and $\mathcal{H} = a'/a$. The conformal time η is defined as $ad\eta = dt$. We will use these notations throughout this thesis. In the case when w is constant, the above equation gives

$$\rho \propto a^{-3(1+w)}. \tag{1.6}$$

The simplest perfect fluids are matter and radiation. Matter is collisionless, nonrelativistic particles, whose $w = 0$. Radiation is the relativistic particles,e.g., photons,

neutrinos, etc, whose $w = 1/3$. The energy density of matter decays as $\rho \propto a^{-3}$, while the energy density of radiation decays as $\rho \propto a^{-4}$. Let us now consider the energy momentum tensor of the cosmological constant. Inserting the cosmological constant Λ into the right hand side of eq. (1.1) one gets

$$G_{\mu\nu} = 8\pi G T_{\mu\nu} - \Lambda g_{\mu\nu} = 8\pi G \left(T_{\mu\nu} - \frac{\Lambda}{8\pi G} g_{\mu\nu} \right) = 8\pi G \left(T_{\mu\nu} + T^{\Lambda}_{\mu\nu} \right). \tag{1.7}$$

One sees that the cosmological constant corresponds to the vacuum energy. Comparing the energy momentum tensor of the cosmological constant $T^{\Lambda}_{\mu\nu}$ with eq. (1.4) we get

$$\rho = -p = \frac{\Lambda}{8\pi G}. \tag{1.8}$$

This means that the cosmological constant has $w = -1$ and therefore its energy density is constant.

Having specified the metric of the spacetime and the forms of matter in the universe, the Einstein equation yields

$$\mathcal{H}^2 = \frac{1}{3\bar{M_p}^2} \rho a^2 - \mathcal{K}, \tag{1.9}$$

$$\mathcal{H}' = -\frac{1}{6\bar{M_p}^2} (\rho + 3p) a^2, \tag{1.10}$$

where $\bar{M_p} = (8\pi G)^{-1/2}$ is the reduced Planck mass. These are the Friedmann equations. These equations and the metric given in eq. (1.2) define the Friedmann-Robertson-Walker (FRW) universe.

Let us introduce some basic cosmological parameters. The expansion rate of the universe is characterized by the Hubble parameter $H = \frac{da/dt}{a}$, whose present value is parametrised as $H^0 = 100\, h\, \mathrm{km\, s^{-1}\, Mpc^{-1}}$. The age of the universe can be estimated using the Hubble parameter as $t = \int da/H$. The amount of matter in the universe is denoted by the density parameter

$$\Omega = \frac{\rho}{3\bar{M_p}^2 H^2} = \frac{\rho}{\rho_{\mathrm{total}}}, \tag{1.11}$$

where ρ_{total} is the total density. The Friedmann equation can be written in terms of the density parameter as

$$\Omega - 1 = \frac{\mathcal{K}}{H^2 a^2}. \tag{1.12}$$

According to observations, the universe is flat and therefore $\Omega = 1$. The parameters Ω, ρ, and p are the sum of all species in the universe. In the simplest case, we can assume that the universe is filled by radiation, matter, and the cosmological constant, so that the Friedmann equation can be written as

$$\mathcal{H}^2 = \left(\mathcal{H}^0\right)^2 \left(\Omega^0_R a^{-4} + \Omega^0_M a^{-3} + \Omega^0_\Lambda \right), \tag{1.13}$$

where the superscript 0 denotes the present value of the parameters and subscripts R, M, and Λ refer to radiation, matter, and cosmological constant, respectively. Here, we have set the present value of a equal to 1. Since the universe is expanding, a increases in time. This implies that the universe can go through different stages where different components in the Friedman equation will dominate. When the energy density in radiation dominates the other two species, the universe is said to be radiation dominated. During radiation domination, the Friedmann equation gives

$$a \propto \eta, \quad \mathcal{H} = \frac{1}{\eta}, \quad a \propto t^{1/2} \quad \text{and} \quad H = \frac{1}{2t}, \tag{1.14}$$

where the last two equations are computed using the relation $ad\eta = dt$. During matter domination, the energy density of the universe is dominated by matter and hence

$$a \propto \eta^2, \quad \mathcal{H} = \frac{2}{\eta}, \quad a \propto t^{2/3} \quad \text{and} \quad H = \frac{2}{3t}. \tag{1.15}$$

If the energy density of the universe is dominated by the vacuum energy, one can show that

$$a \propto -\eta^{-1}, \quad \mathcal{H} = \frac{1}{\eta}, \quad a \propto e^{Ht} \quad \text{and} \quad H = \text{constant}. \tag{1.16}$$

It is easy to check that d^2a/dt^2 is positive for the case of vacuum domination but negative for the cases of radiation and matter domination. Thus, the universe undergoes the period of accelerated expansion during vacuum domination. Since the expansion of the universe is accelerating, we will find a range of w which leads to the accelerated expansion of the universe. Using the Friedmann equations, one can show that

$$\frac{d^2a}{dt^2} = -\frac{1}{6\bar{M}_p{}^2}(1+3w)a\rho. \tag{1.17}$$

This equation shows that the universe will accelerate if $w < -1/3$.

1.2 Standard Cosmological Model

Since the universe is expanding, one expects that a must have been zero at some time in the past. At $a = 0$ the Friedmann and also the Einstein equations become singular. At the singularity, the universe is supposed to originate from the big bang. The big bang represents the creation of the universe from a singular state, not explosion of matter into a pre-existing spacetime. This model of the universe is the big bang model. However, at very high energy quantum corrections might change the Friedmann equation and perhaps there is no singularity and also no big bang.

After the bang, the universe was governed by Planck-scale Physics. Since the theory for the Planck-scale Physics has not yet been formulated, we do not know the

nature of the universe at the Planck epoch. The universe underwent the period of inflation after the Planck epoch [21, 22]. During the inflationary epoch, the universe was driven by one or more inflaton fields. The slowly rolling inflaton field leads to a rapid expansion of the universe. As a result, the particle horizon at the time of inflation became larger than the size of the observable universe. After inflation, the observable universe has been in causal contact. Because the observable universe was a patch of the universe that was in thermal equilibrium before inflation, the observed Cosmic Microwave Background has a black body spectrum and is nearly homogeneous and isotropic. Since a increases at least e^{50} times during inflation, eq. (1.12) gives $\Omega \approx 1$ after inflation. This leads to the flatness of the spacetime of the observable universe. Hence, we will consider only the case of flat universe in this thesis.

At the end of the inflationary epoch, the inflaton oscillated near the minimum of its potential and decayed into elementary particles. The created particles interacted with each other and came to a state of thermal equilibrium with some temperature T_R, which is called the re-heating temperature. This process is known as re-heating [23, 24]. At the initial stage of re-heating, bosons were explosively produced due to the parametric resonance. The created bosons were not in thermal equilibrium. This stage is called pre-heating. After pre-heating, bosons decayed into elementary particles. Those particles reached a state of thermal equilibrium at the last stage of re-heating. Since our universe contains mostly particles and no anti-particles, we need the processes of CP and baryon number violation for explaining these phenomena. Several mechanisms have been proposed. Nevertheless, we will not discuss here.

The universe cools down as it expands. When the temperature was in the range of the nuclear binding energy, the nuclei of light elements, such as Deuterium, Helium, Lithium and Beryllium, were formed. The process of nuclei formation in the early universe is known as Big Bang Nucleosynthesis (BBN) [25]. This process is quite well understood, because the nuclear reactions can be studied in the laboratory and the light elements abundances can be estimated from the observations. The measured abundances are in agreement with the predictions of BBN. Because the temperature was too high, the nuclei and electrons could not combine and hence the universe was in the ionized state. In this epoch, photons and charged particles were tightly coupled by Compton scattering so the mean free path of the photons was very short.

When the temperature dropped below 0.4 eV, the nuclei and electrons could combine, i.e. the atoms were formed. The universe becomes neutral so photons can travel freely. The photons decoupled from baryons after the time of last scattering at redshift z about 1100. Light emitted at last scattering was red-shifted to microwave frequencies when it traveled through space. This microwave radiation is known as

the Cosmic Microwave Background (CMB). Since the photons have traveled freely after last scattering, the CMB power spectrum contains the information about the density fluctuations around the time of last scattering. The photons and baryons were tightly coupled before the last scattering. Thus, they can be treated as a single fluid. The acoustic oscillations of the photon-baryon fluid around the time of last scattering lead to the acoustic peaks and troughs of the observed CMB power spectrum [26].

The absence of absorption by neutral Hydrogen in quasar spectra, the Gunn-Peterson effect, implies that the universe was in the ionized state by the redshift of the most distant known quasars, about 5. The universe was reionized by the ultraviolet photons [27]. The popular models of the photon sources are massive stars in the first generation of galaxies, or early generations of quasars. After reionization, the CMB photons can scatter from the liberated electrons. This leads to a damping of the observed anisotropies, i.e. damping of acoustic peaks and troughs. Since the number density of electrons after reionization is low, some fraction of the original anisotropy is preserved.

At the present epoch, the universe contains many stars, galaxies and other collapsed objects. Moreover, the observed CMB is not precisely isotropic. The small anisotropies in the observed CMB reflect the small inhomogeneities at the time of last scattering. Thus, one expects that the present structure in the universe originates from the growth of initially small inhomogeneities in the early universe. The source of the inhomogeneities might be the quantum fluctuations in the inflaton field [28] or the quantum fluctuations in the other light fields [29, 30]. As cosmological scales leave the Hubble radius, the quantum fluctuations are converted to classical Gaussian perturbations with an almost flat spectrum [31]. One can evolve these perturbations forward in time to the present epoch and then compute the observable quantities such as the CMB and matter power spectrum, using the theory of cosmological perturbation. Comparing the predicted quantity with the observed one, one can constrain the models of the very early universe such as inflationary models or constrain the models of the present universe such as dark energy models. Thus, the theory of cosmological perturbation plays an important role in modern cosmology. In the context of cosmological perturbation theory, the small inhomogeneities are treated as the fluctuations in the homogeneous universe. We will review the fundamental idea of cosmological perturbation theory in chapter 2.

1.3 Observations

The current cosmological models are mainly constrained by CMB, large scale structure and SNeIa observations. We briefly consider the cosmological constraints from these observations in this section.

The CMB Spectrum

In 1965, Penzias and Wilson discovered microwave background radiations which coincide well with the predictions of the big bang theory. The discovery of cosmic microwave background is one of the main pieces of evidence for the big bang. In 1991, the COBE satellite [32] detected the temperature anisotropies in the CMB. The CMB anisotropies are sensitive to the spectral index n_s and amplitude A of primordial energy density fluctuations, the baryon density Ω_B, the matter density Ω_M, the Hubble constant h, the dark energy density Ω_d, the equation of state parameter of dark energy w_d, the optical depth to the last scattering τ, etc. For example, we roughly consider the dependence of the position and height of the acoustic peaks on cosmological parameters. The position of the first peak is determined by the ratio of the comoving angular diameter distance to the last scattering epoch and the sound horizon at that epoch [33]. Therefore it depends on $\Omega_d + \Omega_M$, h, Ω_M, w_d and $\Omega_B h^2$. From the observed value of the first peak position, we have $\Omega_d + \Omega_M \approx 1$ [34], i.e. the universe has a flat geometry. This is in agreement with the prediction of the inflationary scenarios. The position of the first peak can put a constraint on $\Omega_M h^2$ but we have to know an upper limit on $\Omega_B h^2$. The ratio of the height of the second peak to the height of the first peak gives an information about the amount of baryon and spectral index. The constraints on the baryon abundance from this ratio are consistent with the constraints from nucleosynthesis.

The recent CMB datasets are provided by WMAP [18], CBI [35], ACBAR [36] and VSA [37]. The dataset from WMAP covers $2 \leq \ell \leq 700$ while the others cover the higher ℓ. Here, ℓ is the multipole moment of temperature fluctuations. We will see in the next chapter that the fluctuations in the photon energy density or equivalently the temperature fluctuations can be expanded in terms of Legendre polynomials $P_\ell(\theta)$. The best fit ΛCDM model for WMAP data [18] is shown in table 1.1.

	$\Omega_B h^2$	$\Omega_M h^2$	h	τ	n_s
best fit$\pm\sigma$	0.024 ± 0.001	0.14 ± 0.02	0.72 ± 0.05	$0.166^{+0.076}_{-0.071}$	0.99 ± 0.04

Table 1.1: The best fit ΛCDM model. The parameter σ refers to the confidence limit.

Large Scale Structure

The anisotropies in the CMB refer to the inhomogeneities at a redshift of 1100. The distribution of inhomogeneities at the present epoch can be measured by measuring the redshift of many observed galaxies. Using this information, one can construct the power spectrum of the galaxies distribution. The galaxy power spectrum reflects

the distribution of luminous matter, so that it is not a power spectrum of matter (luminous+dark matter) fluctuations. To obtain the power spectrum of matter fluctuations, we multiply the power spectrum of galaxies by the bias parameter [38]. The shape of the matter power spectrum depends mainly on the matter density and the evolution of the universe after radiation-matter equality. It might be affected by dark energy fluctuations, but only on very large scales. To constrain cosmological models in a linear perturbation theory, we use the data at scales where the inhomogeneities are linear, $k/h \leq 0.15\mathrm{Mpc}^{-1}$. The two major collaborations which measure the distribution of the galaxies are the 2-degree Field Galaxy Redshift Survey (2dFGRS) [39] and the Sloan Digital Sky Survey (SDSS) [40].

An alternative method for measuring the matter power spectrum is based on the gravitational lensing effect [41]. Light from distant sources is distorted by a mass distribution between the sources and the observer due to the gravitational lensing. The matter power spectrum can be obtained from the observed distortions of distant and faint galaxies. Since this method detects the dark matter distribution directly, it is not necessary to use the bias parameter. The matter power spectrum can also be obtained from the observations of a Lyman-α forest of the quasar spectrum [42].

Supernovae Ia

The CMB and matter power spectrum give the information about the universe at a particular redshift. Their shapes depend on the average evolution of the universe, so that they cannot be used to constrain the expansion history of the universe very well. One possible method for probing the expansion history of the universe is to measure the luminosity distance of objects at different redshifts. The definition of the luminosity distance is given in section 5.2. To compute the luminosity distance, one has to know the absolute luminosity of the observed objects. The supernovae of the type Ia (SNe Ia) can be used as standard candles for this purpose. This is because their absolute luminosity can be determined by light-curve fitting. Moreover, they have approximately the same absolute luminosity and they are very bright. Thus it is possible to observe them over cosmological distances. The recent supernova data is provided by High-Z Supernova Search Team [43]. The best fit dark energy model with $w = w_0 + w'z$ for SNeIa data only is $w_0 = -1.31 \pm^{0.22}_{0.28}$ and $w' = 1.48 \pm^{0.81}_{0.90}$. Here, the prior $\Omega_M = 0.27 \pm 0.04$ is used. This shows that the expansion of the universe is accelerating today.

1.4 About this Thesis

Dark energy or quintessence with $w \neq -1$ is a time-varying component. It has been argued that a time-varying component should not be perfectly homogeneous because

a smoothly distributed, time-varying component violates the equivalence principle. In this thesis, we study the behavior and effect of the quintessence fluctuations. We review the theory of cosmological perturbation in chapter 2. The evolution of quintessence fluctuations in a FRW universe and their effect on the CMB power spectrum are discussed in chapter 3. In chapter 4, we consider the evolution of quintessence in the inflationary universe and consider the effect of the quantum fluctuations on the classical evolution of the quintessence field. We use the recent observational datasets to constrain the dark energy evolution in chapter 5. Finally, we conclude in chapter 6.

Chapter 2

Cosmological Perturbation Theory

In this chapter, we review the fundamental ideas of cosmological perturbation theory. We concentrate on linear perturbation theory. The gauge transformation properties and the gauge invariant combinations of the metric and matter perturbations are considered in section 2.1. The energy-momentum conservation, Einstein, and Klein-Gordon equations are given in section 2.2. In section 2.3, we give the definitions of adiabatic and isocurvature perturbations, and consider the correlation between them. Finally, we give the evolution equations for the fluctuations in photons, massless neutrinos, cold dark matter, baryons and dark energy.

2.1 Gauge Invariant Perturbation Variables

2.1.1 Metric Decomposition

The metric tensor $g_{\mu\nu}$ can be expanded about the FRW background metric as

$$g_{\mu\nu} = g^{(0)}_{\mu\nu} + h_{\mu\nu}, \tag{2.1}$$

here the metric perturbation $h_{\mu\nu}$ is a function of space and time, while the background metric $g^{(0)}_{\mu\nu}$ depends only on time. The background metric is given by

$$g^{(0)}_{\mu\nu} = a^2(\eta) \begin{pmatrix} -1 & 0 \\ 0 & \gamma_{ij} \end{pmatrix}, \tag{2.2}$$

where η is the conformal time and $\gamma_{\mu\nu}$ is the metric on the 3-dimensional space. For the flat universe, $\gamma_{\mu\nu}$ is the Kronecker delta. Since $g_{\mu\nu}$ is a symmetric tensor, $h_{\mu\nu}$ has 10 degrees of freedom. We will split $h_{\mu\nu}$ into scalar, vector, and tensor parts according to their transformation properties on spatial hypersurfaces [44]. In linear perturbation theory, these parts are decoupled. Thus, they evolve independently. The metric perturbations can be written in a general form as [45]

$$h_{\mu\nu} = 2a^2(\eta) \begin{pmatrix} -A & -B_i \\ -B_i & H_{ij} \end{pmatrix}, \tag{2.3}$$

where A is a scalar, while B_i and H_{ij} are a vector and a symmetric tensor on the 3-dimensional space, respectively. In general, a vector can be decomposed into the curl-free and divergence-free parts as

$$B_i = B_{|i} + B_i^{(V)}, \tag{2.4}$$

where $X_{|i}$ denotes three-dimensional covariant derivative of X, B is a scalar function and $B_i^{(V)|i} = 0$. Because of the constraint $B_i^{(V)|i} = 0$, the divergence-free vector $B_i^{(V)}$ has 2 degrees of freedom. The vector $B_i^{(V)}$ gives no contribution to the scalar perturbation A, while B gives. Thus, $B_i^{(V)}$ corresponds to the vector perturbations and B corresponds to the scalar perturbations. The tensor H_{ij} can be decomposed as

$$H_{ij} = H_L\gamma_{ij} + \left(\nabla_i\nabla_j - \frac{1}{3}\nabla^2\gamma_{ij}\right)H_T + \frac{1}{2}\left(H_{i|j}^{(V)} + H_{j|i}^{(V)}\right) + H_{ij}^{(T)}, \tag{2.5}$$

here the scalar functions H_L, H_T correspond to the scalar perturbations, the divergence-free vector $H_i^{(V)}$ corresponds to the vector perturbations, and a symmetric transverse traceless tensor $H_{ij}^{(T)}$ corresponds to the tensor perturbations. The transverse $H_{ij}^{(T)|j} = 0$ and traceless $H_i^{(T)\,i} = 0$ conditions give 4 constraints on 6 components of the symmetric tensor. Hence, $H_{ij}^{(T)}$ has 2 degrees of freedom which correspond to the 2 polarization states of gravitational waves. We now have 4 scalar functions with 4 degrees of freedom, 2 divergence-free vectors with 4 degrees of freedom, and 1 symmetric transverse traceless tensor with 2 degrees of freedom. Hence, we have 10 degrees of freedom, the same number as the degrees of freedom of the perturbed metric.

In the case of linear perturbations, the gravitational waves do not couple to the matter fluctuations. The vector fluctuations decay in an expanding universe, so that they are not usually cosmologically important. Since the scalar fluctuations couple to matter inhomogeneities, they are the important modes of metric fluctuations.

According to eqs. (2.2) and (2.3), the general line element for a perturbed Robertson-Walker metric can be written as

$$ds^2 = a^2(\eta)\left[-(1+2A)d\eta^2 - 2B_i d\eta dx^i + (\gamma_{ij} + 2H_{ij})\,dx^i dx^j\right]. \tag{2.6}$$

2.1.2 Energy Momentum Tensor

The energy momentum tensor of a perfect fluid is given by

$$T_\nu^\mu = p\delta_\nu^\mu + (\rho + p)u^\mu u_\nu + \pi_\nu^\mu, \tag{2.7}$$

where ρ is the energy density, p is the isotropic pressure, u^μ is the covariant 4-velocity, and π_ν^μ is the anisotropic stress tensor. The linear perturbed velocity can

be written as [46]

$$u^\mu = \frac{1}{a}\left(1 - A, v^i\right), \tag{2.8}$$

$$u_\mu = g_{\mu\nu}u^\nu = a\left(-1 - A, v_i - B_i\right), \tag{2.9}$$

where $u^\mu u_\mu = -1$. To split the perturbations in the energy momentum tensor into the scalar, vector, and tensor modes, we decompose a fluid velocity v^i as

$$v^i = v^{|i} + v^{(V)i}, \tag{2.10}$$

and decompose the anisotropic stress tensor as

$$\Pi^j_i = \left(\nabla_i\nabla^j - \frac{1}{3}\nabla^2\gamma^j_i\right)\Pi + \frac{1}{2}\left(\Pi^{(V)|j}_i + \Pi^{(V)j}_{\quad|i}\right) + \Pi^{(T)j}_i, \tag{2.11}$$

where $\pi^j_i = \bar{p}\Pi^j_i$. The anisotropic stress tensor has only spatial components, π_{ij}, and has no unperturbed part due to the isotropy of the background universe. Hence, it follows from eq. (2.37) that it is gauge invariant. The isotropic pressure is defined as $p = \bar{p}(1 + \pi_L)$. Thus, the components of the energy momentum tensor are

$$T^0_0 = -\bar{\rho}(1 + \delta), \tag{2.12}$$

$$T^i_0 = -\bar{\rho}(1 + w)(v^{|i} + v^{(V)i}), \tag{2.13}$$

$$T^0_i = \bar{\rho}(1 + w)(v_{|i} - B_{|i} + v^{(V)}_i - B^{(V)}_i), \tag{2.14}$$

$$T^i_j = \bar{p}\left[(1 + \pi_L)\gamma^i_j + \Pi^i_j\right], \tag{2.15}$$

here $w = \bar{p}/\bar{\rho}$ is the equation of state parameter, $\bar{p}$ and $\bar{\rho}$ are the background value of pressure and energy density. The energy density contrast δ is defined as $\rho = \bar{\rho}(1+\delta)$. It follows from these equations that the quantity $(\bar{\rho} + \bar{p})\left(v^{|i} + v^{(V)i}\right)$ corresponds to the momentum of the fluid.

Let us now consider the energy momentum tensor of a scalar field. A minimally coupled scalar field is specified by the Lagrangian density

$$\mathcal{L} = -\frac{1}{2}\phi^{|\mu}\phi_{|\mu} - V(\phi). \tag{2.16}$$

The energy momentum tensor for a scalar field is defined as

$$T^\mu_\nu = \phi^{|\mu}\phi_{|\nu} + \delta^\mu_\nu\mathcal{L}. \tag{2.17}$$

We decompose a field ϕ into a homogeneous and a perturbed part as $\phi = \bar{\phi} + \delta\phi$. Using eq. (2.17), we obtain

$$T^0_{\ 0} = -\frac{1}{2}a^{-2}\bar{\phi}'^2 - V(\bar{\phi}) + a^{-2}\left(\bar{\phi}'^2\,\Phi - \delta\phi'\bar{\phi}'\right) - V_{,\bar{\phi}}(\bar{\phi})\delta\phi, \tag{2.18}$$

$$T^i_0 = a^{-2}\bar{\phi}'\delta\phi^{|i}, \tag{2.19}$$

$$T^i_j = a^{-2}\frac{1}{2}\bar{\phi}'^2 - V(\bar{\phi}) + a^{-2}\left(-\bar{\phi}'^2\Phi + \bar{\phi}'\delta\phi'\right) - V_{,\bar{\phi}}(\bar{\phi}), \tag{2.20}$$

where $V_{,\bar{\phi}} = \frac{dV}{d\phi}$. It is obvious that the scalar field fluctuations give no contribution to the vector and tensor perturbations. Comparing these equations with eqs. (2.12), (2.13), and (2.15), one can define the velocity, pressure and energy density fluctuations of the scalar field as

$$\begin{aligned} \delta\rho_\phi &= \bar{\rho}_\phi\delta_\phi = a^{-2}\left(-\bar{\phi}'^2\Phi + \delta\phi'\bar{\phi}'\right) + V_{,\bar{\phi}}(\bar{\phi})\delta\phi, && (2.21)\\ v^{|i} &= -(\bar{\phi}')^{-1}\delta\phi^{|i}, && (2.22)\\ \delta p &= \bar{p}_\phi\pi_L = a^{-2}\left(-\bar{\phi}'^2\Phi + \delta\phi'\bar{\phi}'\right) - V_{,\bar{\phi}}(\bar{\phi})\delta\phi, && (2.23) \end{aligned}$$

here we have defined the background energy density and pressure of a scalar field as

$$\begin{aligned} \bar{\rho}_\phi &= a^{-2}\frac{1}{2}\bar{\phi}'^2 + V(\bar{\phi}), && (2.24)\\ \bar{p}_\phi &= a^{-2}\frac{1}{2}\bar{\phi}'^2 - V(\bar{\phi}). && (2.25) \end{aligned}$$

We note that $v(k,\eta) = k(\bar{\phi}')^{-1}\delta\phi(k,\eta)$ after the Harmonic decomposition.

The notation $\bar{X}$ denotes the background value of the quantity X. We use this notation only in this subsection to split X into a homogeneous and a perturbed part. For notational convenience, a bar will be omitted after this subsection.

2.1.3 Harmonic Decomposition

The evolution equations for metric and matter perturbations are partial differential equations. It is not convenient to solve them in real space, so we expand the metric and matter perturbations in terms of Harmonic functions. In the context of the harmonic expansion, a vector is decomposed into the curl-free and divergence-free parts, and a tensor is decomposed into 4 parts according to eq. (2.5). In the flat space, the harmonic expansion of the scalar quantity f is the Fourier expansion

$$f(\mathbf{x},\eta) = \int d^3k\hat{f}(\mathbf{k},\eta)e^{i\mathbf{kx}} = \int d^3k\hat{f}(\mathbf{k},\eta)Q_{\mathbf{k}}(\mathbf{x}). \quad (2.26)$$

In the curve spacetime, the above expansion also exists, but the functions $Q_{\mathbf{k}}(\mathbf{x})$ are different. The functions $Q_{\mathbf{k}}(\mathbf{x})$ form the complete orthogonal set of eigenfunctions of the Laplacian, [45]

$$\nabla^2 Q^{(S)} = -k^2 Q^{(S)}, \quad (2.27)$$

here a superscript S denotes the scalar mode. A vector and a tensor quantities can be expanded using the basis $Q_j^{(V)}$ and $Q_{ji}^{(T)}$, which are the eigenfunctions of the Laplacian operator

$$\begin{aligned} \nabla^2 Q_j^{(V)} &= -k^2 Q_j^{(V)}, && (2.28)\\ \nabla^2 Q_{ji}^{(T)} &= -k^2 Q_{ji}^{(T)}, && (2.29) \end{aligned}$$

where $Q_j^{(V)}$ is a transverse vector and $Q_{ji}^{(T)}$ is a symmetric transverse traceless tensor. Using these basis, we can expand a vector quantity as

$$\mathcal{V}_i = \mathcal{V} Q_i^{(S)} + \mathcal{V}^{(V)} Q_i^{(V)}, \tag{2.30}$$

and expand a tensor quantity as

$$\mathcal{T}_{ij} = \mathcal{T}_L Q^{(S)} \gamma_{ij} + \mathcal{T}_T Q_{ij}^{(S)} + \mathcal{T}^{(V)} Q_{ij}^{(V)} + \mathcal{T}^{(T)} Q_{ij}^{(T)}, \tag{2.31}$$

where $\mathcal{V}$, $\mathcal{V}^{(V)}$, $\mathcal{T}_L$, $\mathcal{T}_T$, $\mathcal{T}^{(V)}$, and $\mathcal{T}^{(T)}$ are the functions of η and $\mathbf{k}$, and

$$Q_j^{(S)} \equiv -k^{-1} Q_{|j}^{(S)}, \tag{2.32}$$

$$Q_{ij}^{(S)} \equiv k^{-2} Q_{|ij}^{(S)} + \frac{1}{3} \gamma_{ij} Q^{(S)}, \tag{2.33}$$

$$Q_{ij}^{(V)} \equiv -\frac{1}{2k} \left(Q_{i|j}^{(V)} + Q_{j|i}^{(V)} \right). \tag{2.34}$$

After this subsection, we will write all perturbation variables in terms of the Harmonic coefficients.

2.1.4 Gauge Transformations

Because of the homogeneity of a FRW spacetime, one can find a coordinate system in which the metric is independent of coordinates. Nevertheless, it is not possible to find such a coordinate system for the perturbed spacetime. Thus, the definitions of metric and matter fluctuations depend on the choice of the coordinates, i.e. they are gauge dependent. To construct the gauge invariant quantities of them, we consider their behavior under coordinate (or gauge) transformations. Let us consider diffeomorphisms ϕ_1 and ϕ_2 which map a space-time manifold of a physical Universe $\mathcal{M}$ to a space-time manifold of a homogeneous and isotropic Universe $\mathcal{M}_0$. For a given coordinate system on $\mathcal{M}_0$, a choice of diffeomorphism corresponds to a choice of coordinates on $\mathcal{M}$. Let $\mathcal{Q}$ be a physical quantity on $\mathcal{M}$ and $\mathcal{Q}^{(0)}$ is the corresponding quantity on $\mathcal{M}_0$. Thus, in the coordinate systems given by the mapping ϕ_1 and ϕ_2, the perturbation $\delta_1\mathcal{Q}$ and $\delta_2\mathcal{Q}$ of $\mathcal{Q}$ at the point $p \in \mathcal{M}$ are defined by [47]

$$\begin{aligned} \delta_1\mathcal{Q}(p) &= \mathcal{Q}(p) - \mathcal{Q}^{(0)}(\phi_1 p), \\ \delta_2\mathcal{Q}(p) &= \mathcal{Q}(p) - \mathcal{Q}^{(0)}(\phi_2 p). \end{aligned} \tag{2.35}$$

Hence, the change in the perturbation of $\mathcal{Q}$ due to the coordinate transformations is

$$\delta_2\mathcal{Q} - \delta_1\mathcal{Q} = \mathcal{Q}^{(0)}(\phi_1 p) - \mathcal{Q}^{(0)}(\phi_2 p). \tag{2.36}$$

To study the effect of infinitesimal coordinate transformations, we use families of diffeomorphisms which arise from vector fields u^μ, where u^μ generates the coordinate transformation [19]. In this case, the right hand side of the above equation can be replaced by Lie derivative $\mathcal{L}_u\mathcal{Q}^{(0)}$, so that under an infinitesimal coordinate transformation the perturbation of $\mathcal{Q}$ transforms as [48]

$$\delta\mathcal{Q} \to \delta\mathcal{Q} + \mathcal{L}_u\mathcal{Q}^{(0)}. \tag{2.37}$$

We now consider the gauge transformation properties of $h_{\mu\nu}$. Setting $\mathcal{Q}^{(0)} = g^{(0)}_{\mu\nu}$ and $u^\mu = (T(\mathbf{x},\eta), L^i(\mathbf{x},\eta))$, the Lie derivative becomes

$$\mathcal{L}_u g^{(0)}_{\mu\nu} = 2a^2(\eta)\begin{pmatrix} -\frac{a'}{a}T - T' & L'_i - T_{|i} \\ L'_i - T_{|i} & \frac{a'}{a}T\gamma_{ij} + \frac{1}{2}\left(L_{i|j} + L_{j|i}\right)\end{pmatrix}, \tag{2.38}$$

where a prime denotes a derivative with respect to conformal time. Using eqs. (2.3), (2.4), (2.5), (2.37), (2.38) and expanding vector $L_i = LQ^{(S)}_i + L^{(V)}Q^{(V)}_i$, one can show that under gauge transformations our perturbation variables transform as

$$\begin{aligned}
A &\to A + \mathcal{H}T + T', && (2.39)\\
B &\to B - L' - kT, && (2.40)\\
B^{(V)} &\to B^{(V)} - L^{(V)\prime}, && (2.41)\\
H_L &\to H_L + \mathcal{H}T + \frac{k}{3}L, && (2.42)\\
H_T &\to H_T - kL, && (2.43)\\
H^{(V)} &\to H^{(V)} - kL^{(V)}, && (2.44)\\
H^{(T)} &\to H^{(T)}. && (2.45)
\end{aligned}$$

To simplify the following expressions, we define $\tilde{\psi} = H_L + \frac{1}{3}H_T$. One can also use eq. (2.37) to study the transformation properties of $\delta\rho$, v, π_L and $\delta\phi$. Under the gauge transformation these quantities transform as

$$\begin{aligned}
\delta\rho &\to \delta\rho + \rho' T, && (2.46)\\
v &\to v - L', && (2.47)\\
\pi_L &\to \pi_L + p' T, && (2.48)\\
\delta\phi &\to \delta\phi + \phi' T. && (2.49)
\end{aligned}$$

Here, we consider only scalar perturbations in the matter sector. Dividing eq. (2.46) by ρ, one obtains $\delta \to \delta - 3(1+w)T$,i.e. transformation property of density contrast.

The vector u^μ generates the coordinates transformation

$$\eta \to \eta + T, \quad x^i \to x^i + L^i. \tag{2.50}$$

The function T determines the choice of constant-η hypersurfaces, while L and $L_i^{(V)}$ select the spatial coordinates in these hypersurfaces. The choice of coordinates is arbitrary for a perturbed spacetime, so that the perturbation variables in eqs. (2.39)-(2.48) are gauge dependent. Since the coordinates of space-time carry no independent physical meaning, one needs the gauge invariant perturbation variables. We will construct them in the net subsection.

2.1.5 Gauge Invariant Variables

There are two possible approaches to eliminate the gauge freedom. The first is to choose a gauge, i.e. to pick conditions on the coordinates which completely eliminate the gauge freedom. The second is to work with a basis of gauge-invariant variables.

Let us consider the first approach. The convenient gauge choice is the Longitudinal (or Conformal) gauge. This gauge is defined by $B = H_T = 0$. It follows from eqs. (2.40) and (2.42) that B and H_T vanish when

$$L = H_T/k, \quad T = \frac{1}{k}(B - k^{-1}H_T') = -\sigma/k, \tag{2.51}$$

where $\sigma = H_T' k^{-1} - B$ is the shear of spacetime. Using these equations one obtains the following gauge-independent perturbation variables

$$\begin{aligned}
\Phi_l &= A - \mathcal{H}\sigma/k - \sigma'/k, && (2.52)\\
\Psi_l &= \tilde{\psi} - \mathcal{H}\sigma/k, && (2.53)\\
\Delta_l &= \delta + 3\mathcal{H}(1+w)\sigma/k, && (2.54)\\
V_l &= v - \frac{1}{k}H_T', && (2.55)\\
\Delta\phi_l &= \delta\phi - \frac{1}{k}\phi'\sigma. && (2.56)
\end{aligned}$$

The gauge freedom can also be eliminated using other gauge choices. We now consider the comoving gauge. This gauge is defined by choosing spatial coordinates such that the 3-velocity of the fluid vanishes, $v = 0$. Since the 4-velocity, u^μ is orthogonal to the constant-η hypersurfaces, one obtains $v - B = 0$. Thus, the conditions for fixing the gauge freedom are $v = 0$ and $B = 0$. Using these conditions, one obtains

$$\begin{aligned}
T &= -(v - B)/k, && (2.57)\\
L &= \int d\eta v + \hat{L}, && (2.58)
\end{aligned}$$

where $\hat{L}$ is a residual gauge freedom, corresponding to a constant shift of the spatial coordinates. However, the evolution equations for scalar perturbations do not depend on $\hat{L}$. The above equations can be used to eliminate the gauge freedom from

the perturbations variables. The results are

$$\Phi_{\rm m} = A - \frac{1}{ak}\left[(v-B)a\right]', \tag{2.59}$$
$$\Psi_{\rm m} = \tilde{\psi} - \mathcal{H}(v-B)/k, \tag{2.60}$$
$$H'_{T\rm m} = H'_T - kv, \tag{2.61}$$
$$\Delta_{\rm m} = \delta + 3\mathcal{H}(1+w)(v-B)/k, \tag{2.62}$$
$$\Delta\phi_{\rm m} = \delta\phi - \frac{1}{k}\phi'(v-B). \tag{2.63}$$

The curvature perturbation in the comoving gauge $\Psi_{\rm m}$ corresponds to $\mathcal{R}$ in the notation of Lyth [49, 38, 50]. On large scales, this quantity is conserved if non-adiabatic pressure perturbations vanish. The conservation of the curvature perturbation does not depend on the evolution of the background universe, so that one might use it to relate the inflaton fluctuations to the primordial density perturbation [51]. In the case of multi-fluid, the comoving gauge is defined by the vanishing of total momentum

$$(\rho+p)(v-B) = \sum_\alpha (\rho_\alpha + p_\alpha)(v_\alpha - B) = 0. \tag{2.64}$$

Here v_α, ρ_α and p_α are the velocity, the density and the pressure of the fluid species α, respectively. Orthogonality of the constant-η hypersurfaces to the total 4-velocity, u^μ, also requires that $B = 0$. Using the Einstein equations one can write $\Psi_{\rm m}$ in terms of Φ_l and Ψ_l as

$$\Psi_{\rm m} = \Psi_l + \frac{3}{2}\frac{\mathcal{H}\Phi_l - \Psi'_l}{\mathcal{H}(1+w)}. \tag{2.65}$$

Instead of the fluid velocity, one can use the density fluctuations of fluid to pick a gauge. The uniform density gauge is defined by $\delta\rho = 0$. In this case, eq. (2.46) becomes

$$T = \frac{\delta}{3\mathcal{H}(1+w)}. \tag{2.66}$$

Thus, the curvature perturbation in this gauge is [52]

$$\zeta = \Psi_{\delta\rho} = \tilde{\psi} + \frac{\delta}{3(1+w)}. \tag{2.67}$$

This quantity is equal to $\mathcal{R}$ on large scales. To pick a condition on L, one can set either B, H_T or v to be zero.

For comparison, we briefly consider the uniform curvature gauge and synchronous gauge. The uniform curvature gauge is defined by $H_T = \tilde{\psi} = 0$, i.e. the induced 3-metric is unperturbed. For this gauge, we have $T = -\frac{\tilde{\psi}}{\mathcal{H}}$ and $L = H_T/k$. The gauge freedom is completely eliminated using this gauge choice. This gauge is often used to compute the fluctuations in the inflaton. The synchronous gauge is defined

by $A = B = 0$. It is well known that there is a residual gauge freedom [46] $\hat{T} = X/a$, where $X(x^i)$ is an arbitrary function of the spatial coordinates, and hence it is not possible to define gauge-independent quantities in this gauge choice.

We now consider the second approach. Since there are two scalar gauge functions (TL), two of the metric perturbations can be eliminated. According to eqs. (2.39), (2.40), (2.42) and (2.43), the remaining metric perturbations can be written in the gauge invariant form as

$$\Phi = A - \mathcal{H}\sigma/k - \sigma'/k, \tag{2.68}$$
$$\Psi = \tilde{\psi} - \mathcal{H}\sigma/k. \tag{2.69}$$

These are called Bardeen potentials [53]. It can be seen that they are similar to the gauge-independent metric perturbations in conformal gauge. From the gauge-transformation properties of δ, v and π_L, which are given by eqs (2.46)-(2.48), one can construct gauge invariant variables of these quantities. The results are

$$\Delta = \delta + 3(1+w)\tilde{\psi}, \tag{2.70}$$
$$V = v - k^{-1}H_T', \tag{2.71}$$
$$\Gamma = \pi_L - \frac{c_a^2}{w}\delta, \tag{2.72}$$
$$\Delta\phi = \delta\phi - \frac{1}{k}\phi'\sigma, \tag{2.73}$$

here Γ is the entropy perturbation and c_a^2 is the adiabatic sound speed defined as

$$c_a^2 = \frac{p'}{\rho'} = 1 + \frac{2a^2 V_{,\phi}}{3\mathcal{H}\phi'}. \tag{2.74}$$

Finally, we give some relations between gauge-independent variables on the specific hypersurfaces and gauge invariant variables.

$$\Phi_l = \Phi, \tag{2.75}$$
$$\Phi_{\rm m} = \Phi - \mathcal{H}V/k - V'/k, \tag{2.76}$$
$$\Psi_l = \Psi, \tag{2.77}$$
$$\Psi_{\rm m} = \Psi - \mathcal{H}V/k, \tag{2.78}$$
$$\Psi_{\delta\rho} = \frac{\Delta}{3(1+w)}, \tag{2.79}$$
$$\Delta_l = \Delta - 3(1+w)\Psi, \tag{2.80}$$
$$\Delta_{\rm m} = \Delta_l + 3\mathcal{H}(1+w)V_l/k,$$
$$= \Delta - 3(1+w)\left(\Psi - \mathcal{H}V/k\right), \tag{2.81}$$
$$V_l = V, \tag{2.82}$$
$$\Delta\phi_l = \Delta\phi, \tag{2.83}$$
$$\Delta\phi_{\rm m} = \Delta\phi - \phi' V/k. \tag{2.84}$$

2.2 Evolution Equations for Scalar Perturbations

2.2.1 Conservation of the Energy Momentum Tensor

The conservation of energy-momentum yields evolution equation for the perturbation in the energy density [46]

$$\delta\rho' + 3\mathcal{H}(\delta\rho + \delta p) = -(\rho + p)\left[3H_L' + kv\right] , \tag{2.85}$$

and an evolution equation for the momentum

$$[(\rho + p)(v - B)]' - k\delta p + \frac{2}{3}kp\Pi = (\rho + p)\left[kA - 4\mathcal{H}(v - B)\right] , \tag{2.86}$$

where $\delta p = p\pi_L$. Using the definition of gauge invariant variables, one obtains the evolution equations

$$\Delta' = -3(c_a^2 - w)\mathcal{H}\Delta - kV(1 + w) - 3\mathcal{H}w\Gamma, \tag{2.87}$$

$$V' = \mathcal{H}(3c_a^2 - 1)V + k[\Phi - 3c_a^2\Psi] + \frac{c_a^2 k}{1 + w}\Delta + \frac{wk}{1 + w}\left[\Gamma - \frac{2}{3}\Pi\right]. \tag{2.88}$$

These equations can be written in a specific gauge using eqs. (2.76)-(2.82).

2.2.2 Einstein Equations

The first-order perturbed Einstein equations yield [67]

$$\begin{aligned} a^2\rho\Delta &= 2\bar{M_p}^2 k^2\Psi - 3a^2\rho(1 + w)\left(\mathcal{H}k^{-1}V - \Psi\right), \\ a^2(\rho + p)V &= 2\bar{M_p}^2 k\left(\mathcal{H}\Phi - \Psi'\right), \\ a^2 p\Pi &= -\bar{M_p}^2 k^2(\Psi + \Phi), \end{aligned} \tag{2.89}$$

where Δ, V and Π are the sum of the contributions of all species α, i.e.

$$\Delta = \sum_\alpha \frac{\rho_\alpha\Delta_\alpha}{\rho}, \quad V = \sum_\alpha \frac{(\rho_\alpha + p_\alpha)V_\alpha}{\rho + p} \quad \text{and} \quad \Pi = \sum_\alpha \frac{p_\alpha\Pi_\alpha}{p}. \tag{2.90}$$

Using eq. (1.9) we can write the perturbed Einstein equations as

$$3\mathcal{H}(\Psi' - \mathcal{H}\Phi) + k^2\Psi + \frac{9}{2}\mathcal{H}^2(1 + w)\Psi = \frac{3}{2}\mathcal{H}^2\Delta, \tag{2.91}$$

$$\Psi' - \mathcal{H}\Phi = -\frac{3}{2}\mathcal{H}^2 k^{-1}(1 + w)V, \tag{2.92}$$

$$\Psi + \Phi = -3\mathcal{H}^2 w\Pi. \tag{2.93}$$

We combine eqs. (2.92) and (2.88) to give

$$\begin{aligned}\Psi'' + 2\mathcal{H}\Psi' - \mathcal{H}\Phi' &= 3\mathcal{H}^2\Phi + 3\mathcal{H}^2(1+w)\Phi - \frac{9}{2}\mathcal{H}^2(1+w)c_a^2\Psi \\ &= -\frac{3}{2}\mathcal{H}^2\left(c_a^2\Delta + w\Gamma - \frac{3}{2}w\Pi\right). \end{aligned} \tag{2.94}$$

In the case of a simple perfect fluid, one can set $\Gamma = \Pi = 0$ and use eq. (2.91) to eliminate $c_a^2\Delta$ from the above equation. As a result, the evolution of metric perturbation does not depend on matter fluctuations.

One can derive the relation between the curvature perturbation on the comoving and uniform density hypersurfaces using eqs. (2.91) and (2.92) as

$$\mathcal{R} + \frac{k^2}{3\mathcal{H}^2(1+w)}\Psi = \Psi_{\delta\rho} = \zeta. \tag{2.95}$$

One sees that $\mathcal{R} = \zeta$ on superhorizon scales.

2.2.3 Klein-Gordon Equations

The evolution of the scalar field is described by the Klein-Gordon equations. The background field obeys the unperturbed Klein-Gordon equation

$$\phi'' + 2\mathcal{H}\phi' + a^2V_{,\phi} = 0, \tag{2.96}$$

while the field perturbations obey the perturbed Klein-Gordon equation [46]

$$\delta\phi'' + 2\mathcal{H}\delta\phi' + k^2\delta\phi + a^2V_{,\phi\phi}\delta\phi = \phi'(A' - 3\tilde{\psi}' + k^2\sigma) - 2a^2V_{,\phi}A, \tag{2.97}$$

where V is the potential of the scalar field, $V_{,\phi} = \frac{dV}{d\phi}$ and $V_{,\phi\phi} = \frac{d^2V}{d\phi^2}$. The gauge invariant version of the perturbed Klein-Gordon equation is

$$\Delta\phi'' + 2\mathcal{H}\Delta\phi' + k^2\Delta\phi + a^2V_{,\phi\phi}\Delta\phi = \phi'(\Phi' - 3\Psi') - 2a^2V_{,\phi}\Phi. \tag{2.98}$$

2.3 Entropy and Adiabatic Perturbations

2.3.1 Entropy Perturbations

In general, the entropy perturbation Γ can be split into two parts as [46]

$$\begin{aligned}\Gamma &= \left(\frac{\delta p}{p} - \frac{c_a^2}{w}\frac{\delta\rho}{\rho}\right), \\ &= \Gamma_{\rm rel} + \Gamma_{\rm int}, \end{aligned} \tag{2.99}$$

where $\Gamma_{\rm int}$ is the intrinsic and $\Gamma_{\rm rel}$ is the relative entropy perturbation.

In the case of a single fluid, the relative entropy perturbation vanishes, so that the intrinsic entropy perturbation is given by

$$p\Gamma_{\rm int} = \delta p - c_a^2 \delta\rho, \tag{2.100}$$

here p and ρ are the pressure and energy density of that fluid. If equation of state parameter w of the fluid is constant, we will get $c_a^2 = w$ and hence $\Gamma_{\rm int} = 0$. The quantity $p\Gamma_{\rm int}$ refers to the non-adiabatic pressure perturbation which may be written as

$$\delta p_{\rm non} = p\Gamma_{\rm int} = p' \left(\frac{\delta p}{p'} - \frac{\delta\rho}{\rho'} \right). \tag{2.101}$$

It is clear that this expression for $\delta p_{\rm non}$ is gauge invariant, and represents the displacement between hypersurfaces of uniform pressure and uniform density.

For the multi-fluid case, the intrinsic entropy perturbation of fluid species α is given by

$$p_\alpha \Gamma_{{\rm int}\alpha} = \delta p_\alpha - c_{a\,\alpha}^2 \delta\rho_\alpha, \tag{2.102}$$

and hence the total intrinsic entropy perturbation is

$$p\Gamma_{\rm int} = \sum_\alpha p_\alpha \Gamma_{{\rm int}\alpha}. \tag{2.103}$$

The total entropy perturbation is defined as

$$p\Gamma = \sum_\alpha (\delta p_\alpha - c_{\rm total}^2 \delta\rho_\alpha), \tag{2.104}$$

where $c_{\rm total}^2$ is the overall adiabatic sound speed, determined by [54]

$$c_{\rm total}^2 = \sum_\alpha \frac{c_{a\,\alpha}^2 \rho'_\alpha}{\rho'}. \tag{2.105}$$

Thus, the relative entropy perturbation can be written as

$$p\Gamma_{\rm rel} = p\Gamma - p\Gamma_{\rm int} = \sum_\alpha (c_{a\,\alpha}^2 - c_{\rm total}^2)\delta\rho_\alpha. \tag{2.106}$$

If there is no energy and momentum transfer between the fluid species, this equation can be expressed in terms of entropy perturbation between any fluid species α and β as [54, 46]

$$w\Gamma_{\rm rel} = \frac{1}{2} \sum_{\alpha>\beta} \Omega_\alpha \Omega_\beta (1+w_\alpha)(1+w_\beta)(c_\alpha^2 - c_\beta^2) S_{\alpha\beta}, \tag{2.107}$$

where $S_{\alpha\beta}$ is defined as

$$S_{\alpha\beta} = \frac{\delta_\alpha}{1+w_\alpha} - \frac{\delta_\beta}{1+w_\beta}. \tag{2.108}$$

The energy and momentum in each fluid are conserved when there is no energy and momentum transfer between the fluids. Thus, one can solve eqs. (2.87) and (2.88) for each fluid separately. The above equations are not necessary for solving eqs. (2.87) and (2.88), but we will use them to define the adiabatic perturbations. If the energy and momentum can transfer between the fluids, the energy and momentum in each fluid will not be conserved, but the total energy and momentum are conserved. Therefore, the quantities Δ, V, w and c_a^2 in eqs. (2.87) and (2.88) are the sum of the contributions of all species and Γ is the total entropy perturbation.

2.3.2 Adiabatic and Isocurvature Conditions

We now consider the conditions for the adiabatic and isocurvature perturbations. The fluctuations in the fluid species α will be adiabatic if the total entropy perturbations vanish. This means that

$$\Gamma_{\mathrm{int}\alpha} = 0 \quad \text{and} \quad S_{\alpha\beta} = 0. \tag{2.109}$$

For a simple perfect fluid with a constant w, the intrinsic entropy perturbations always vanish, so that the condition for the adiabatic perturbations is

$$S_{\alpha\beta} = 0. \tag{2.110}$$

In general, the intrinsic entropy perturbations of the scalar field do not vanish because w is not constant. Thus, the scalar field fluctuations are not adiabatic. However, a scalar field can undergo a period of nearly constant w, e.g. tracking quintessence. In this case, $\Gamma_{\mathrm{int}\alpha} \approx 0$, and hence the scalar field fluctuations are adiabatic when eq. (2.110) is satisfied. For the adiabatic perturbations, the curvature perturbation does not vanish and refers to the amplitude of adiabatic perturbation.

The isocurvature perturbations are defined by the vanishing of fluctuations in total energy density, or equivalently the vanishing of curvature perturbation on comoving hypersurfaces. Since curvature perturbations on comoving and uniform density hypersurfaces are equivalent on large scale, one can use one of them to define the isocurvature perturbations. Using eqs. (2.70) and (2.67), one can write the curvature perturbation on hypersurfaces of uniform energy density of species α as

$$\zeta_\alpha = \frac{\Delta_\alpha}{3(1+w_\alpha)}, \tag{2.111}$$

and write the curvature perturbation on slices of uniform total energy density as

$$\zeta = \frac{\sum_\alpha \Delta_\alpha \Omega_\alpha}{\sum_\alpha 3(1+w_\alpha)\Omega_\alpha}, \tag{2.112}$$

where Ω_α is the density parameter of the species α. Hence the isocurvature perturbations are defined by

$$\zeta = 0. \tag{2.113}$$

We use the definitions of the adiabatic and isocurvature perturbations to specify the initial value of the perturbations. In the case of fluid with constant w, the adiabatic initial condition is defined by $S_{\alpha\beta} = 0$ for all species α and β. Assuming that the universe contains photons, baryons, neutrinos, and cold dark matter, the adiabatic initial condition for these species is

$$\frac{\Delta_\gamma}{1+w_\gamma} = \frac{\Delta_\nu}{1+w_\nu} = \frac{\Delta_B}{1+w_B} = \frac{\Delta_C}{1+w_C}, \tag{2.114}$$

where subscripts γ, ν, B, and C denote photons, neutrinos, baryons, and cold dark matter, respectively. It is well known that initially adiabatic perturbations remain purely adiabatic until the onset of matter domination.

The isocurvature initial conditions are obtained by setting $\zeta = 0$. One can distinguish different isocurvature modes from one another by setting $S_{\sigma\beta} = 0$ except for an interesting species. For example, the neutrino isocurvature mode is defined by

$$\zeta = 0, \quad S_{\gamma B} = S_{\gamma C} = 0 \quad \text{and} \quad S_{\gamma\nu} \neq 0. \tag{2.115}$$

These conditions show that the entropy perturbation $S_{\gamma\nu}$ can be used to determine the amplitude of isocurvature perturbation. It can be seen that there are $\sigma - 1$ isocurvature modes if there are σ species.

2.3.3 Correlated Adiabatic and Isocurvature Perturbations

In the context of inflation, the primordial density perturbation is generated by quantum fluctuations in the inflaton. For the simplest models of inflation driven by a single scalar field, only adiabatic primordial perturbation can be generated. The amplitude of adiabatic perturbation is characterized by the comoving curvature perturbation. According to the high energy physics theory, there may exist more than one scalar fields that contribute to the dynamics of inflation. In this case, the isocurvature perturbation can be generated. As remarked in the previous subsection, the amplitude of the isocurvature perturbation is determined by the entropy perturbation. This isocurvature perturbation may have a correlation with an adiabatic perturbation [55, 56, 57]. We now consider the generation of such a correlation.

The transformation of the comoving curvature perturbation $\mathcal{R}$ and the entropy perturbation $\mathcal{S}$ from the time of the horizon exit during inflation to the beginning of radiation dominated era can be parameterized by [57]

$$\begin{pmatrix} \mathcal{R}_r \\ \mathcal{S}_r \end{pmatrix} = \begin{pmatrix} 1 & T_{RS} \\ 0 & T_{SS} \end{pmatrix} \begin{pmatrix} \mathcal{R}_\star \\ \mathcal{S}_\star \end{pmatrix}_{k=aH}, \tag{2.116}$$

where the subscripts r and $\star$ denote the beginning of radiation dominated era and time of horizon exit, respectively. The transfer functions $T_{RR} = 1$ and $T_{SR} = 0$,

because $\mathcal{R}$ is conserved for purely adiabatic perturbations and $\mathcal{R}$ cannot source $\mathcal{S}$. We are interested in the superhorizon modes, so that T_{RS} and T_{SS} are weakly scale-dependent. This means that the k dependence of $\mathcal{R}_r$ comes from the initial k dependence of $\mathcal{R}_\star$ and $\mathcal{S}_\star$, and the k dependence of $\mathcal{S}_r$ comes from the initial k dependence of $\mathcal{S}_\star$. Thus we write

$$\mathcal{R}_r = A_r k^{n_1} \hat{a_r} + A_s k^{n_3} \hat{a_s}, \tag{2.117}$$

$$\mathcal{S}_r = B k^{n_2} \hat{a_s}, \tag{2.118}$$

where $\hat{a_r}$ and $\hat{a_s}$ are independent Gaussian random variables with unit variance, $\langle \hat{a_r} \hat{a_s} \rangle = \delta_{rs}$. The above equations show that the adiabatic perturbation can have a correlation with the isocurvature perturbation if $A_s \neq 0$. The correlation between $\mathcal{R}$ and $\mathcal{S}$ may be parameterized by an angle θ as

$$\cos\theta = \frac{\langle \mathcal{R}_r \mathcal{S}_r \rangle}{\langle \mathcal{R}_r^2 \rangle^{1/2} \langle \mathcal{S}_r^2 \rangle^{1/2}} = \frac{\mathrm{sign}(B) A_s k^{n_3}}{\sqrt{A_r^2 k^{2n_1} + A_s^2 k^{2n_3}}}. \tag{2.119}$$

It can be seen that $\cos\theta$ is scale dependent and $-1 \leq \cos\theta \leq 1$. We consider the simple case when $n_1 = n_3 \neq n_2$, i.e. $\cos\theta$ is scale independent. In this case, $\cos\theta = \mathrm{sign}(B) A_s / A$, where $A = \sqrt{A_r^2 + A_s^2}$. Using the above equations, we can write the power spectra and the cross-correlation spectrum as

$$\Delta^2_{\mathcal{R}}(k) = (A_r^2 + A_s^2) k^{2n_1} = A^2 k^{n_{ad}-1}, \tag{2.120}$$

$$\Delta^2_{\mathcal{S}}(k) = B^2 k^{2n_2} = A^2 f_{iso}^2 k^{n_{iso}-1}, \tag{2.121}$$

$$\Delta_{RS}(k) = A_s B k^{n_2+n_3} = A^2 f_{iso} \cos\theta k^{(n_{ad}+n_{iso})/2-1}, \tag{2.122}$$

where $f_{iso} = B/A$ denotes the relative amplitude of $\mathcal{S}$ to $\mathcal{R}$. We have defined $2n_1 = n_{ad} - 1$ and $2n_2 = n_{iso} - 1$ to coincide with the standard notation for the scalar spectral index. The temperature anisotropies are given by these power spectra:

$$C_\ell^{ad} \propto A^2 \int \frac{dk}{k} \left(\frac{k}{k_0}\right)^{n_{ad}-1} \left[g_\ell^{ad}(k)\right]^2, \tag{2.123}$$

$$C_\ell^{iso} \propto A^2 f_{iso}^2 \int \frac{dk}{k} \left(\frac{k}{k_0}\right)^{n_{iso}-1} \left[g_\ell^{iso}(k)\right]^2, \tag{2.124}$$

$$C_\ell^{corr} \propto A^2 f_{iso} \cos\theta \int \frac{dk}{k} \left(\frac{k}{k_0}\right)^{(n_{ad}+n_{iso})/2-1} \left[g_\ell^{ad}(k) g_\ell^{iso}(k)\right], \tag{2.125}$$

and the total anisotropy is $C_\ell^{tot} = C_\ell^{ad} + C_\ell^{iso} + 2C_\ell^{corr}$. Here, $g_\ell(k)$ is the radiation transfer function. This transfer function can be expressed as [58]

$$g_\ell(k) = \int_0^{\eta_0} S^{(S)}(k,\eta) j_\ell[k(\eta_0 - \eta)] d\eta, \tag{2.126}$$

where j_ℓ is the spherical Bessel function, η_0 is the conformal time at the present epoch, and $S^{(S)}$ is the source function for the temperature anisotropy. The quantities n_{ad}, n_{iso}, and f_{iso} are defined at a specific wavenumber k_0. The source function is a function of metric and matter perturbations whose initial conditions may be adiabatic or isocurvature. The transfer functions Ag_ℓ^{ad} and $Af_{iso}g_\ell^{iso}$ correspond to the adiabatic and isocurvature initial conditions, respectively. If the initial conditions are a combination of isocurvature and adiabatic perturbations, we can write

$$S_i^{(S)}(\Psi_{ad}\pm f_{iso}\Psi_{iso}, \Delta_{ad}\pm f_{iso}\Delta_{iso}, V_{ad}\pm f_{iso}V_{iso}) = S_i^{(S)}(\Psi_{ad}, \Delta_{ad}, V_{ad})\pm f_{iso}S_i^{(S)}(\Psi_{iso}, \Delta_{iso}, V_{iso}), \tag{2.127}$$

where $S_i^{(S)}$ is the initial value of $S^{(S)}$. This equation is valid because we consider only the linear perturbation. Using this equation one obtains

$$C_\ell^{tot} \propto \int \frac{dk}{k}\left(\frac{k}{k_0}\right)^{(n_{ad}+n_{iso})/2-1} [g_\ell(k)]^2 = C_\ell^{ad} + C_\ell^{iso} + 2C_\ell^{corr}. \tag{2.128}$$

It is clear that $\cos\theta = \pm 1$ in this case. The correlation between adiabatic and isocurvature perturbations is called full correlation when $\cos\theta = 1$, and called (full) anti-correlation when $\cos\theta = -1$. To compute the CMB power spectrum for the partial correlation case, we compute C_ℓ^{ad} for the pure adiabatic case, C_ℓ^{iso} for the pure isocurvature case, and C_ℓ^{tot} for the full correlation case. After that, we compute C_ℓ^{corr} for the partial correlation case using $2C_\ell^{corr} = \cos\theta\left(C_\ell^{tot} - C_\ell^{ad} - C_\ell^{iso}\right)$. Finally, we use this value of C_ℓ^{corr} to compute C_ℓ^{tot} for partial correlation case. If $\cos\theta = 0$, the correlation between adiabatic and isocurvature perturbation vanishes and therefore $C_\ell^{tot} = C_\ell^{ad} + C_\ell^{iso}$.

2.4 Evolution Equations for Matter and Radiation

2.4.1 Photons and Massless Neutrinos

The perfect fluid descriptions of the photons and neutrinos are not quite correct, because the neutrinos are not very tightly coupled, and the photons can diffuse significantly inside the horizon. One therefore useds the phase-space distribution function $\mathcal{F}$ to describe their properties. In this subsection, we will derive the evolution equations for the perturbations of photons and massless neutrinos using a distribution function. We follow the derivation in [59] but used only the longitudinal gauge in the following derivation. The energy momentum tensor is defined in terms of a distribution function $\mathcal{F}$ as

$$T_{\mu\nu} = \int dP_1 dP_2 dP_3\,(-g)^{-1/2}\,\frac{P_\mu P_\nu}{P^0}\mathcal{F}(x^i, P_j, \eta), \tag{2.129}$$

where g denotes the determinant of $g_{\mu\nu}$. The 4-momentum P_μ is related to the proper energy and momentum by

$$P_i = a(1+\Psi_l)p_i = (1+\Psi_l)q_i, \quad P_0 = -a(1+\Phi_l)\sqrt{p_i^2+m^2} = -(1+\Phi_l)\epsilon, \tag{2.130}$$

where $q_i = ap_i$ and $\epsilon = \sqrt{q^2+a^2m^2}$. In the perturbed spacetime, the distribution function might be split into a zeroth-order component and a perturbation as

$$\mathcal{F}(x^i, P_i, \eta) = \mathcal{F}(x^i, q, n_i, \eta) = f_0(q)(1+f(x^i, q, n_i, \eta)), \tag{2.131}$$

where q is the magnitude of q_i and n_i is the unit vector in direction of q_i. The zeroth-order phase space distribution f_0 is given by

$$f_0(q) = \frac{g_s}{h_{\rm P}^3}\frac{1}{e^{\epsilon(q)/k_{\rm B}T_0}\pm 1}, \tag{2.132}$$

where $T_0 = aT$ is the temperature of the particles today, the factor g_s is the number of spin degrees of freedom, and $h_{\rm P}$ and $k_{\rm B}$ are the Planck and the Boltzmann constants. The plus sign in this equation corresponds the Fermi-Dirac distribution for fermions, while the minus sign corresponds the Bose-Einstein distribution for bosons.

From eq. (2.130), we can write $dP_1dP_2dP_3 = (1+3\Psi_l)q^2dqd\Omega$, where Ω is the solid angle associated with direction n_i. Since $\int d\Omega n_i n_j = 4\pi\delta_{ij}/3$, $\int d\Omega n_i = \int d\Omega n_i n_j n_k = 0$ and $(-g)^{-1/2} = a^{-4}(1-\Phi_l-3\Psi_l)$, we obtain

$$\begin{aligned}
T^0{}_0 &= -a^{-4}\int q^2dq\,d\Omega\,q\,f_0(q)\,(1+f)\,,\\
T^0{}_i &= a^{-4}\int q^2dq\,d\Omega\,q\,n_i\,f_0(q)\,f\,,\\
T^i{}_j &= a^{-4}\int q^2dqd\Omega\,q\,n_in_j\,f_0(q)\,(1+f).
\end{aligned} \tag{2.133}$$

Here, we set $m=0$ for photons and massless neutrinos. Comparing these equations with eqs. (2.12) - (2.15) and performing the Fourier transformation, one gets

$$\begin{aligned}
\rho &= 3p = a^{-4}\int d\Omega\int q^3dqf_0(q),\\
(\delta\rho)_l &= 3\,(\delta p)_l = a^{-4}\int d\Omega\int q^3dqf_0(q)\,f,\\
\rho(1+w)V_l &= ia^{-4}\int\Omega\hat{k}\cdot\hat{n}\int q^3dq\,f_0(q)\,f,\\
\frac{2}{3}p\Pi_l &= -a^{-4}\int d\Omega\left(\hat{k}\cdot\hat{n}^2-\frac{1}{3}\right)\int q^3dqf_0(q)f.
\end{aligned} \tag{2.134}$$

Here, we have used eqs. (2.32) and (2.33) to relate the Fourier components of the perturbation variables to the coefficients of the harmonic expansion. The q-dependence in the distribution function can be integrated out and the angular dependence of the perturbation variables can be expanded in a series of Legendre polynomials $P_\ell(\hat{k}\cdot\hat{n})$ as

$$F(\vec{k},\hat{n},\eta) = \frac{\int q^3 dq f_0(q) f}{\int q^3 dq f_0(q)} = \sum_{\ell=0}^{\infty}(-i)^\ell(2\ell+1)F_\ell(\vec{k},\eta)P_\ell(\hat{k}\cdot\hat{n}). \tag{2.135}$$

Thus one obtains

$$\begin{aligned}
\Delta_l &= \frac{1}{4\pi}\int d\Omega F(\vec{k},\hat{n},\eta) = F_0, \\
V_l &= \frac{3i}{16\pi}\int d\Omega(\hat{k}\cdot\hat{n})F(\vec{k},\hat{n},\eta) = \frac{3}{4}F_1, \qquad (2.136)\\
\Pi_l &= -\frac{9}{8\pi}\int d\Omega\left[(\hat{k}\cdot\hat{n})^2 - \frac{1}{3}\right]F(\vec{k},\hat{n},\eta) = 3F_2. \qquad (2.137)
\end{aligned}$$

The phase space distribution $\mathcal{F}$ evolves according to the Boltzmann equation. Since the perturbations of the photons and massless neutrinos can be calculated from the function F, we derive the evolution equations for the perturbations by writing the Boltzmann equation in terms of this function as

$$\frac{\partial F}{\partial\eta} + ik\mu F = -4(\Psi_l' + ik\mu\Phi_l) + \left.\frac{\partial F}{\partial\eta}\right|_C, \tag{2.138}$$

where $\mu \equiv \hat{k}\cdot\hat{n}$. The collision term $\left.\frac{\partial F}{\partial\eta}\right|_C$ vanishes for the neutrinos. For the photons, this term represents photons scattering off electrons. For simplicity, we neglect the photon polarization and write this term as

$$\left.\frac{\partial F}{\partial\eta}\right|_C = \dot{\tau}\left[-F + F_0 + 4\hat{n}\cdot\vec{v}_B - \frac{1}{2}F_2P_2\right], \tag{2.139}$$

where $P_2(\mu) = \frac{1}{2}(3\mu^2-1)$ is the Legendre polynomial of degree 2 and $\vec{v}_B$ is the baryon velocity. The differential optical depth for Thomson scattering is denoted as $\dot{\tau} = an_e x_e \sigma_T$, where $a(\eta)$ is the scale factor, n_e is the electron density, x_e is the ionization fraction and σ_T is the Thomson cross section. The total optical depth at time η is obtained by integrating $\dot{\tau}$, $\tau(\eta) = \int_\eta^{\eta_0}\dot{\tau}(\eta)d\eta$.

Expanding F in a Legendre series and using the relation $\hat{n}\cdot\vec{v}_B = -iv_BP_1(\hat{k}\cdot\hat{n})$ and eqs. (2.76)-(2.82), the Boltzmann equation can be written in terms of the gauge

invariant variables as

$$\begin{aligned}
\Delta'_\gamma &= -\frac{4}{3}kV_\gamma, \\
V'_\gamma &= k\left(\frac{1}{4}\Delta_\gamma - \frac{1}{6}\Pi_\gamma + \Phi - \Psi\right) + \dot{\tau}(V_B - V_\gamma), \\
F'_{\gamma\,2} &= \frac{1}{3}\Pi'_\gamma = \frac{8}{15}kV_\gamma - \frac{3}{5}kF_{\gamma\,3} - \frac{3}{10}\dot{\tau}\Pi_\gamma, \\
F'_{\gamma\,\ell} &= \frac{k}{2\ell+1}\left[\ell F_{\gamma\,(\ell-1)} - (\ell+1)F_{\gamma\,(\ell+1)}\right] - \dot{\tau}F_{\gamma\,\ell}\,, \quad \ell \geq 3,
\end{aligned} \tag{2.140}$$

here the subscript γ denotes the photons. In the early epoch, the universe was filled with the ionized matter, so that the photons are tightly coupled to the ionized baryons. Hence, $\dot{\tau}$ is large and $F_{\gamma\,\ell}$ is suppressed for $\ell \geq 2$. Moreover, we will see in the next subsection that the photon velocity is equal to the baryon velocity in this case.

The evolution equations for the neutrinos fluctuations are easily obtained by setting $\dot{\tau} = 0$. The results are

$$\begin{aligned}
\Delta'_\nu &= -\frac{4}{3}kV_\nu, \\
V'_\nu &= k\left(\frac{1}{4}\Delta_\nu - \frac{1}{6}\Pi_\nu + \Phi - \Psi\right), \\
\Pi'_\nu &= \frac{8}{5}kV_\nu - \frac{9}{5}kF_{\nu\,3}, \\
F'_{\nu\,\ell} &= \frac{k}{2\ell+1}\left[\ell F_{\nu\,(\ell-1)} - (\ell+1)F_{\nu\,(\ell+1)}\right], \quad \ell \geq 3.
\end{aligned} \tag{2.141}$$

We note that the multipole expansion of the neutrino distribution function can be truncated beyond the quadrupole at early time [59, 48]. Since $w = c_a^2 = 1/3$ and $\Gamma = 0$ for the neutrinos, the first 2 lines of the above equations are equivalent to eqs. (2.87) and (2.88).

The Boltzmann equation for the temperature fluctuations can be derived using the above analysis. According to eq. (2.132), one may write [59, 60]

$$\mathcal{F} = f_0\left(\frac{q}{1+\Delta_T}\right), \tag{2.142}$$

where $\Delta_T = \delta T/T$ is the photon brightness temperature perturbations. Expanding this equation around q, we get

$$\mathcal{F} = f_0(q) - q\frac{df_0}{dq}\Delta_T. \tag{2.143}$$

Integrating this equation over the photon energies, we can write

$$\Delta_T = \frac{1}{4}\frac{4\pi}{\rho}\int dq q^3 f_0\ f = \frac{1}{4}F. \tag{2.144}$$

From this equation, we get $4\Delta_{T\,0} = \Delta_\gamma$, $3\Delta_{T\,1} = V_\gamma$, $12\Delta_{T\,2} = \Pi_\gamma$, and $\Delta_{T\,\ell} = F_{\gamma\,\ell}/4$. Substituting these relations into eq. (2.140), one obtains the evolution equations for the temperature fluctuations.

2.4.2 Cold Dark Matter and Baryons

CDM can be treated as a pressure-less perfect fluid so the evolution equations for its perturbations can be obtained from eqs. (2.87) and (2.88). Setting w, c_a^2, Π and Γ equal to zero, these equations give

$$\begin{aligned} \Delta_C' &= -kV_C, \\ V_C' &= -\mathcal{H}V_C + k\Phi. \end{aligned} \tag{2.145}$$

The baryons behave like a non-relativistic fluid, so that $c_a^2 = w \ll 1$, $\Gamma \approx 0$ and $\Pi = 0$. If they do not interact with the radiation, their evolution is governed by the energy-momentum conservation equations. Although c_a^2 of the baryon is small, the acoustic term $c_a^2 k\Delta$ in eq. (2.88) cannot be neglected for sufficiently large k. In the early epoch, the baryons and photons are coupled due to the Thomson scattering. Thus there is the momentum transfer between them. The second line of eq. (2.140) shows that the momentum transfer into the photons is equal to $4\rho_\gamma\dot{\tau}(V_B - V_\gamma)/3$. Since the total momentum is conserved, the baryon receives momentum $4\rho_\gamma\dot{\tau}(V_\gamma - V_B)/3$. This means that we have to add $4\rho_\gamma\dot{\tau}(V_\gamma - V_B)/(3\rho_B)$ on the right hand side of eq. (2.88). Thus, the evolution equations for the baryon perturbations are given by

$$\begin{aligned} \Delta_B' &= -kV_B, \\ V_B' &= -\mathcal{H}V_B + c_B^2 k\Delta_B + k\left(\Phi - 3c_B^2\Psi\right) + \frac{4\rho_\gamma}{3\rho_B}\dot{\tau}(V_\gamma - V_B), \end{aligned} \tag{2.146}$$

where c_B^2 is the baryon sound speed.

Let us now consider the evolution of the photons and baryons fluctuations when they are tightly coupled. Using eqs. (2.140) and (2.146), one will get $V_\gamma' - V_B' \propto -\dot{\tau}\left(1 + 4\rho_\gamma/(3\rho_B)\right)(V_\gamma - V_B)$ if $\dot{\tau}$ is large. This implies that $V_\gamma - V_B$ decreases exponentially and hence $V_\gamma \approx V_B$. Therefore, the evolution equations for the photons and baryons fluctuations become

$$\begin{aligned} \Delta_\gamma' &= -\frac{4}{3}kV_\gamma, \\ V_\gamma' &= \frac{k}{4}\Delta_\gamma + k\Phi - k\Psi, \\ \Delta_B' &= -kV_\gamma. \end{aligned} \tag{2.147}$$

2.4.3 Dark Energy

There are two possible approaches for calculating the fluctuations in dark energy. One possibility is to use the perturbed Klein-Gordon equation. The other possibility is to use the energy-momentum conservation equations. One can verify that these approaches are equivalent. However, it is convenient to use the conservation equations for the general dark energy models. For general dark energy, its adiabatic sound speed c_{aQ}^2 is not equal to its equation of state parameter w_Q, so its intrinsic entropy perturbations do not vanish. If dark energy is uncoupled from other species, the entropy perturbation in the conservation equations will be equal to the intrinsic entropy perturbation. Hence, the evolution of the fluctuations in dark energy depends on w_Q, c_{aQ}^2, $\Gamma_{\rm int}$ and Π. Usually, Π is set to zero. On small scales, the dark energy can collapse faster than dark matter during dark energy domination if $\Gamma_{\rm int} = 0$ [61]. To prevent the clustering of dark energy, the suitable form of $\Gamma_{\rm int}$ has been proposed. For the general scalar field,i.e., k-essence, the intrinsic entropy perturbation can be written as [62]

$$w_Q \Gamma_{\rm int} = (c_s^2 - c_{aQ}^2)\left(\Delta_Q - 3(1+w_Q)\Psi + 3\mathcal{H}(1+w_Q)V_Q/k\right), \tag{2.148}$$

where $c_s^2 = \partial p/\partial\rho$ is the effective sound speed which equals to 1 for the canonical scalar field, i.e. quintessence. Using eq. (2.100), this equation can be obtained from a specific form of the scalar field potential. Using eqs. (2.87), (2.88) and (2.148) and setting $c_s^2 = 1$, one obtains the evolution equations for the quintessence fluctuations

$$\begin{aligned} \Delta_Q' &= 3\mathcal{H}(w_Q - 1)\Delta_Q - 9\mathcal{H}(1+w_Q)(c_{aQ}^2 - 1)\Psi \\ &+ 9\mathcal{H}^2(c_{aQ}^2 - 1)U_Q/k - kU_Q, \qquad (2.149) \\ U_Q' &= \mathcal{H}(3w_Q - 3c_{aQ}^2 + 2)U_Q + k\Delta_Q + k(1+w_Q)(\Phi - 3\Psi), \qquad (2.150) \end{aligned}$$

here $U_Q = (1+w_Q)V_Q$. The relations between the gauge invariant field fluctuations ΔQ and the gauge invariant velocity V_Q, energy density fluctuations Δ_Q are given by

$$\begin{aligned} \Delta_Q &= (1+w_Q)\left[3\Psi - \Phi + \frac{\Delta Q'}{Q'}\right] + \Delta Q \frac{dV(Q)}{dQ}\rho_Q^{-1}, \\ V_Q &= k\Delta Q/Q'. \end{aligned} \tag{2.151}$$

Chapter 3

Fluctuations in Quintessence

In this chapter, we will discuss the evolution of the quintessence fluctuations in the flat FRW universe. We parameterize the quintessence evolution with the equation of state parameter w_Q and the adiabatic sound speed c^2_{aQ}. We will not consider k-essence here, so that the effective sound speed is equal to 1. The evolution of quintessence fluctuations on superhorizon scales is considered in section 3.2. Quintessence is treated as a uncoupled fluid. The results in this section are used to study the fluctuations in tracking quintessence whose background evolution is reviewed in section 3.1. On subhorizon scales, it is easier to solve the perturbed Klein-Gordon equation than the energy-momentum conservation equations, so that in section 3.3 we use the Klein-Gordon equation to compute the evolution of the quintessence fluctuations on subhorizon scales. The uncoupled quintessence is an un-thermalized component in the universe, so that the non-adiabatic or isocurvature perturbations should exist in this component. It is well known that the isocurvature modes of tracking quintessence decrease rapidly when it is in the tracking regime [63, 64]. However, it is possible that the quintessence field enters the tracking regime at late time and the isocurvature perturbations can leave the imprint on the CMB spectrum. The effects of quintessence fluctuations on the CMB spectrum are discussed in section 3.4.

3.1 Evolution of Tracking Quintessence

The evolution of tracking quintessence has been studied by many authors [65, 66]. We review some basic ideas in this section. Tracking quintessence is quintessence whose evolution converges to a common track for a very wide range of initial conditions. This behavior of tracking quintessence avoids the coincidence problem. The potential V of tracking quintessence satisfies the condition [65]

$$\gamma = \frac{V_{,QQ}V}{(V_{,Q})^2} \sim \text{constant}. \tag{3.1}$$

The evolution of tracking quintessence in the very early era (after inflation) depends on its initial conditions. We assume for simplicity that the quintessence field Q is released from rest. If the initial value of its energy density is much larger than the tracker solution value, w_Q will initially increase and reach $+1$. When w_Q is close to 1, its kinetic energy dominates its potential energy so $c_{aQ}^2 = w_Q = 1$. During this stage, it follows from the Klein-Gordon equation that $Q = Q_f - A/a$, where Q_f and A are constant. This implies that Q is approximately constant when A/a is small. As a increases, $V(Q)$ reaches the constant value while the kinetic energy decreases. Consequently, w_Q decreases from $+1$ towards -1, and therefore Q becomes nearly frozen. This means that $V_{,Q} \approx$ constant and hence the Klein-Gordon equation gives

$$Q' = -\frac{2a^2 V_{,Q}}{3(w_B+3)\mathcal{H}} \propto a^{\frac{3}{2}\left(w_B+\frac{5}{3}\right)}. \tag{3.2}$$

Substituting this equation into eq. (2.74) one gets

$$c_{aQ}^2 = -2 - w_B, \tag{3.3}$$

where w_B is the equation of state parameter of the dominant component in the universe. One can see that w_Q and c_{aQ}^2 are constant during this stage but are not equal. Moreover, eq. (3.2) shows that the kinetic energy increases as $a^{-2}Q'^2/2 \propto a^{3(w_Q+1)}$ while $V(Q)$ is nearly frozen. Hence, w_Q will increase from -1 towards the tracking value.

The quintessence field will be frozen initially if the initial value of ρ_Q is much less than the tracker value. The value of w_Q increases and reaches the tracker value as the quintessence field evolves. The time, when the tracking behaviour starts, depends on the initial value of ρ_Q. If the initial value of ρ_Q decreases, the quintessence field will enter the tracking regime at lower redshift. The evolution of w_Q and c_{aQ}^2 of the tracking quintessence is shown in figure 3.1. It can be seen from this figure that there are 4 regimes of evolution. The first is the kinetic regime ($w_Q = c_{aQ}^2 = 1$). The second is the transition regime ($w_Q = -1, c_{aQ}^2 = 1$). The third is the potential regime ($w_Q = -1, c_{aQ}^2 = -2 - w_B$). The fourth is the tracking regime ($w_Q \approx c_{aQ}^2 \approx$ constant). This implies that the evolution of quintessence can be described by w_Q and c_{aQ}^2. To describe the evolution of quintessence and its fluctuations by both parameters, one should write $V_{,Q}$ and $V_{,QQ}$ in terms of them. Using the relations $2V(Q) = (1 - w_Q)\rho_Q$ and $dV/d\eta = V_{,Q}Q'$, one gets

$$\frac{dV}{dQ} = V_{,Q} = \frac{3}{2}(c_{aQ}^2 - 1)\mathcal{H}Q'a^{-2}, \tag{3.4}$$

$$\frac{d^2V}{dQ^2} = V_{,QQ} = \frac{3}{2}\mathcal{H}c_{aQ}^{2\prime}a^{-2} + \frac{9}{4}\mathcal{H}^2(1 - c_{aQ}^2)(w_B + c_{aQ}^2 + 2a^{-2}). \tag{3.5}$$

We note that only the case $c_{aQ}^{2\prime} \approx 0$ is considered in this thesis.

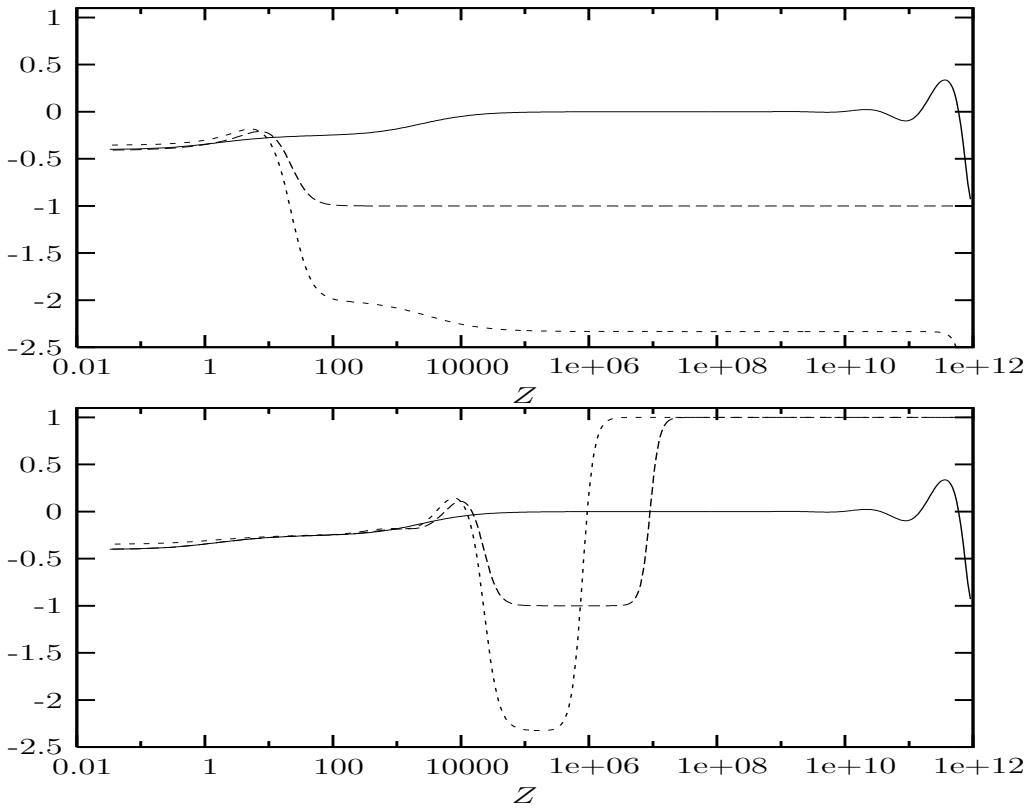

Figure 3.1: Evolution of w_Q and c_{aQ}^2 as a function of redshift z. The upper panel shows the case of small initial value of ρ_Q, while the lower panel shows the case of large initial value of ρ_Q. In both panels, the long dashed curve represents the evolution of w_Q, the dashed curve represents the evolution of c_{aQ}^2, and the solid curve represents the evolution of w_Q for the tracking solution. We use an inverse power-law potential $V(Q) \propto Q^{-6}$ in this plot.

3.2 Superhorizon Scales Fluctuations

We first consider the density fluctuations during the radiation dominated era. It can be seem from eq. (1.14) that $\mathcal{H} = k/x$, where $x = k\eta$. Using eq. (2.89) one can show that the gauge invariant potential Ψ evolves on superhorizon scales as

$$\Psi = \frac{1}{4}\left[\Omega_\gamma \Delta_\gamma + \Omega_\nu \Delta_\nu + 4(V_\gamma \Omega_\gamma + V_\nu \Omega_\nu)/x\right]. \tag{3.6}$$

Here, we have assumed that the density parameter of CDM, baryon, and quintessence are small. In the early epoch, the photons and baryons are tightly coupled, so that the photon fluctuations obey

$$\frac{d\Delta_\gamma}{d\ln x} = -\frac{4}{3}x^2 \tilde{V}_\gamma, \qquad \frac{d\tilde{V}_\gamma}{d\ln x} = \frac{1}{4}\Delta_\gamma - \tilde{V}_\gamma + \Omega_\nu \Pi_\nu + 2\Phi. \tag{3.7}$$

For the neutrinos, we truncate the neutrino moments beyond $\ell \geq 2$, therefore the evolution equations for the neutrino fluctuations become

$$\frac{d\Delta_\nu}{d\ln x} = -\frac{4}{3}x^2\tilde{V}_\nu, \qquad \frac{d\tilde{V}_\nu}{d\ln x} = \frac{1}{4}\Delta_\nu - \tilde{V}_\nu + \Omega_\nu\Pi_\nu + 2\Phi - \frac{1}{6}x^2\tilde{\Pi}_\nu,$$
$$\frac{d\tilde{\Pi}_\nu}{d\ln x} = \frac{8}{5}\tilde{V}_\nu + 2\tilde{\Pi}_\nu. \tag{3.8}$$

In the above equations we have defined $\tilde{V} = V/x$ and $\tilde{\Pi} = \Pi/x^2$. On superhorizon scales, the dominant solutions for the adiabatic perturbations are

$$\Delta_\gamma = \Delta_\nu, \qquad V_\gamma = V_\nu = -\frac{5}{4}Px\Delta_\gamma, \tag{3.9}$$
$$\Pi_\nu = -x^2P\Delta_\gamma, \qquad \Psi = \frac{1}{4}(1-5P)\Delta_\gamma = -\Phi - \Omega_\nu\Pi_\nu/x^2, \tag{3.10}$$

where $P = 1/(4\Omega_\nu + 15)$ and $\Delta_\gamma, \Delta_\nu, \Psi, \Phi$ are approximately constant. During the radiation dominated era, eqs. (2.149) and (2.150) become

$$\frac{d\Delta_Q}{dx} = \frac{3}{x}(w_Q - 1)\Delta_Q - \frac{9}{x}(1+w_Q)(c_{aQ}^2 - 1)\Psi$$
$$+\frac{9}{x^2}(c_{aQ}^2 - 1)U_Q - U_Q, \tag{3.11}$$
$$\frac{dU_Q}{dx} = \frac{1}{x}(3w_Q - 3c_{aQ}^2 + 2)U_Q + \Delta_Q + (1+w_Q)(\Phi - 3\Psi), \tag{3.12}$$

where $U_Q = (1+w_Q)V_Q$. Assuming that w_Q and c_{aQ}^2 are nearly constant compared with the expansion time, the above equations have the solution

$$\Delta_Q = \Delta_{aR}, \qquad U_Q = (1+w_Q)V_Q = (1+w_Q)V_{aR}x, \tag{3.13}$$

where Δ_{aR}, V_{aR} are constant and

$$\frac{3w_Q(c_{aQ}^2 - 1) - (w_Q - 1)(3w_Q - 2)}{3(1+w_Q)(c_{aQ}^2 - 1)}\Delta_{aR} = \frac{1}{4}\left[(5P-1)(3w_Q - 3c_{aQ}^2) + 2\right]\Delta_\gamma, \tag{3.14}$$
$$\frac{3w_Q(c_{aQ}^2 - 1) - (w_Q - 1)(3w_Q - 2)}{3(c_{aQ}^2 - 1)}V_{aR} = \frac{1}{4}\left[\frac{(5P-3)(w_Q-1)}{3(c_{aQ}^2-1)} - 5P + 1\right]\Delta_\gamma.$$

This solution shows that $\Delta_{aR}/(1+w_Q) = 3\Delta_\gamma/4$ when $w_Q \approx c_{aQ}^2$. Moreover, one can use eq. (2.100) or (2.148) to show that the intrinsic entropy perturbation vanishes in this case. Thus, this solution corresponds to the adiabatic perturbations. Nevertheless, in the potential regime, we have $w_Q \neq c_{aQ}^2$ so the above equation does not satisfy the adiabatic condition. However, we use this solution to define the

adiabatic initial conditions. The other solution of eqs. (3.11) and (3.12) can be obtained by combining eq. (3.13) with

$$\Delta_Q = \Delta_{nR} x^s, \quad U_Q = (1+w_Q) V_{nR} x^{s+1}, \tag{3.15}$$

and substituting them into eqs. (3.11) and (3.12). The result is

$$s = \frac{1}{2}\left[6w_Q - 3c_{aQ}^2 - 2 \pm \sqrt{9c_{aQ}^4 + 12c_{aQ}^2 - 20}\right], \tag{3.16}$$

$$\frac{\Delta_{nR}}{(1+w_Q)V_{nR}} = s - 3w_Q + 3c_{aQ}^2 - 1. \tag{3.17}$$

It is easy to see that eq. (3.15) is the solution of eqs. (3.11) and (3.12) when $\Psi \simeq \Phi \simeq \Delta_\Gamma \simeq \Delta_\nu \simeq V_\gamma \simeq V_\nu \simeq 0$. This implies that this solution corresponds to the isocurvature mode [62, 68], because the curvature perturbation $\zeta \sim \mathcal{O}(\Delta_Q \Omega_Q)$ is very small. This mode is constant in the potential regime and decreases in the tracking regime. This mode can increase if $w_Q > c_{aQ}^2/2 + 1/3$. The solutions (3.14) and (3.17) are valid for any quintessence models whose w_Q is approximately constant. In this case, the isocurvature mode will decrease if $-1 < w_Q < c_{aQ}^2/2 + 1/3$. Since Δ_{nR} and V_{nR} do not depend on Ψ, their magnitude might be large compared with Ψ, and therefore they might give a significant contribution to the CMB spectrum. We will discuss the effects of quintessence fluctuations on the CMB spectrum in section 3.4. In section 3.4, we compute the CMB spectrum by assuming that the isocurvature fluctuations in quintessence are fully correlated with the adiabatic fluctuations in the other matter components. Thus, we can write the initial conditions for the quintessence fluctuations as

$$\Delta_Q^i = \Delta_{aR}^i + \Delta_{nR}^i x^s \quad \text{and} \quad U_Q^i = (1+w_Q)\left[V_{aR}^i x + V_{nR}^i x^{s+1}\right], \tag{3.18}$$

where a superscript i denotes the initial value in the radiation dominated epoch. One can compute Δ_{aR}^i and V_{aR}^i using eq. (3.14) and compute the ratio Δ_{nR}^i/Ψ^i using the inflation scenario. The coefficient V_{nR}^i can be computed using eq. (3.17). It is possible to apply the above analysis to the case where the isocurvature fluctuations in the other components, e.g., CDM etc, exist. Because the Ψ and Φ terms are canceled by the adiabatic solution, eqs. (3.17) and (3.16) are still valid in this case.

Next, we consider the quintessence fluctuations in the matter dominated epoch. In this epoch, $\mathcal{H} = 2k/x$ and

$$\Psi = \frac{\Delta_M}{3} + 2\tilde{V}_M, \tag{3.19}$$

where the subscript M refers to matter, e.g. cold dark matter. Since matter has $w = c_a^2 = \Gamma = 0$, the energy-momentum conservation equations become

$$\frac{d\Delta_M}{d\ln x} = -x^2 \tilde{V}_M, \tag{3.20}$$

$$\frac{d\tilde{V}_M}{d\ln x} = -3\tilde{V}_M - \Psi, \tag{3.21}$$

here we have neglected the anisotropic stress of neutrino and set $\Psi = -\Phi$. The dominant solution of the above equations is

$$\Delta_M \approx \text{constant}, \quad V_M = -\frac{x}{15}\Delta_M, \quad \Psi = \frac{\Delta_M}{5}. \tag{3.22}$$

The evolution of quintessence fluctuations during the matter dominated era can be described by

$$\begin{aligned} \frac{d\Delta_Q}{dx} &= \frac{6}{x}(w_Q - 1)\Delta_Q - \frac{18}{x}(1 + w_Q)(c_{aQ}^2 - 1)\Psi \\ &\quad + \frac{36}{x^2}(c_{aQ}^2 - 1)U_Q - U_Q, \end{aligned} \tag{3.23}$$

$$\frac{dU_Q}{dx} = \frac{2}{x}(3w_Q - 3c_{aQ}^2 + 2)U_Q + \Delta_Q + (1 + w_Q)(\Phi - 3\Psi). \tag{3.24}$$

Using the similar approach to the one that we apply to the case of the radiation dominated era, the solutions of these equations are

$$\Delta_Q = \Delta_{aM} + \Delta_{nM} x^q, \tag{3.25}$$

$$U_Q = (1 + w_Q)V_Q = (1 + w_Q)\left[V_{aM} x + V_{nM} x^{q+1}\right], \tag{3.26}$$

where $\Delta_{aM}, \Delta_{nM}, V_{aM}, V_{nM}$ are constant and satisfy the relations

$$\begin{aligned} \frac{6w_Q(c_{aQ}^2 - 1) - 3(2w_Q - 1)(w_Q - 1)}{3(c_{aQ}^2 - 1)(1 + w_Q)}\Delta_{aM} &= \frac{1}{5}(6c_{aQ}^2 - 6w_Q + 5)\Delta_M, \\ \frac{6w_Q(c_{aQ}^2 - 1) - 3(2w_Q - 1)(w_Q - 1)}{3(c_{aQ}^2 - 1)}V_{aM} &= \left[\frac{1}{5} - \frac{4(w_Q - 1)}{15(c_{aQ}^2 - 1)}\right]\Delta_M, \end{aligned} \tag{3.27}$$

and

$$\frac{\Delta_{nM}}{(1 + w_Q)V_{nM}} = q + 6c_{aQ}^2 - 6w_Q - 3. \tag{3.28}$$

One can compute q using the formula

$$q = \frac{1}{2}\left(12w_Q - 6c_{aQ}^2 - 3 \pm 3\sqrt{4c_{aQ}^4 + 4c_{aQ}^2 - 7}\right). \tag{3.29}$$

It can be seem that eq. (3.27) satisfies the adiabatic condition when $w_Q \approx c_{aQ}^2$. Hence, the first terms on the right hand side of eqs. (3.25) and (3.26) correspond to the adiabatic modes. On superhorizon scales, the adiabatic fluctuations in quintessence are constant both in the radiation dominated and matter dominated epoch. In the matter dominated era, the isocurvature mode will increase if $12w_Q > 6c_{aQ}^2 + 3$ and will be constant if $q = 0$. This means that the isocurvature mode is constant during potential regime but decreases during the tracking regime.

We now consider the evolution of the quintessence fluctuations during the quintessence dominated era. The gauge invariant potential Ψ can be computed using the formula

$$\Psi \simeq \frac{\Delta_Q}{3(1+w_Q)} + \mathcal{H}V_Q/k. \tag{3.30}$$

Substituting the above equation into eqs. (2.149) and (2.150), one gets

$$\Delta_Q' = 3\mathcal{H}(w_Q - c_{aQ}^2)\Delta_Q = \frac{w_Q'}{1+w_Q}\Delta_Q, \tag{3.31}$$

$$V_Q' = -2\mathcal{H}V_Q - \frac{k}{3}\frac{\Delta_Q}{1+w_Q}. \tag{3.32}$$

The solution of eq. (3.31) has a simple form

$$\frac{\Delta_Q}{\Delta_{Q0}} = \frac{1+w_Q}{1+w_{Q0}}, \tag{3.33}$$

where Δ_{Q0} and w_{Q0} are evaluated at an arbitrarily chosen time during the quintessence dominated era. The evolution of V_Q is given by

$$V_Q = -\frac{k\Delta_Q}{3(1+w_Q)}a^{-2}\int a^2 d\eta. \tag{3.34}$$

It can be seen that eqs. (3.33) and (3.34) are valid though w_Q is not constant. Inserting eq. (3.30) into eq. (2.148), we will find that the intrinsic entropy fluctuations of quintessence vanish. Thus, we will check whether eq. (3.33) corresponds to the adiabatic perturbation. For simplicity, we consider the case where w_Q is constant. When w_Q is constant, eqs. (3.30) and (3.34) give

$$V_Q \simeq -x\frac{\Delta_Q}{3(1+w_Q)}\frac{3w_Q+1}{3w_Q+5}, \tag{3.35}$$

$$\Psi \simeq \frac{\Delta_Q}{3w_Q+5}. \tag{3.36}$$

The fluctuations in matter obey eq. (2.145). The possible solution of this equation is

$$\Delta_M = C, \quad V_M = V_Q, \tag{3.37}$$

where C is a constant parameter whose value depends on the value of Δ_M in the matter dominated epoch. The parameter C might be equal to $4\Delta_Q/(3w_Q+3)$, and hence the fluctuations in matter and quintessence might be adiabatic.

3.3 Subhorizon Scales Fluctuations

In this section, we assume that the universe is filled with a perfect fluid and a scalar field quintessence, so that $\Pi = 0$ and $\Psi = -\Phi$. Using this assumption and $w = c_a^2 = 1/3$ for the radiation dominated era, one find from eqs. (2.94) and (2.91) that

$$\Psi'' + 4\mathcal{H}\Psi' + \frac{k^2}{3}\Psi = 0, \tag{3.38}$$

here we have set $\Gamma = 0$ for the adiabatic perturbations. The solution of this equation is

$$\begin{aligned}
\Psi &= y^{-3/2}\left(c_1 J_{3/2}(y/\sqrt{3}) + c_2 N_{3/2}(y/\sqrt{3})\right), \\
&= y^{-3} c_1 \left(\frac{y}{\sqrt{3}}\cos\frac{y}{\sqrt{3}} - \sin\frac{y}{\sqrt{3}}\right) \\
&\quad + y^{-3} c_2 \left(\frac{y}{\sqrt{3}}\sin\frac{y}{\sqrt{3}} + \cos\frac{y}{\sqrt{3}}\right),
\end{aligned} \tag{3.39}$$

where $J_{3/2}(y), N_{3/2}(y)$ are the Bessel functions, $y = a/a_c$, a_c is the scale factor at the horizon crossing ($\mathcal{H}(a_c) = k$), and c_1, c_2 are constant. This equation shows that Ψ is approximately constant outside the horizon ($y < 1$), and decreases as $\Psi \propto y^{-2}$ inside the horizon ($y > 1$). we use eqs. (3.39), (3.4), (3.5), (2.98) and variable $u = y^{1/2}\Delta Q$ to derive the evolution equation for the quintessence fluctuations during the radiation dominated era. The result is

$$\begin{aligned}
&\frac{d^2u}{dy^2} + \frac{1}{y}\frac{du}{dy} + \left(1 - \frac{\mu^2}{y^2}\right) u \\
&= Q_{yc} y^{-\frac{3w_Q}{2}} \left[\frac{3}{y}(c_{aQ}^2 + 3)\Psi + \frac{4c_1}{3y^2}\sin\frac{y}{\sqrt{3}} - \frac{4c_2}{3y^2}\cos\frac{y}{\sqrt{3}}\right] = I_1(y),
\end{aligned} \tag{3.40}$$

where $\mu^2 = \frac{1}{4} + \frac{9}{4}(c_{aQ}^2 - 1)(c_{aQ}^2 + 7/2)$ and $dQ/dy = Q_{yc} y^{-(3w_Q+1)/2}$. The left hand side of the above equation is the Bessel equation, so that the solution of the homogeneous equation is the combination of the Bessel function $(J_\mu(y), N_\mu(y)$. The particular solution can be constructed via Green's method. Since it is difficult to find the particular solution which is valid over the whole range of y, we discuss only the case of very small scales ($y \gg 1$). Using the asymptotic representation of the Bessel

function, we obtain

$$\begin{aligned}
\Delta Q &\simeq \frac{u_1}{y}\sin(y)+\frac{u_2}{y}\cos(y)+\frac{1}{\sqrt{y}}\int_{y_i}^{y} G(y,y_1)I_1(y_1)dy_1, \\
&\simeq \frac{u_1}{y}\sin(y)+\frac{u_2}{y}\cos(y) \\
&\quad +\frac{1}{\sqrt{y}}\int_{y_i}^{y}\left(\cos(y)\sin(y_1)-\sin(y)\cos(y_1)\right)y^{-1/2}y_1^{1/2}I_1(y_1)dy_1, \\
&\approx \frac{u_1}{y}\sin(y)+\frac{u_2}{y}\cos(y) \\
&\quad +\begin{cases} y^{-3w_Q/2-3/2}\times\text{oscillation terms} & \text{for } -\frac{1}{3}<w_Q\leq\frac{1}{3} \\ y^{-3w_Q/2-5/2}\times\text{oscillation terms} & \text{for } -1<w_Q\leq-\frac{1}{3}\end{cases}+\ldots
\end{aligned} \tag{3.41}$$

here y_i is the initial value of y. We neglect the constant phase in the trigonometric functions and use the formulas in [69] to evaluate the integration. We now compute the density contrast using eqs. (2.151) and (3.41). As the universe evolves, Ψ decreases faster than $\Delta Q'/Q'$ and $\Delta Q V_{,Q}/\rho_Q$. For this reason, the dominant term on the right hand side of eq. (2.151) becomes $(1+w_Q)\Delta Q'/Q'$, so that we get

$$\Delta_Q \propto \left(\frac{a}{a_c}\right)^{\frac{1}{2}(3w_q-1)}. \tag{3.42}$$

Since the dominant contribution to $\Delta Q'$ comes from the homogeneous solution of eq. (3.40), the evolution of Δ_Q inside the horizon does not depend on the evolution of Ψ. Physically, this is because the gravitational potential damps away in side the horizon. One can see from eq. (3.42) that Δ_Q will be constant if $w_Q = 1/3$. This is the case of the exponential quintessence. During the kinetic regime, the quintessence fluctuations can grow in side the horizon, because $w_Q > 1/3$. However, they decay rapidly, and therefore become negligible during the potential regime.

In the matter dominated era, the evolution equation for Ψ can be obtained from eq. (2.94), by setting $w = \Gamma = c_a^2 = 0$. The result is

$$\Psi'' + 3\mathcal{H}\Psi' = 0. \tag{3.43}$$

Thus, Ψ evolves as

$$\Psi = c_3 + c_4\left(\frac{a}{a_c}\right)^{-\frac{5}{2}}, \tag{3.44}$$

where c_3 and c_4 are constant. During this era, the evolution of Ψ does not depend on the time of horizon crossing. The gravitational potential Ψ is approximately constant both inside and outside the horizon. We write the expression for Ψ in terms of a/a_c because we will use the variable $y = \sqrt{a/a_c}$ in the following calculation. Using

$y = \sqrt{a/a_c}$ and $u = y^{3/2}\Delta Q$, we can write eq. (2.98) as

$$\begin{aligned} \frac{d^2u}{dy^2} + \frac{1}{y}\frac{du}{dy} &+ \left(4 - \frac{\alpha^2}{y^2}\right) u \\ &= Q_{yc} y^{-3w_Q - \frac{1}{2}} \left[6(c_{aQ}^2 - 1)c_3 + \mathcal{O}(y^{-5})\right] = I_2(y), \end{aligned} \tag{3.45}$$

where $\alpha^2 = \frac{9}{4} + 9(c_{aQ}^2 - 1)(c_{aQ}^2 + 2)$ and $dQ/dy = Q_{yc} y^{-3w_Q - 1}$. As in the case of radiation domination, one can write the solution for the sub-horizon modes as

$$\begin{aligned} \Delta Q &= \frac{u_3}{y^2}\sin(2y) + \frac{u_4}{y^2}\cos(2y) + \frac{1}{y^{3/2}}\int_{y_i}^{y} G(y, y_1) I_2(y_1) dy_1, \\ &\simeq \frac{u_3}{y^2}\sin(2y) + \frac{u_4}{y^2}\cos(2y) \\ &\quad + \frac{1}{y^{3/2}}\int_{y_i}^{y} \left(\cos(2y)\sin(2y_1) - \sin(2y)\cos(2y_1)\right) y^{-1/2} y_1^{1/2} I_2(y_1) dy_1, \\ &\approx \frac{u_3}{y^2}\sin(2y) + \frac{u_4}{y^2}\cos(2y) \\ &\quad + \begin{cases} y^{-3w_Q - 3} \times \text{oscillation terms} & \text{for } -\frac{1}{3} \le w_Q < 0 \\ y^{-3w_Q - 4} \times \text{oscillation terms} & \text{for } -\frac{2}{3} \le w_Q < -\frac{1}{3} \\ y^{-3w_Q - 5} \times \text{oscillation terms} & \text{for } -1 < w_Q < -\frac{2}{3} \end{cases} + \ldots . \end{aligned} \tag{3.46}$$

Since Ψ is approximately constant, it gives the main contribution to Δ_Q. As a result, the density contrast of quintessence evolves as

$$\Delta_Q \approx 4(1 + w_Q)\Psi. \tag{3.47}$$

The term $(1 + w_Q)\Delta Q'/Q'$ depends on w_Q, hence it may give a contribution to Δ_Q for a specific range of w_Q. Using eq. (3.46), one gets

$$\frac{\Delta Q'}{Q'} \propto \left(\frac{a}{a_c}\right)^{\frac{1}{2}(3w_Q - 1)}. \tag{3.48}$$

This means that Δ_Q will increase as $\Delta_Q \propto a^{(3w_Q - 1)/2}$ if $w_Q > 1/3$. However, in most realistic quintessence models, $w_Q < 1/3$ during the matter dominated era.

3.4 Effects of Quintessence Fluctuations on the CMB

The quintessence fluctuations affect the CMB spectrum only on large scales, because the small scale fluctuations damp and become negligible before the onset of the quintessence dominated era. On large scales, the contributions to the CMB spectrum

come from the Sachs Wolfe effect which can be written in the Longitudinal gauge as [70]

$$\begin{aligned}\frac{\Theta_\ell(\eta)}{2\ell(\ell+1)} &= [\Theta_0+\Phi_l](\eta_*)j_\ell\left(k(\eta-\eta_*)\right)+\int_{\eta_*}^{\eta}(\Phi_l'-\Psi_l')j_\ell\left(k(\eta-\bar{\eta})\right)d\bar{\eta},\\ &= -\frac{1}{3}\Psi_l(\eta_*)j_\ell\left(k(\eta-\eta_*)\right)-2\int_{\eta_*}^{\eta}\Psi_l'j_\ell\left(k(\eta-\bar{\eta})\right)d\bar{\eta}, \qquad (3.49)\end{aligned}$$

where Θ_ℓ is the temperature fluctuations $\delta T_\ell(k,\eta)/T$ in momentum space, j_ℓ is the spherical Bessel function, ℓ is the multipole moment and η_* is the conformal time at last scattering. The angular power spectrum of the CMB is related to the temperature fluctuations Θ_ℓ by the formula

$$\frac{\ell(\ell+1)}{2\pi}C_\ell=\frac{1}{2\pi^2}\int\frac{dk}{k}k^3\frac{|\Theta_\ell|^2}{2\ell(\ell+1)}. \qquad (3.50)$$

The first term on the right hand side of eq. (3.49) corresponds to the gravitational redshift effects due to the photon's climb out of the potential well Φ_l at last scattering. This is the ordinary Sachs Wolfe (SW) effect. The second term describes the fluctuations induced by the passage of CMB photons through the time evolving gravitational potential. This is the Integrated Sachs Wolfe (ISW) effect. To obtain the second line, we assume that the density fluctuations are adiabatic before quintessence domination, and $\Psi=-\Phi$.

If one neglects the density fluctuations in eq. (2.91), i.e., set $\Delta_l=\Delta-3(1+w)\Psi=0$, one will find that Ψ decreases as $\Psi\propto 1/a$ on large scales due to the expansion of the universe. Hence, the ISW effect partially cancels the SW effect. If the ratio Δ_Q/Ψ is negative at the present era, the contribution from the quintessence fluctuations will increase the decay rate of gravitational potential. As a result the CMB spectrum at low multipoles might be suppressed. If the ratio Δ_Q/Ψ is positive, the decay rate of gravitational potential may decrease. This might lead to the enhancement of the CMB spectrum at low multipoles. It has been shown in [71] that the contribution from quintessence fluctuations enhances the CMB spectrum at low multipoles if $w_Q=-0.6$, and suppresses the CMB spectrum at low multipoles if $w_Q=-2$.

The isocurvature fluctuations in the quintessence field may be generated if this field is already present during inflation. This primordial isocurvature fluctuation might be correlated with the adiabatic density perturbations, which are generated by the inflaton. We assume for simplicity that there are no primordial isocurvature fluctuations in CDM, baryons and neutrino. The CMB spectrum at low multipoles is enhanced if the primordial fluctuation of the quintessence field ΔQ is uncorrelated with the adiabatic density fluctuations [68, 72]. However, it is possible that the primordial fluctuation ΔQ has a correlation with the adiabatic density fluctuations.

In this case, the CMB spectrum at low multipoles can be suppressed [73, 62]. This might be used to explain the low quadrupole of the measured CMB spectrum.

The isocurvature fluctuations in quintessence can give a significant contribution to the CMB spectrum if their magnitude is large enough compared with the adiabatic density fluctuations during the present epoch. For tracking quintessence, isocurvature modes decrease rapidly during the tracking regime. Hence, the isocurvature fluctuations can affect the CMB spectrum if the quintessence field enters the tracking regime after matter domination. In this section, we will consider the case when quintessence is in the potential regime until the onset of the quintessence dominated era. Since quintessence is a light field during inflation, it acquires the usual quantum fluctuations [89]

$$\Delta Q_{\rm inf}(k) = \frac{H_e}{\sqrt{2k^3}}, \tag{3.51}$$

where H_e is the Hubble parameter evaluated at the time of the horizon exit and k is the wavenumber. At the beginning of the radiation dominated era, the field is nearly frozen, thus its density contrast is given by

$$\Delta_Q^i = \frac{V_{,Q}(Q^i)}{V(Q^i)} \Delta Q_{\rm inf}, \tag{3.52}$$

where the superscript i denotes the initial value at the beginning of the radiation dominated era. It is easy to see that Δ_Q^i does not satisfy the adiabatic condition. Since quintessence is sub-dominant during the radiation dominated era, the perturbation Δ_Q^i gives a negligible contribution to the curvature perturbation. Roughly speaking, Δ_Q^i corresponds to the isocurvature initial condition. The quantity Δ_Q^i depends on the ratio $V_{,Q}/V$ and H_e. According to observations, $H_e \approx 10^{-5} M_p$ [74]. the ratio $V_{,Q}/V$ depends on the model of quintessence. For the potential $V(Q) \propto Q^{\pm\alpha}$, one gets $V_{,Q}/V = \pm\alpha/Q^i$. It has been shown that $Q^i \approx \bar{M}_p$ for inverse power law quintessence [75]. For $\alpha > 0$, the energy density of quintessence can dominate at the present epoch if the quintessence field Q is nearly frozen until today. One can check that $Q^i \approx \bar{M}_p$ in this case. Thus $\Delta_Q^i \approx \pm 10^{-5}$ for the simple power law quintessence. The magnitude of the primordial adiabatic density perturbation, i.e., the curvature perturbation $\mathcal{R}$, is approximately 10^{-5}, as required by observations. Because the ratio of Δ_Q to the curvature perturbation does not change dramatically as the universe evolves, the magnitude of quintessence fluctuations at the present epoch is not large enough to give a significant contribution to the CMB spectrum in this case. However, it is possible that the field fluctuation ΔQ is large, and therefore quintessence fluctuations can give a significant contribution to the CMB spectrum [73, 76]. We will briefly discuss this possibility at the end of this section. Alternatively, we will show that the large magnitude of Δ_Q^i can be generated if $|V_{,Q}/V|$ is large. Let us consider the exponential quintessence ($V(Q) \propto e^{-\lambda Q/\bar{M}_p}$).

This quintessence model gives $V_{,Q}/V = -\lambda/\bar{M}_p$, so that the magnitude of Δ_Q^i is large when λ is large. The large value of λ corresponds to the small Ω_Q in the radiation dominated epoch, because $\Omega_Q = 4/\lambda^2$. According to the slow roll conditions $V_{,Q}^2/(6\bar{M}_p{}^2 H^4) \ll 1$ and $|V_{,QQ}/(3H^2)| \ll 1$, a simple exponential quintessence cannot be frozen until the present epoch if λ is large. For this reason, quintessence cannot dominate matter and therefore the expansion of the universe is not accelerating today. Thus, we use the exponential quintessence which its kinetic coefficient is a function of the quintessence field. The Lagrangian of this quintessence is [77]

$$\mathcal{L}(\chi) = \frac{1}{2}(\partial\chi)^2 \kappa^2(\chi) + \exp[-\chi/\bar{M}_p]\,. \tag{3.53}$$

Using the field variable $Q = K(\chi)$, where $\kappa(\chi) = \partial Q/\partial\chi$, the above Lagrangian becomes

$$\mathcal{L}(Q) = \frac{1}{2}(\partial Q)^2 + \exp[-K^{-1}(Q)/\bar{M}_p]\,. \tag{3.54}$$

We are interested in the evolution of field Q which depends on the form of $\kappa(\chi)$. We use [77]

$$\kappa(\chi) = \kappa_{\min} + \tanh\left(\frac{\beta}{\bar{M}_p}[\chi - \chi_1]\right) + 1, \tag{3.55}$$

where $\kappa_{\min}$, χ_1 and β are constant. In the radiation dominated era, $\chi \ll \chi_1$, so that $\kappa \simeq \kappa_{\min}$ and hence the quintessence field Q evolves like a simple exponential quintessence. This implies that $V_{,Q}/V \simeq -(\kappa_{\min}\bar{M}_p)^{-1}$ and $\Omega_Q = 4\kappa_{\min}^2$. Thus the magnitude of Δ_Q^i increases when Ω_Q in the early epoch decreases. During the matter dominated era, the coefficient $\kappa(\chi)$ increases rapidly when $\chi \approx \chi_1$. Consequently, w_Q will decrease towards -1 and quintessence becomes dominant. The present value of w_Q and Ω_Q depend on β and χ_1, respectively. The value of $\kappa_{\min}$ corresponds to the value of Ω_Q in the early epoch. The evolution of w_Q is shown in figure 3.2.

The quintessence field might be in the potential regime until the present epoch if its initial value is large compared with the tracking value. In our consideration, we set the initial value of Q' to be zero. We set $\Omega_Q = 0.7$ at the present epoch, and set $\beta = 1$. We can specify a value of $\kappa_{\min}$ through a value of Ω_Q at a chosen time during the early epoch. We first estimate $\kappa_{\min}$ numerically from the value of Ω_Q at last scattering (Ω_{Qls}). The evolution of w_Q is shown in figure 3.3. For a given Ω_{Qls}, w_Q has to increase from -1 before the matter dominated era, because the increasing rate of Ω_Q has to decrease. If we increase the initial value of Q, the quintessence field will not enter the tracking regime at the present time. However, w_Q still deviates from -1 before the matter dominated era. The quintessence field can be frozen until the quintessence dominated era if Ω_{Qls} is very small. We will consider this case in the next paragraph. Since the quintessence field is nearly frozen in the early epoch, the ratio Δ_Q/Ψ is negative and constant before the onset of the

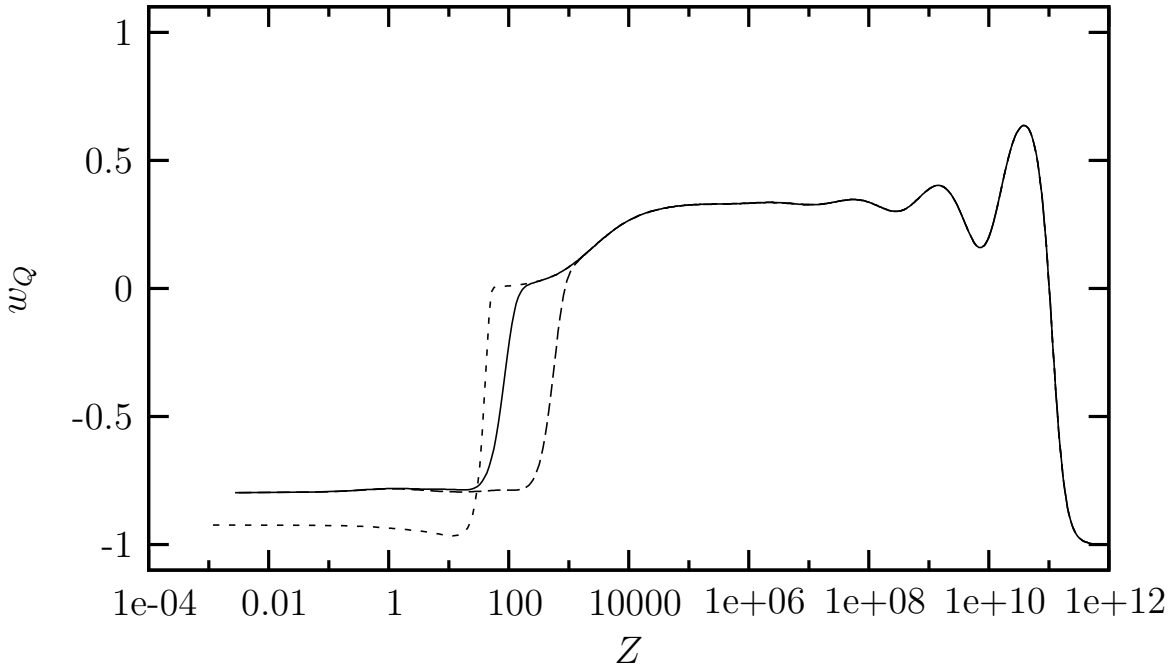

Figure 3.2: Evolution of w_Q. the solid line is $\beta = 1.0, \kappa_{\min} = 5 \times 10^{-3}$. The long dashed line is $\beta = 1.0, \kappa_{\min} = 5 \times 10^{-4}$. The dashed line is $\beta = 5.0, \kappa_{\min} = 5 \times 10^{-3}$. In this plot, we set $\Omega_Q = 0.7$ at the present epoch.

matter dominated era. When w_Q increases from -1, the magnitude of Δ_Q decreases and becomes small during quintessence domination. Thus the isocurvature fluctuations in quintessence cannot give a significant contribution to the CMB fluctuations during the present epoch. However, they might affect the CMB fluctuations during the matter dominated epoch if Ω_{Qls} is not too small. Unfortunately, a large Ω_{Qls} corresponds to a small Δ_Q^i. As a result, the isocurvature fluctuations in quintessence have a small effect on the CMB spectrum. We use CMBEASY [78] to compute the CMB spectrum for a case of $\Omega_{Qls} = 10^{-2}$. The result is show in figure 3.3.

If the quintessence field is in the tracking regime during the radiation dominated epoch, its density parameter Ω_Q is constant and equal to the tracking value Ω_{Qtr}. We now compute $\kappa_{\min}$ using the formula $\Omega_{Qtr} = 4\kappa_{\min}^2$. We still set $\Omega_Q = 0.7$ at the present epoch, $Q' = 0$ at the initial epoch and $\beta = 1$. The initial value of Q is chosen to be greater than the tracking value. This means that Ω_Q during the radiation dominated era does not equal to Ω_{Qtr}. Since Ω_Q can be small during the matter dominated era, its increasing rate need not be reduced. As a result, w_Q can be close to -1 until today. The evolution of w_Q is shown in figure 3.4. If we increase the initial value of Q, the quintessence field will enter the tracking regime at lower

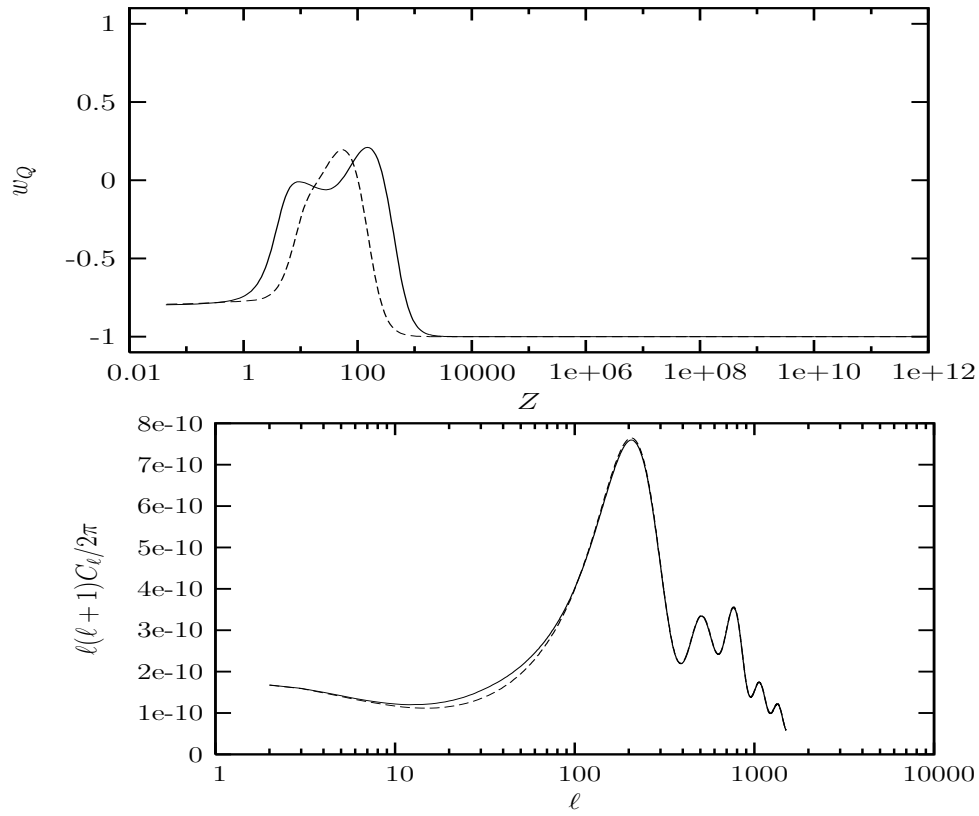

Figure 3.3: The upper panel shows the evolution of w_Q for $\Omega_{Qls} = 10^{-2}$ (solid line) and $\Omega_{Qls} = 10^{-4}$ (long dashed line). The lower panel shows the CMB spectrum for $\Omega_{Qls} = 10^{-2}$. The solid line corresponds to the adiabatic initial condition (eq 3.14), while the long dashed line corresponds to the isocurvature initial condition (eqs. 3.52 and 3.17). In this plot, we set $\Omega_Q = 0.7, \Omega_C = 0.26, \Omega_B h^2 = 0.023, h = 0.72$, $n_s = 0.99$, and $\tau = 0.1$.

redshift. In this case, the magnitude of Δ_Q can be large during the quintessence dominated era, so that Δ_Q can give a large contribution to the ISW effect. For $\Omega_{Qtr} = 10^{-6}$, The ISW effect can dominate the SW effect if Q enters the tracking regime after redshift about 10. This leads to the enhancement of the CMB spectrum at low multipoles. To suppress the CMB spectrum at low multipoles, the magnitude of Δ_Q should not be too large or too small. Thus the quintessence field should enter the tracking regime at the appropriate time. The CMB spectrum is shown in figure 3.4.

Finally, we compare the above results with the results in [76]. In this paper quintessence, with the ratio $V_{,Q}/V \sim \mathcal{O}(\bar{M_p}^{-1})$, is used. Thus quintessence fluctuations can have a significant effect on the CMB spectrum if ΔQ is large enough during the present epoch. Since the upper bound of ΔQ at the end of inflation is

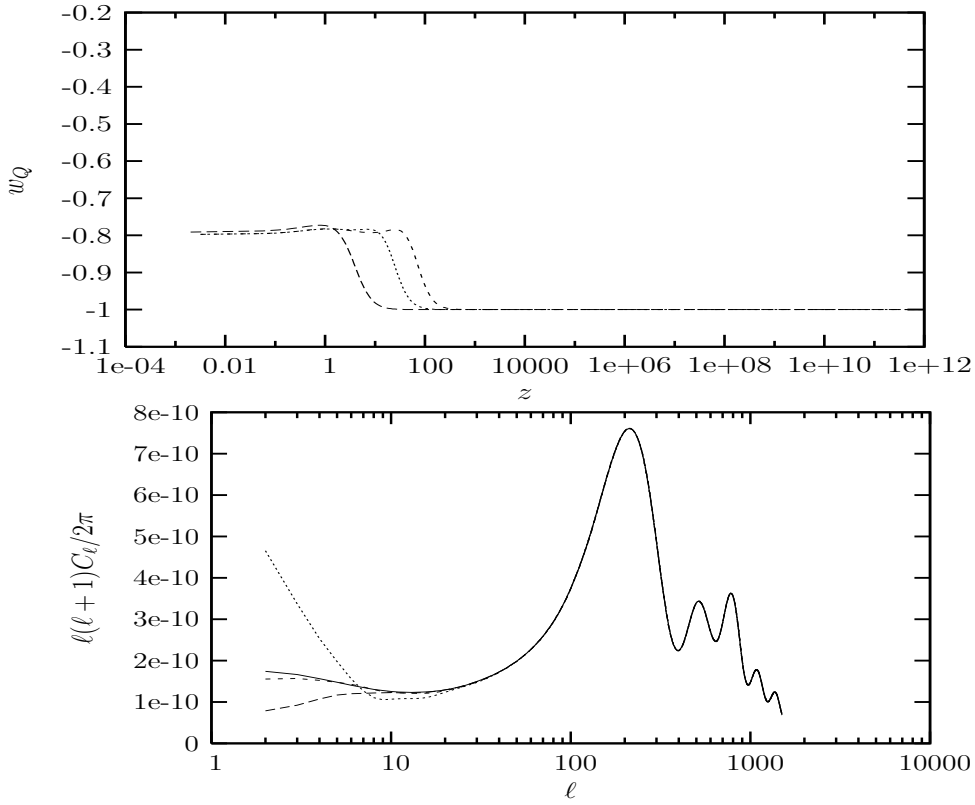

Figure 3.4: The upper panel shows the evolution of w_Q for a different value of Ω_{Qtr}. The lower panel shows the corresponding CMB spectrum. The solid curve denotes the adiabatic initial condition, while the other three curves denote isocurvature initial condition. In both panels the long dashed curve corresponds to $\Omega_{Qtr} = 10^{-3}$, while the dashed curve and the dotted curve corresponds to $\Omega_{Qtr} = 10^{-6}$ with the different initial value of Q. In this plot, we set $\Omega_Q = 0.7, \Omega_C = 0.26, \Omega_B h^2 = 0.023, h = 0.72$, $n_s = 0.99$, and $\tau = 0.1$.

limited by observations and ΔQ is constant when Q is nearly frozen, one needs a mechanism to amplify the magnitude of ΔQ. The amplification of ΔQ can occur if the coefficient of the kinetic term in the Lagrangian can vary. To suppress the CMB spectrum at low multipoles significantly, the ratio of ΔQ at the present epoch to ΔQ at the end of inflation has to be larger than 45. As a result, the ratio of the the kinetic coefficient at the present epoch to the one at the end of inflation is larger than 45. In our analysis, the varying kinetic coefficient is used to push the density parameter of quintessence from a small value to a value larger than 0.5 at the present epoch. It follows from eq. (3.55) that the maximum change in the kinetic coefficient is 2. The evolution of ΔQ and Δ_Q is shown in figure 3.5. This figure shows that the magnitude of ΔQ and Δ_Q decrease when the kinetic coefficient

increase. The redshift when the kinetic coefficient starts to increase might be read from figure 3.4, using the fact that w_Q and the kinetic coefficient start to increase at about the same time. Thus our results are quite different from [76].

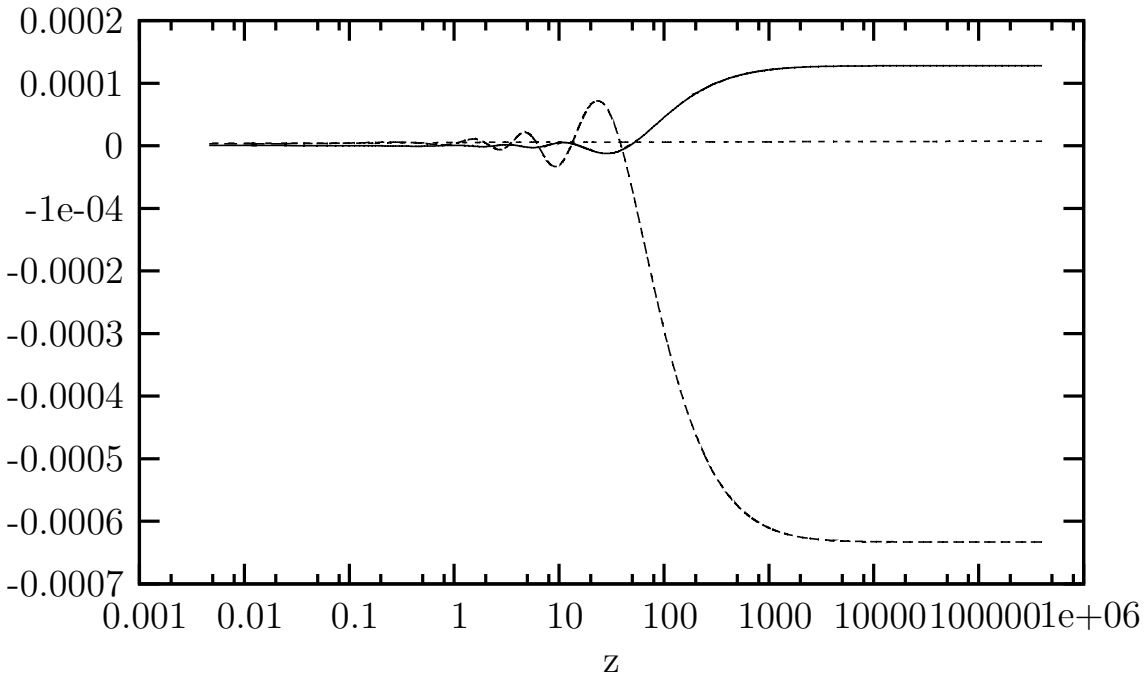

Figure 3.5: Evolution of dq (solid line), δ_Q (long dashed line) and Ψ (dashed line) for the $\Omega_{Qtr} = 10^{-3}$ model in figure 3.4. In this plot we set the initial value of $\mathcal{R}$ equal to 10^{-5} and use the mode whose $k = 0.002\mathrm{Mpc}^{-1}$.

Chapter 4

Initial Conditions from Inflation

According to section 3.4, the quintessence fluctuations can give a large contribution to the CMB spectrum if the quintessence field is nearly frozen until the quintessence dominated epoch, or equivalently starts the tracking behavior at the present epoch. In this chapter, we will discuss whether the quintessence field can be frozen until the present epoch. The quintessence field will be frozen for a long time after inflation, if the initial value of its energy density in the radiation dominated era is much smaller than the tracking value. In our consideration, we set $Q' = 0$ at the initial time, so that the initial value of the energy density depends on the initial value of the field. To estimate the initial value of the quintessence field in the radiation dominated epoch, we consider its evolution during inflation. It has been shown that the evolution of the quintessence field in the inflationary universe is influenced by its quantum fluctuations [75, 79]. The coarse-grained field is driven towards a large value by its quantum fluctuations. In the case of inverse power law quintessence, the value of the coarse-grained quintessence field is about M_p at the end of inflation [75]. As a result, the quintessence field can be frozen until the present epoch, but the initial value of its density fluctuations is not large enough to give a significant contribution to the CMB spectrum. Hence, we concentrate on the leaping kinetic term quintessence model, whose fluctuations are able to give a large contribution to the CMB spectrum. We study the effects of quantum fluctuations on the evolution of quintessence field using the stochastic approach.

The basic equations for the stochastic approach is reviewed in section 4.1. The classical evolution of the quintessence field during the inflationary era is discussed in section 4.2. In section 4.3, the effect of quantum fluctuations on the classical evolution is considered.

4.1 Stochastic Approach

The stochastic approach is one possible approach to model the evolution of quantum field in an inflationary universe [80]-[83]. This approach describes the dynamics of quantum field on the basis of a splitting of field into a superhorizon and a subhorizon part. The superhorizon part, which arises from a coarse-grained over a volume larger than the observable universe, is treated as classical. In the case of the inflaton, this part drives the de Sitter expansion of the universe. The evolution of this coarse-grained field, which is governed by a Langevin-like equation, is influenced by classical noise, that generates from the quantum fluctuations in the subhorizon part. In this section, we review the basic ideas of the stochastic approach.

We assume that the universe has a flat space time, whose metric has a form $ds^2 = -dt^2 + a^2(t)dx^2$, so the evolution of scalar field $\phi(\mathbf{x}, t)$ is described by the Klein-Gordon equation

$$\ddot{\phi} + 3H\dot{\phi} - \frac{\nabla^2\phi}{a^2} + \frac{dV}{d\phi} = 0, \tag{4.1}$$

where a dot denotes the derivative with respect to cosmic time. The field ϕ can be split into a long wavelength and a short wavelength component as $\phi = \phi_L + \phi_S$, where

$$\phi_S(\mathbf{x}, t) = \int \frac{d^3k}{(2\pi)^{3/2}}\Theta(k - \epsilon/|\eta|)\left[a(k)u_k(t)e^{-i\mathbf{kx}} + a^\dagger(k)u_k^*(t)e^{i\mathbf{kx}}\right], \tag{4.2}$$

here Θ is the step function, η is the conformal time, ϵ is a numerical constant whose value is smaller than 1. The step function is used to filter out the long wavelength modes with $k|\eta| < \epsilon$. Since $\epsilon \ll 1$, The coarse-grained field ϕ_L contains modes whose wavelength is much larger than the horizon size. We use the absolute value of η in this expression because η is negative during the inflationary era. The annihilation $a(k)$ and creation $a^\dagger(k)$ operators satisfy the usual commutation relations

$$\left[a(k), a^\dagger(k')\right] = \delta(k - k'), \quad [a(k), a(k')] = \left[a^\dagger(k), a^\dagger(k')\right] = 0. \tag{4.3}$$

Substituting $\phi = \phi_L + \phi_S$ into eq. (4.1), and using the evolution equation

$$\ddot{u_k} + 3H\dot{u_k} + \left[\frac{k^2}{a^2} + \left.\frac{d^2V(\phi)}{d\phi^2}\right|_{\phi=\phi_L}\right] u_k = 0, \tag{4.4}$$

we get [84]

$$\ddot{\phi_L} + 3H\dot{\phi_L} + \frac{dV(\phi_L)}{d\phi_L} - a^{-2}\nabla^2\phi_L = \int \frac{d^3k}{(2\pi)^{3/2}}\delta(k - \epsilon/|\eta|)\left[a(k)y(\mathbf{x}, \mathbf{k}, t)e^{-i\mathbf{kx}} + h.c.\right] = \xi(\mathbf{x}, t), \tag{4.5}$$

where a dot denotes the derivative with respect to $|t|$. The function $y(\mathbf{x},\mathbf{k},t)$ is defined as

$$\begin{aligned}
&\delta(k-\epsilon/|\eta|)y(\mathbf{x},\mathbf{k},t) \\
&= -\left[\ddot{\Theta}+3H\dot{\Theta}\right]u_k - 2\dot{\Theta}\dot{u}_k = \delta(k-\epsilon/|\eta|)\times \qquad (4.6)\\
&\left\{\frac{2\epsilon}{a^2|\eta|^3}\left[1-\frac{|\eta|}{a}\frac{da}{d|\eta|}\right]u_k - \frac{2\epsilon}{a^2|\eta|^2}\frac{du_k}{d|\eta|} + e^{i\mathbf{kx}}\frac{\epsilon^2}{a^2|\eta|^4}\frac{\partial}{\partial k^\alpha}\left[\frac{k^\alpha}{|\mathbf{k}|}e^{-i\mathbf{kx}}u_k\right]\right\}. \qquad (4.7)
\end{aligned}$$

The second line in eq. (4.7) is obtained using the relations

$$\dot{\Theta} = \frac{\epsilon}{a|\eta|^2}\delta(k-\epsilon/|\eta|), \quad \dot{\delta}(k-f(t)) = -\dot{f}(t)\frac{k^\alpha}{|\mathbf{k}|}\frac{\partial}{\partial k^\alpha}\delta(k-f(t)),$$

and

$$\ddot{\Theta} = -\frac{\epsilon}{a^2|\eta|^3}\left[2+\frac{|\eta|}{a}\frac{da}{d|\eta|}\right]\delta(k-\epsilon/|\eta|) + \frac{\epsilon^2}{a^2|\eta|^4}\frac{k^\alpha}{|\mathbf{k}|}\frac{\partial}{\partial k^\alpha}\delta(k-\epsilon/|\eta|).$$

In our approach, the field ϕ_L can be viewed as a classical field which evolves in the external random force $\xi(\mathbf{x},t)$. The statistical properties of this random force is characterized by the quantum expectation values of $\xi(\mathbf{x},t)$ and $\xi(\mathbf{x}_1,t_1)\xi(\mathbf{x}_2,t_2)$. We assume that the short wavelength modes ($k|\eta|<\epsilon$) are in a vacuum state, so that the mean of $\xi(\mathbf{x},t)$ is $\langle\xi(\mathbf{x},t)\rangle = 0$. The two-point correlation function is

$$\begin{aligned}
&\langle\xi(\mathbf{x}_1,t_1)\xi(\mathbf{x}_2,t_2)\rangle \\
&= \int\frac{d^3k}{(2\pi)^3}\delta(k-\epsilon/|\eta|_1)\delta(k-\epsilon/|\eta|_2)y(\mathbf{x}_1,\mathbf{k},t_1)y^*(\mathbf{x}_2,\mathbf{k},t_2)e^{-i\mathbf{k}(\mathbf{x}_1-\mathbf{x}_2)}, \\
&= \delta(\epsilon/|\eta|_1-\epsilon/|\eta|_2)\int\frac{d^3k}{(2\pi)^3}\delta(k-\epsilon/|\eta|_1)y(\mathbf{x}_1,\mathbf{k},t_1)y^*(\mathbf{x}_2,\mathbf{k},t_2)e^{-i\mathbf{k}(\mathbf{x}_1-\mathbf{x}_2)}, \\
&= \frac{|\eta|_1^2 a(t_1)}{\epsilon}\delta(t_1-t_2)\int\frac{d^3k}{(2\pi)^3}\delta(k-\epsilon/|\eta|_1)yy^*e^{-i\mathbf{k}(\mathbf{x}_1-\mathbf{x}_2)}. \qquad (4.8)
\end{aligned}$$

One can see that the two-point correlation function of the noise ξ is proportional to a Dirac delta function in time. This is a consequence of the sharp splitting of ϕ into short and long wavelength modes. A noise, whose two-point correlation function is proportional to a Dirac delta function, is a white noise. The white noise has a singular correlation at $t_1=t_2$ [85]. One may avoid this singular by using a smooth version of step function to split the field ϕ. This leads to a color noise [86]-[88]. For simplicity, we concentrate on a white noise in this thesis.

We now apply the above formulas to the case of the de Sitter expansion. During the de Sitter stage, $a(t)\propto e^{Ht}$, $\eta = -\frac{1}{a(t)H}$ and $H = dot(a)/a =$ constant, so that

$$y(\mathbf{x},\mathbf{k},\eta) = \frac{4\epsilon H^2}{|\eta|}u_k - 2\epsilon H^2\frac{\partial u_k}{\partial|\eta|} + e^{i\mathbf{kx}}\frac{\epsilon^2H^2}{|\eta|^2}\frac{\partial}{\partial k^\alpha}\left[\frac{k^\alpha}{|\mathbf{k}|}u_k e^{-i\mathbf{kx}}\right]. \qquad (4.9)$$

We are interested in the two-point correlation function of the noise ξ, so that the explicit expression for $y(\mathbf{x}, \mathbf{k}, \eta)$ has to be computed. The mode functions u_k obey the evolution equation (4.4), which can be written in terms of the variable $\bar{u}_k = a(t)u_k$ as

$$\frac{d^2\bar{u}_k}{d\eta^2} + \left[k^2 - \frac{1}{\eta^2}\left(\mu^2 - \frac{1}{4}\right)\right]\bar{u}_k = 0, \tag{4.10}$$

where $\mu^2 = \frac{9}{4} - \frac{M^2(t)}{H^2}$ and $M^2(t) = \left.\frac{d^2V(\phi)}{d\phi^2}\right|_{\phi=\phi_L}$. If we assume that $M^2(t)$ is approximately constant and $M^2(t)/H^2 < 1$, the solution of above equation is [89]

$$u_k = \bar{u}_k/a = |\eta|^{\frac{3}{2}} H\left[c_1 H_\mu^{(1)}(k|\eta|) + c_2 H_\mu^{(2)}(k|\eta|)\right], \tag{4.11}$$

where $H_\mu^{(1)}$ and $H_\mu^{(2)}$ are the Hankel functions of the first and second kind, respectively. For the short wavelength modes ($k|\eta| \gg 1$), eq. (4.10) has a plane-wave solution. Matching this solution to eq. (4.11) at $k|\eta| \gg 1$, one can compute c_1, c_2 and obtain [89]

$$u_k = \frac{\sqrt{\pi}}{2} e^{i\left(\mu+\frac{1}{2}\right)\frac{\pi}{2}} |\eta|^{\frac{3}{2}} H\, H_\mu^{(1)}(k|\eta|). \tag{4.12}$$

Because of the function $\delta(k - \epsilon/|\eta|)$, only the long wavelength modes of $y(\mathbf{x}, \mathbf{k}, \eta)$ give a contribution to the correlation function. At the long wavelength limit ($k|\eta| \ll 1$), $y(\mathbf{x}, \mathbf{k}, \eta) \simeq \frac{1}{\sqrt{2}} 3\epsilon H^3 |\eta|^{1/2} (k|\eta|)^{-\mu} e^{-i\pi/2}$ [84]. Substituting this expression for y into eq. (4.8), one gets

$$\langle \xi(\mathbf{x}_1, t_1)\xi(\mathbf{x}_2, t_2)\rangle = \epsilon^{\frac{4M^2}{9H^2}} \frac{9H^5}{4\pi^2} \frac{\sin\left[\epsilon a H(\mathbf{x}_1 - \mathbf{x}_2)\right]}{\epsilon a H(\mathbf{x}_1 - \mathbf{x}_2)} \delta(t_1 - t_2). \tag{4.13}$$

At $\mathbf{x}_1 = \mathbf{x}_2$ and $M^2 \ll H^2$, the above equation becomes

$$\langle \xi(t_1)\xi(t_2)\rangle = \frac{9H^5}{4\pi^2}\delta(t_1 - t_2). \tag{4.14}$$

This expression will not depend on the form of the potential of the field ϕ if H does not depend on ϕ. Moreover, this equation is valid for the case of quasi de Sitter expansion because $\dot{H}/H \ll 1$. Using the slow-roll approximation, eq. (4.5) can be written as

$$\dot{\phi}_L = -\frac{1}{3H}\frac{dV}{d\phi_L} + \tilde{\xi}, \tag{4.15}$$

where $\tilde{\xi} = \xi/3H$. We set $a^{-2}\nabla^2\phi_L = 0$ because we are interested in the very long wavelength modes. It is easy to show that the two-point correlation function of $\tilde{\xi}$ is

$$\langle \tilde{\xi}(t_1)\tilde{\xi}(t_2)\rangle = \frac{H^3}{4\pi^2}\delta(t_1 - t_2). \tag{4.16}$$

The Brownian motion of the coarse-grained field ϕ_L can be described by the probability distribution $P(\phi_L, t|\chi)$, which is the solution of the Fokker-Planck equation

$$\frac{\partial P(\phi_L,t|\chi)}{\partial t} = \frac{1}{2}\frac{\partial}{\partial\phi_L}\left(\frac{H^{3/2}}{2\pi}\frac{\partial}{\partial\phi_L}\left(\frac{H^{3/2}}{2\pi}P(\phi_L,t|\chi)\right)+\frac{V'(\phi_L)}{3H}P(\phi_L,t|\chi)\right), \tag{4.17}$$

where the Hubble parameter H will be a function of ϕ_L if ϕ_L is the inflaton. This equation can be derived from the Langevin equation (4.15) [90]. It gives the probability that the field has the value ϕ_L at time t for a fixed initial value χ.

Now, let us consider the physics of eq. (4.15). Inside the horizon, the quantum fluctuations of any physical fields can be considered as waves with all possible wavelengths, moving in all possible directions. If the average value of these fluctuations vanishes, they can be called vacuum fluctuations. During the inflationary era, the wavelengths of vacuum fluctuations of the scalar field ϕ grow exponentially. When the wavelength of the fluctuations becomes larger than H^{-1}, the amplitude of this fluctuation is approximately constant. Thus its value, averaged over some macroscopically large space and time, does not vanish. As a result, the value of the field outside the horizon is perturbed by its vacuum fluctuations. The average amplitude of the fluctuations, which exit the horizon during a time interval H^{-1}, is $|\delta\phi(x)| \approx H/(2\pi)$. Since phase of each fluctuations is random, the sum of all fluctuations at a given point outside the horizon leads to the random jump of the field value at that point. During a time interval H^{-1}, the field value outside the horizon changes by $|\delta\phi_{\rm cl}| \simeq \left|\frac{dV/d\phi_L}{3H^2}\right|$ due to the classical evolution. Thus the evolution of the field will be dominated by the quantum effect if $\left|\frac{H}{2\pi}\frac{3H^2}{dV/d\phi_L}\right| > 1$. In this case, the field will be extremely inhomogeneous. Moreover, there exists a probability that the field is driven toward the large value ϕ_p, where $V(\phi_p) \sim M_p^4$. This will lead to the self-reproduction of the universe [90, 91] if ϕ is an inflaton. For simplicity, we consider only the case when the classical evolution of the inflaton dominates the quantum evolution. In this case, the inflaton field can be treated as a classical field.

4.2 Classical Evolution

As discussed in the previous section, the coarse-grained field ϕ_L can be treated as a classical field. If this field is quintessence, it drives the accelerated expansion of the universe at the present epoch. We now consider the classical evolution of this field by setting the noise term equal to zero. We assume that the quintessence field is not coupled to the inflaton. Thus, using the slow-roll approximation, the evolution equation for the inflaton $\tilde{\phi}$ and coarse-grained quintessence field $\tilde{Q}$ can be written

as

$$\frac{d\tilde{\phi}}{dN} = -\frac{1}{3\bar{M}_p{}^2 H^2}\frac{dW(\tilde{\phi})}{d\tilde{\phi}}, \tag{4.18}$$

$$\frac{d\tilde{Q}}{dN} = -\frac{1}{3\bar{M}_p{}^2 H^2}\frac{dV(\tilde{Q})}{d\tilde{Q}}, \tag{4.19}$$

where $N = \ln(a/a_i)$ and a_i is the initial value of scale factor. We suppose that the inflation is driven by the single inflaton field, whose potential can be written as

$$W(\tilde{\phi}) = W_0\tilde{\phi}^{\alpha}, \tag{4.20}$$

where $\tilde{\phi} = \phi/\bar{M}_p$ and $\alpha \geq 2$. For quintessence, we focus on the leaping kinetic term quintessence model. Since this quintessence evolves like an ordinary exponential quintessence in the early universe, we write the potential of quintessence as

$$V(\tilde{Q}) = \bar{M}_p{}^4 \exp\left(-\lambda\tilde{Q}\right), \tag{4.21}$$

here $\tilde{Q} = Q/\bar{M}_p$. This evolution equation for the quintessence field is valid when the condition $\left|\frac{d^2V/dQ^2}{3H^2}\right| \ll 1$ is satisfied. This means that the quintessence field will roll slowly if its value is larger than

$$\tilde{Q}_s(N) \simeq \frac{1}{\lambda}\ln\left[\frac{\lambda^2}{3\bar{M}_p{}^2 H^2(N)}\right]. \tag{4.22}$$

In our analysis, we set $\lambda > 1$, so that the inflaton energy dominates quintessence energy when $\tilde{Q}(N) \geq \tilde{Q}_s(N)$. If $\tilde{Q}(N) \ll \tilde{Q}_s(N)$, the energy of quintessence might dominate the inflaton energy. However, the quintessence field will rapidly move to a value larger than $\tilde{Q}_s(N)$, if $\tilde{Q}(N) < \tilde{Q}_s(N)$. Consequently, the universe becomes dominated by the inflaton and therefore the Hubble parameter can be written as

$$H^2 \simeq \frac{1}{3\bar{M}_p{}^2}W(\tilde{\phi}), \tag{4.23}$$

so that the solution of eq. (4.18) is

$$\tilde{\phi} = \sqrt{\tilde{\phi}_i^2 - 2\alpha N}, \tag{4.24}$$

where $\tilde{\phi}_i$ is the initial value of $\tilde{\phi}$. Because we restrict ourselves to the case when the classical evolution of the inflaton dominates the quantum evolution, we set $\tilde{\phi}_i = \tilde{\phi}_m$. The parameter $\tilde{\phi}_m$ is the maximum value of $\tilde{\phi}$, which the classical evolution still

dominates the quantum evolution. Thus we can compute $\tilde{\phi}_i$ using the relation $\left|\frac{H}{2\pi}\frac{3H^2}{dV/d\phi}\right| \simeq 1$. The result is

$$\tilde{\phi}_i = \left(\frac{12\alpha^2\pi^2 \bar{M_p}^4}{W_0}\right)^{\frac{1}{\alpha+2}}. \tag{4.25}$$

At the end of inflation, the slow-roll conditions

$$\epsilon_s = \frac{\bar{M_p}^2}{2}\left(\frac{dW/d\phi}{W}\right)^2 \ll 1, \tag{4.26}$$

$$\eta_s = \bar{M_p}^2\left|\frac{d^2W/d\phi^2}{W}\right| \ll 1 \tag{4.27}$$

are violated, so that we can compute the value of $\tilde{\phi}$ at the end of inflation using the relations $\epsilon_s \simeq 1$ or $\eta_s \simeq 1$. Because these slow-roll conditions are not violated at the same time, the condition, which is violated earliest, is used to compute the value of $\tilde{\phi}$ at the end of inflation ($\tilde{\phi}_e$). The result is

$$\tilde{\phi}_e = \max\left(\frac{\alpha}{\sqrt{2}}, \sqrt{\alpha(\alpha-1)}\right). \tag{4.28}$$

Using eqs. (4.23) and (4.24), the Hubble parameter can be written in terms of N as

$$H^2 = \frac{1}{3\bar{M_p}^2} W_0 \left(\tilde{\phi}_i^2 - 2\alpha N\right)^{\frac{\alpha}{2}}. \tag{4.29}$$

Let us now consider the evolution of the quintessence field. Substituting eq. (4.29) into eq. (4.19) we get

$$e^{\lambda\tilde{Q}} - e^{\lambda\tilde{Q}_i} = \frac{\lambda^2\bar{M_p}^4}{W_0}\int_0^N \frac{d\tilde{N}}{(\tilde{\phi}_i^2 - 2\alpha\tilde{N})^{\alpha/2}}. \tag{4.30}$$

Evaluating the integrals, one obtains

$$\tilde{Q}(N) = \begin{cases} \frac{1}{\lambda}\ln\left[e^{\lambda\tilde{Q}_i} + \frac{\lambda^2\bar{M_p}^4}{\alpha(2-\alpha)W_0}\left(\tilde{\phi}_i^{2-\alpha} - (\tilde{\phi}_i^2 - 2\alpha N)^{\frac{2-\alpha}{2}}\right)\right] & \text{for } \alpha > 2 \\ \frac{1}{\lambda}\ln\left[e^{\lambda\tilde{Q}_i} + \frac{\lambda^2\bar{M_p}^4}{4W_0}\ln\left[\frac{\tilde{\phi}_i^2}{\tilde{\phi}_i^2 - 2\alpha N}\right]\right] & \text{for } \alpha = 2 \end{cases}. \tag{4.31}$$

At the end of inflation, the value of the field $\tilde{Q}$ is

$$\tilde{Q}_e = \begin{cases} \frac{1}{\lambda}\ln\left[e^{\lambda\tilde{Q}_i} + \frac{\lambda^2\bar{M_p}^4}{\alpha(2-\alpha)W_0}\left(\tilde{\phi}_i^{2-\alpha} - \tilde{\phi}_e^{2-\alpha}\right)\right] & \text{for } \alpha > 2 \\ \frac{1}{\lambda}\ln\left[e^{\lambda\tilde{Q}_i} + \frac{\lambda^2\bar{M_p}^4}{2W_0}\ln\left[\frac{\tilde{\phi}_i}{\tilde{\phi}_e}\right]\right] & \text{for } \alpha = 2 \end{cases}. \tag{4.32}$$

This implies that the field $\tilde{Q}$ is frozen if

$$\tilde{Q}_i > \tilde{Q}_f = \begin{cases} \frac{1}{\lambda}\ln\left[\frac{\lambda^2 \bar{M_p}^4}{\alpha(2-\alpha)W_0}\left(\tilde{\phi}_i^{2-\alpha} - \tilde{\phi}_e^{2-\alpha}\right)\right] & \text{for } \alpha > 2 \\ \frac{1}{\lambda}\ln\left[\frac{\lambda^2 \bar{M_p}^4}{2W_0}\ln\left[\frac{\tilde{\phi}_i}{\tilde{\phi}_e}\right]\right] & \text{for } \alpha = 2 \end{cases} . \tag{4.33}$$

It follows from table 4.1 that $\tilde{Q}_s(0) < \tilde{Q}_f$, so that the slow-rolling quintessence field, which $\ddot{\tilde{Q}} \ll \dot{\tilde{Q}}$, needs not to be frozen. The value of the quintessence field at the end of inflation $\tilde{Q}_e$ depends on $\tilde{Q}_i$. If $\tilde{Q}_i > \tilde{Q}_f$, $\tilde{Q}_e \simeq \tilde{Q}_i$. If $\tilde{Q}_s(0) < \tilde{Q}_i < \tilde{Q}_f$, the value of $\tilde{Q}_e$ is given by eq. (4.32). Moreover, the value of $\tilde{Q}_e$ also depends on the duration of inflation through the inflation model. The evolution of the slow-rolling quintessence field is shown in figure 4.1.

λ	Ω_{Qr}	$\tilde{Q}_s(0)$	$\tilde{Q}_f$
2000	10^{-6}	0.012	0.021
632.5	10^{-5}	0.035	0.062
200	10^{-4}	0.1	0.19
63.25	10^{-3}	0.28	0.55

Table 4.1: The value of $\tilde{Q}_s(0)$ and $\tilde{Q}_f$. The parameter Ω_{Qr} is the density parameter of quintessence in the radiation dominated era. We use the potential $W(\tilde{\phi}) = \frac{1}{2}m_\phi^2 \bar{M_p}^2 \tilde{\phi}^2$ for the inflaton, where $m_\phi \simeq 10^{-6} M_p$.

Now, we consider the evolution of the quintessence field when $\tilde{Q}_i < \tilde{Q}_s(0)$. In this case, the field does not roll slowly during the initial stage. Although the kinetic energy of the field is set to zero at the beginning, it will dominate the potential energy in a short period of time. Hence, we assume that the kinetic energy of the field dominates the potential energy at about the initial stage, and write

$$\frac{d\tilde{Q}}{dN} = \frac{\dot{\tilde{Q}}_i}{H} e^{-3N}, \tag{4.34}$$

where $\dot{\tilde{Q}}_i$ is $d\tilde{Q}/dt$ evaluated at the initial time. We assume that H is approximately constant during the initial stage, so we get

$$\tilde{Q}(N) = \tilde{Q}_i - \frac{\dot{\tilde{Q}}_i}{3H_i} e^{-3N} + \frac{\dot{\tilde{Q}}_i}{3H_i}, \tag{4.35}$$

here the subscript i denotes the initial value. This equation shows that $\tilde{Q} \to$ constant as N increases. Consequently, the potential energy of the field $\tilde{Q}$ dominates the kinetic energy, and this field becomes nearly frozen. Since the initial value of the

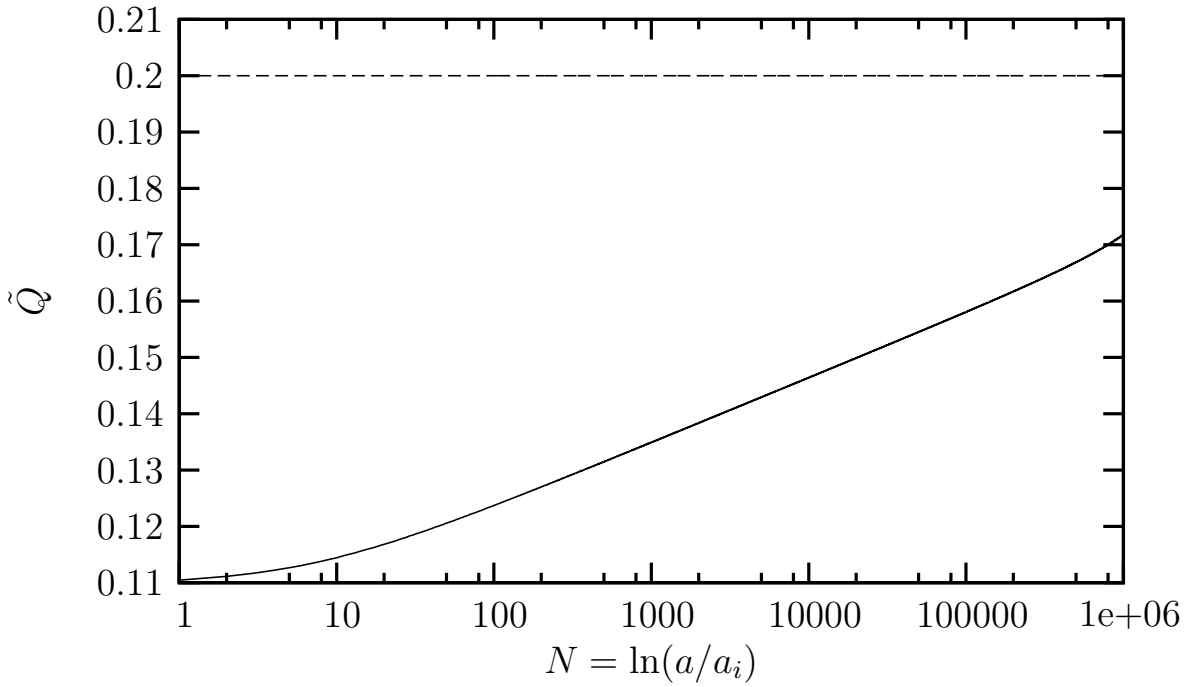

Figure 4.1: Evolution of the quintessence field in the slow-roll limit. We use the same inflaton potential as in table 4.1, and set $\lambda = 200$. The solid curve represents the case of $\tilde{Q}_i = 0.11$, while the long dashed curve represents the case of $\tilde{Q}_i = 0.2$.

kinetic energy is set to zero, the initial value of the energy density is equal to the potential energy. To compute $\dot{\tilde{Q}}_i$, we assume that the kinetic energy dominates the potential energy before the energy density changes significantly. Thus we obtain

$$\tilde{Q} \to \tilde{Q}_c = \tilde{Q}_i + \frac{\sqrt{2V(\tilde{Q}_i)}}{3H_i\bar{M}_p}. \tag{4.36}$$

We note that this expression agrees very well with the numerical solution. The evolution of the quintessence field in this case is shown in figure 4.2. It can be seen from this figure that the value of $\tilde{Q}_c$ rapidly increases when $\tilde{Q}_i$ decreases. If $\tilde{Q}_i$ is not much smaller than $\tilde{Q}_s(0)$, $\tilde{Q}_c$ will be smaller than $\tilde{Q}_f$. This means that the quintessence field will evolve according to eq. (4.31) after it reaches $\tilde{Q}_c$. Nevertheless, if $\tilde{Q}_i$ is small enough, $\tilde{Q}_c$ will be larger than $\tilde{Q}_f$ and therefore the quintessence field can be frozen until the end of inflation.

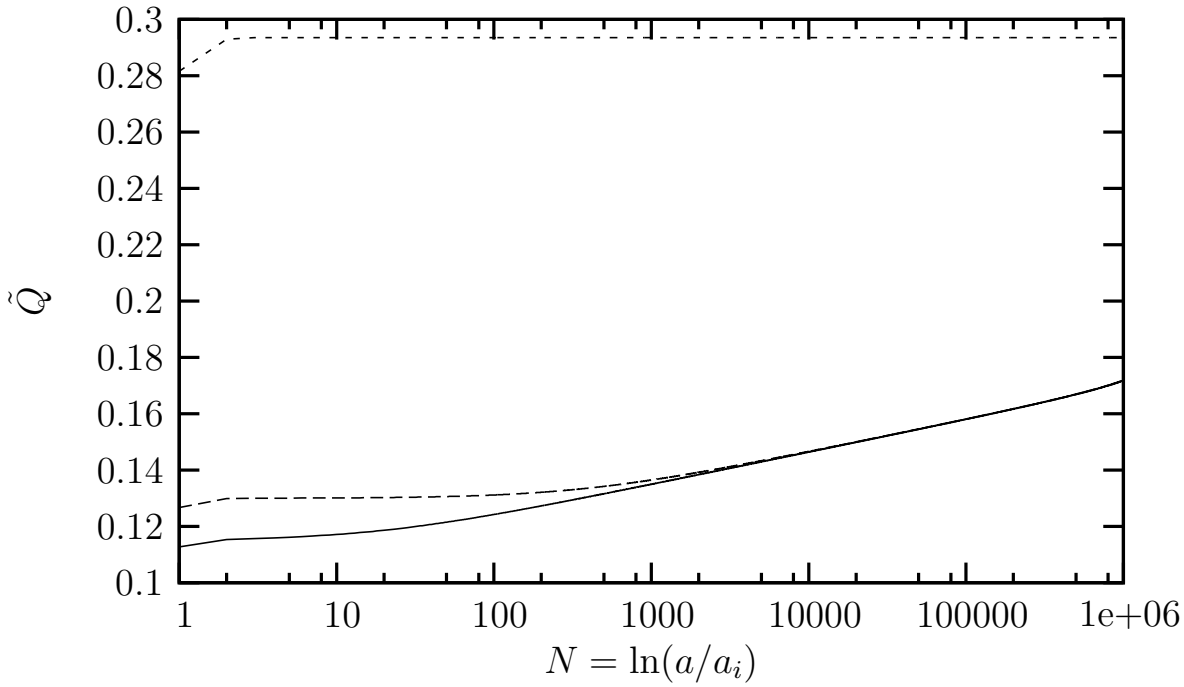

Figure 4.2: Evolution of the quintessence field in the case when it does not roll slowly at the initial time. We use the same inflaton potential as in figure 4.1, and set $\lambda = 200$. The solid curve represents the case of $\tilde{Q}_i = 0.08$, the long dashed curve represents the case of $\tilde{Q}_i = 0.075$ and the dashed curve represents the case of $\tilde{Q}_i = 0.06$. The numerical integration gives $\tilde{Q}_c = 0.293$ and $\tilde{Q}_c = 0.13$ when $\tilde{Q}_i = 0.06$ and $\tilde{Q}_i = 0.075$ respectively, while eq. (4.36) gives $\tilde{Q}_c = 0.290$ and $\tilde{Q}_c = 0.13$ when $\tilde{Q}_i = 0.06$ and $\tilde{Q}_i = 0.075$ respectively.

4.3 Quantum Evolution

We now discuss the effect of quantum fluctuations on the evolution of the coarse-grained quintessence field $\tilde{Q}$. For simplicity, we use the potential $W(\tilde{\phi}) = \frac{1}{2}m_\phi^2 \bar{M_p}^2 \tilde{\phi}^2$ for the inflaton. Here, $m_\phi \simeq 10^{-6} M_p$. In the slow-roll limit, the Langevin equation for the exponential quintessence can be written as

$$\frac{d\tilde{Q}}{dN} = \frac{\lambda}{3H^2 \bar{M_p}^2} e^{-\lambda \tilde{Q}} + \frac{H}{2\pi \bar{M_p}} \tilde{\xi}, \tag{4.37}$$

where the two-point correlation function of $\tilde{\xi}$ is given by

$$\langle \tilde{\xi}(N) \tilde{\xi}(N') \rangle = \delta(N - N'). \tag{4.38}$$

We will see in the following discussion that the slow-roll approximation is not always valid. Thus we use eq. (4.37) to study qualitatively the evolution of $\tilde{Q}$ instead of

finding its solution. Since $\langle\tilde{\xi}(N)\rangle = 0$, we have $\langle d\tilde{Q}/dN\rangle = \lambda \exp(-\lambda\tilde{Q})/(3H^2\bar{M_p}^2)$. Thus we assume that the mean of $\tilde{Q}$ is given by $\langle\tilde{Q}(N)\rangle = \tilde{Q}_{\rm cl}(N)$, where $\tilde{Q}_{\rm cl}$ corresponds the classical evolution of $\tilde{Q}$. It follows from figure 4.3 that the effects of the quantum noise on the evolution of $\tilde{Q}$ is negligible during the initial stage, but becomes significant after this stage. Since the quantum noise leads to the deviation of $\tilde{Q}$ from $\tilde{Q}_{\rm cl}$, we further suppose that

$$\tilde{Q}(N) = \tilde{Q}_{\rm cl}(N) + \int_0^N dN' \frac{H\tilde{\xi}(N')}{2\pi\bar{M}_p}, \tag{4.39}$$

here we have set $\tilde{Q}(N=0) = \tilde{Q}_{\rm cl}(N=0)$. It is clear that this equation is not the solution of eq. (4.37). However, we will use this equation to study the evolution of $\tilde{Q}$ under the random force $\tilde{\xi}$. The variance of $\tilde{Q}$ is defined by

$$\sigma^2_{\tilde{Q}} = \langle\tilde{Q}^2\rangle - \langle\tilde{Q}\rangle^2 = \langle\tilde{Q}^2\rangle - \tilde{Q}^2_{\rm cl}. \tag{4.40}$$

Using eqs. (4.39) and (4.38), one obtains

$$\begin{aligned} \sigma^2_{\tilde{Q}} &= \int_0^N dN' \frac{H^2}{4\pi^2\bar{M_p}^2}, \\ &= \frac{W_0}{12\pi^2\alpha(\alpha+2)\bar{M_p}^4}\left(\tilde{\phi}_i^{\alpha+2} - \tilde{\phi}^{\alpha+2}(N)\right) = \sigma_o^2. \end{aligned} \tag{4.41}$$

It follows from eq. (4.39) that the value of field $\tilde{Q}$ might be smaller than $\tilde{Q}_s(N)$ due to the random force. When the random force drives the field $\tilde{Q}$ to a value close to $\tilde{Q}_s$, the slow-roll approximation is not valid and the classical drift term $dV/d\tilde{Q}$ dominates the random force. Consequently, the field $\tilde{Q}$ will be rapidly driven towards a large value by the classical drift term. Hence the classical drift behaves like a reflecting wall, which prevents $\tilde{Q}$ to become smaller than $\tilde{Q}_s$. We will put the reflecting wall into the probability distribution of $\tilde{Q}$ and compute its mean and also its variance using this distribution function. Let us consider the normalized probability distribution $p(x)$. If we put a reflecting wall at $x = x_s$ such that only the values $x > x_s$ are allowed, the new probability distribution is $P(x) + P(2x_s - x)$ [79]. It can be checked that this probability distribution is normalized. We suppose that the probability distribution of the field $\tilde{Q}$ is a Gaussian distribution, so

$$P(\tilde{Q}) = \left[\exp\left(-\frac{(\tilde{Q}-\tilde{Q}_{\rm cl})^2}{2\sigma_o^2}\right) + \exp\left(-\frac{(\tilde{Q}+(\tilde{Q}_{\rm cl}-2\tilde{Q}_s))^2}{2\sigma_o^2}\right)\right] / \left(\sqrt{2\pi}\sigma_o\right). \tag{4.42}$$

Using this probability distribution, one obtains

$$\bar{\tilde{Q}} = \sigma_0\sqrt{\frac{2}{\pi}}\exp\left[-\frac{(\tilde{Q}_{\rm cl}-\tilde{Q}_s)^2}{2\sigma_o^2}\right] + \left(\tilde{Q}_{\rm cl}-\tilde{Q}_s\right) E\left(\frac{\tilde{Q}_{\rm cl}-\tilde{Q}_s}{\sqrt{2\sigma_o^2}}\right) + \tilde{Q}_s, \tag{4.43}$$

and

$$\bar{\tilde{Q}}^2 = \sigma_0^2 + \frac{2\sqrt{2}\tilde{Q}_s\sigma_0}{\sqrt{\pi}} \exp\left[-\frac{(\tilde{Q}_{\rm cl}-\tilde{Q}_s)^2}{2\sigma_0^2}\right] + 2(\tilde{Q}_s\tilde{Q}_{\rm cl}-\tilde{Q}_s^2)E\left(\frac{\tilde{Q}_{\rm cl}-\tilde{Q}_s}{\sqrt{2\sigma_o^2}}\right) + \tilde{Q}_{\rm cl}^2 - 2\tilde{Q}_{\rm cl}\tilde{Q}_s + 2\tilde{Q}_s^2, \quad (4.44)$$

where $E(x)$ is the error function defined by

$$E(x) = \frac{2}{\sqrt{\pi}}\int_0^x e^{-t^2}dt. \quad (4.45)$$

We note that the quantities $\bar{\tilde{Q}}$, $\bar{\tilde{Q}}^2$, $\tilde{Q}_{\rm cl}$, $\tilde{Q}_s$ and σ_0 are functions of N. The variance of $\tilde{Q}$ can be computed using the relation $\sigma_{\tilde{Q}} = \bar{\tilde{Q}}^2 - \bar{\tilde{Q}}^2$. To check these analytic expressions for $\bar{\tilde{Q}}$ and $\sigma^2_{\tilde{Q}}$, we solve the Langevin equation for $\tilde{Q}$ numerically. We do not use the slow-roll approximation in the numerical integration. The results are shown in table 4.2. One sees from this table that eqs. (4.43) and (4.44) agree quite well with the numerical solution.

λ	$\bar{\tilde{Q}}_a$	$\bar{\tilde{Q}}_n$	$\sigma_{\tilde{Q}a}$	$\sigma_{\tilde{Q}n}$
2000	0.583	0.583	0.426	0.428
632.5	0.623	0.618	0.426	0.426
200	0.739	0.731	0.426	0.431
63.25	1.08	1.09	0.427	0.404

Table 4.2: The mean and variance of $\tilde{Q}$ at the end of inflation. We use the same inflation potential as in table 4.1. The subscripts a and n denote the analytic and numerical solutions, respectively.

We plot the evolution of $\tilde{Q}$ in figure 4.3. From this figure, we see that the value of $\tilde{Q}$ cannot be smaller than $\tilde{Q}_s(N)$. This is because the classical drift will drive the field towards a large value if $\tilde{Q} \approx \tilde{Q}_s$. The probability distribution of $\tilde{Q}$ is shown in figure 4.4. The mean value of $\tilde{Q}$ is not equal to the peak of the probability distribution because there is a reflecting wall at $\tilde{Q}_s$. Finally, we set the initial value of the quintessence field at the beginning of the radiation dominated era equal to $\bar{\tilde{Q}}$ at the end of inflation, and then compute $w_Q(z)$ in the FRW universe. The evolution of $w_Q(z)$ is shown in figure 4.5. The quintessence field is frozen until the present epoch when $\lambda = 2000$ and $\lambda = 632.5$, while it enters the tracking regime in the radiation dominated era when $\lambda = 63.25$ and $\lambda = 200$. However, the probability that the quintessence field is frozen until the present epoch does not vanish in all cases. We note that the value of $\bar{\tilde{Q}}$ at the end of inflation also depends on the the model of inflation.

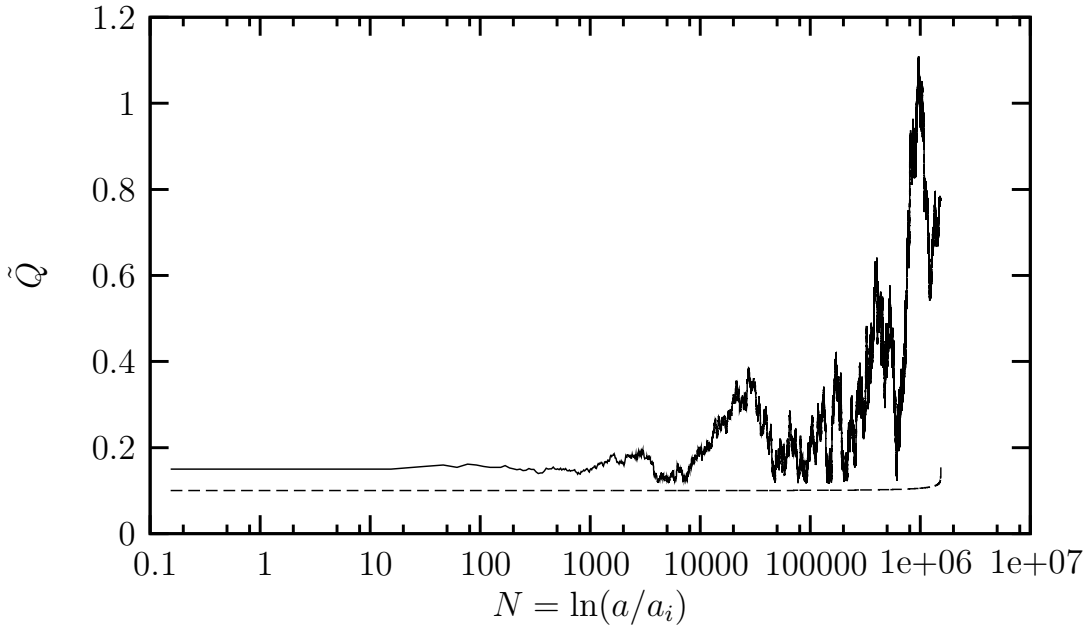

Figure 4.3: Evolution of $\tilde{Q}$ under the random force $\tilde{\xi}$. The solid line shows the evolution of $\tilde{Q}$ while the long dashed line shows the slow roll limit $\tilde{Q}_s(N)$. In this plot we set $\lambda = 200$ and $\tilde{Q}(0) = 0.12$.

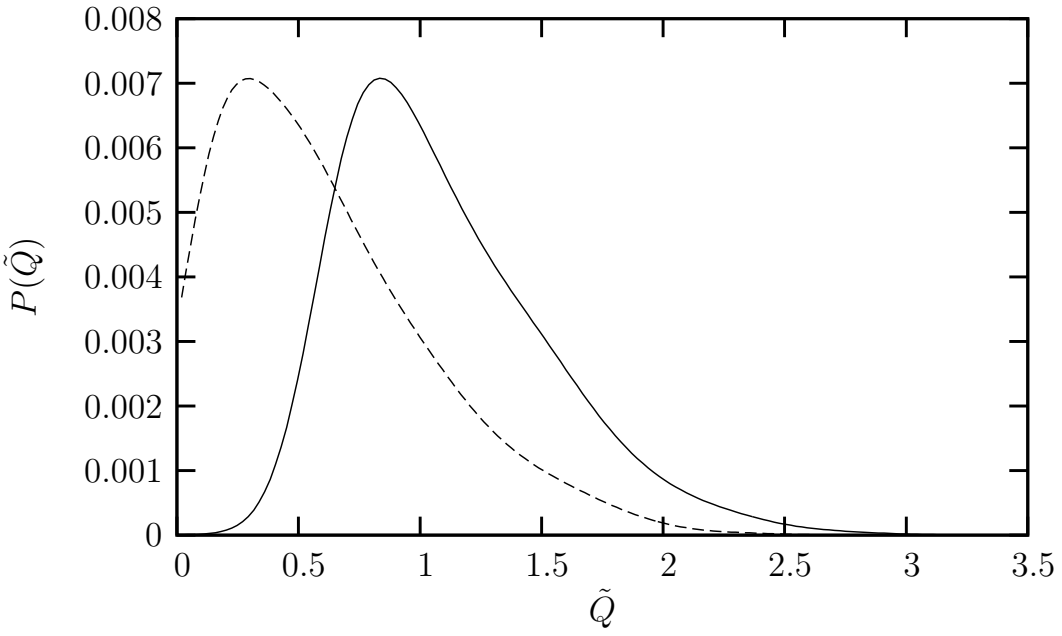

Figure 4.4: Probability distribution of $\tilde{Q}$. The solid line represents the case of $\lambda = 63.25$, while the long dashed line represents the case of $\lambda = 2000$.

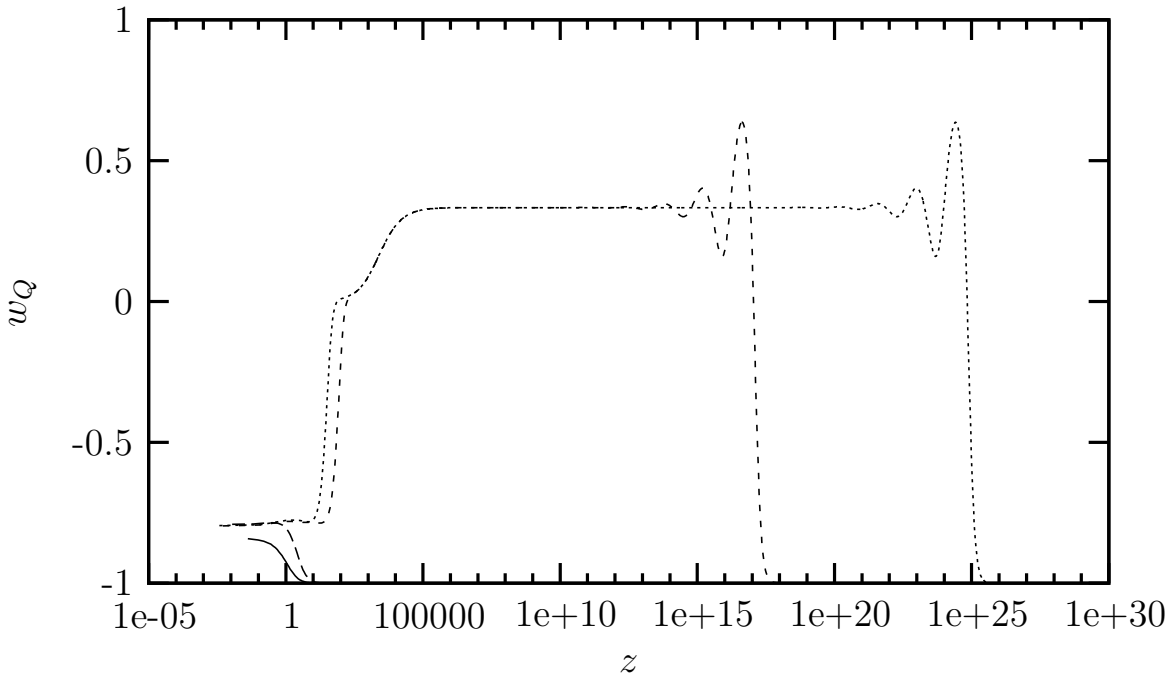

Figure 4.5: The evolution of leaping kinetic term quintessence in the FRW universe. We set the initial value of quintessence equal to $\tilde{Q}$ in table 4.2. The solid curve represents the case of $\lambda = 2000$, the long dashed curve represents the case of $\lambda = 632.5$, the dashed curve represents the case of $\lambda = 200$ and the dotted curve represents the case of $\lambda = 63.25$. In this plot, we set $\Omega_Q = 0.7$, $\Omega_M = 0.3$ and $h = 0.7$.

Chapter 5

Observational Constraints on Dark Energy

Observations [43, 18, 35, 92, 37, 40, 93] indicate that a mysterious form of dark energy [4, 5, 7, 12] is driving an accelerated expansion of our universe. A possible form of dark energy is a scalar field which is generated naturally in many particle physics models. There are many models of dark energy with different potentials proposed in the literature. To test their general features, one may parameterize their evolution using a suitable parameterization of the equation of state parameter w_d. Various parameterizations of w_d as a function of the scale factor a or redshift z have been investigated [95, 96, 97, 98]. In the early epoch, the universe is influenced by the amount of dark energy Ω_d rather than the equation of state. For example, the CMB anisotropies are very sensitive to the averaged fraction of dark energy at last scattering $\bar{\Omega}_{\rm ls}$ [99], and structure formation depends on the averaged amount of dark energy during structure formation $\bar{\Omega}_{\rm sf}$ [100]. Thus, these quantities can be used to describe the effects of dark energy in the early epoch.

Yet, some essential key features for a viable model seem to be the following: today, the amount of dark energy should be $\sim 70\%$. Going back in time, this value must have decreased considerably, as current constraints yield a fraction of dark energy at the time of last scattering $\bar{\Omega}_{\rm ls} \leq 8\%$ [101]. Supernovae measurements tell us that this decrease must have occurred swiftly, as the slope of this decrease is reflected in $w_0 \leq -0.7$.

Usually, observations at low redshift, such as SNe Ia measurements are combined with structure formation and CMB observations that probe earlier epochs. In this thesis, we will take a different point of view. Given the uncertainties in parameterizing Ω_d or equivalently w_d, we look at high redshift and low redshift constraints separately.

In section 5.1, we study the general properties of the dark energy parameterization used in this chapter. We constrain this parameterization using SNe Ia data

in section 5.2, and using structure formation and CMB observations in section 5.3, respectively.

5.1 Dark Energy Parameterization

We use a particularly simple and direct parameterization of the dark energy evolution [102]. The parameters are the amount of dark energy today Ω_d^0, the present equation of state parameter w_0, and the bending parameter b or, equivalently, the amount of dark energy at early times Ω_d^e to which it asymptotes for very large z. To derive this parameterization, we consider the evolution of Ω_d during the present epoch. Assuming that the radiation energy can be neglected, the evolution equation for Ω_d is given by

$$\frac{d\Omega_d}{dy} = 3\Omega_d(1-\Omega_d)w_d \qquad , \qquad y = \ln(1+z) = -\ln a. \tag{5.1}$$

Using the variable

$$R(y) = \ln\left(\frac{\Omega_d(y)}{1-\Omega_d(y)}\right), \tag{5.2}$$

eq. (5.1) becomes

$$\frac{\partial R(y)}{\partial y} = 3w_d(y). \tag{5.3}$$

This equation can be integrated by introducing the parameterization

$$\int_0^y w_d(y')dy' = \frac{w_0 y}{1+by}, \tag{5.4}$$

where the bending parameter b is zero for a constant w_d. Substituting this parameterization into eq. (5.3), we get

$$R(y) = R_0 + \frac{3w_0 y}{1+by}, \tag{5.5}$$

where $R_0 = \ln\left(\frac{\Omega_d^0}{1-\Omega_d^0}\right)$. The density parameter Ω_d can be written in terms of R as

$$\Omega_d = \frac{e^R}{1+e^R}. \tag{5.6}$$

This equation shows that the evolution of Ω_d depends on the parameters Ω_d^0, w_0, and b. Thus, w_d can be expressed in terms of these parameters. It follows from eq. (5.4), that

$$w_d(y) = \frac{w_0}{(1+by)^2}. \tag{5.7}$$

It is clear that w_d reaches 0 at large redshift and hence dark energy evolves like dark matter. Since we neglect the radiation in our derivation, this expression for w_d should be valid after the matter-radiation equality. If we use this expression in the radiation dominated epoch, the ratio of dark energy to dark matter will reach a constant value at large redshift, while the ratio of dark energy to radiation will decrease as redshift increases. Thus, it is reasonable to use this expression both before and after matter-radiation equality. However, if one would like to parametrise dark energy by the amount of dark energy at high redshift, one may assume that w_d has a complicated form in the radiation dominated epoch, and therefore the expression for Ω_d at high redshift is

$$\Omega_d^e = \Omega_d(z \to \infty) = \frac{e^{R_0+3w_0/b}}{1+e^{R_0+3w_0/b}}. \tag{5.8}$$

This expression for Ω_d is obtained from eq. (5.6) by setting $y \to \infty$. To compare our model with the cosmological constant, we plot the evolution of Ω_d in figure 5.1.

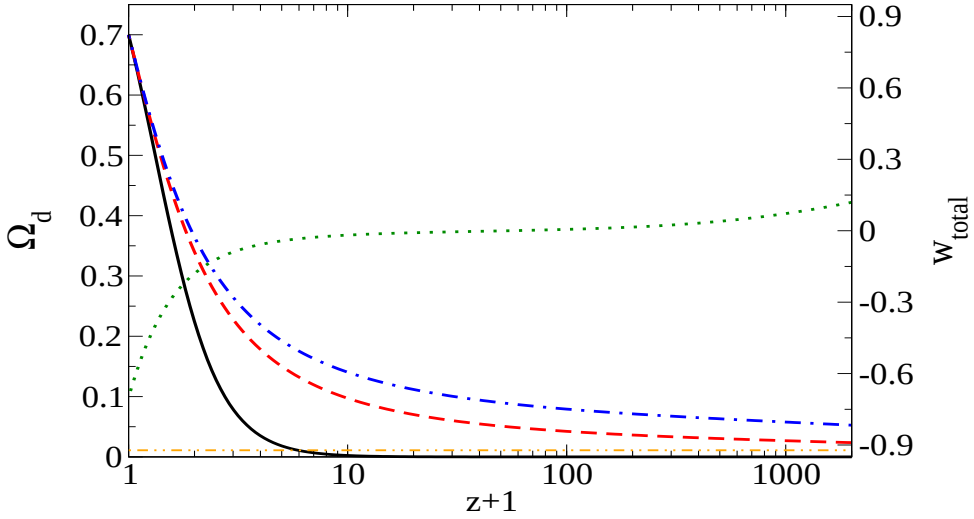

Figure 5.1: Evolution of a typical dark energy model considered in this section with $\Omega_d^0 = 0.7$, $w_0 = -0.999$, and $\Omega_d^e = 0.01$ depicted as dashed (red) line and with $\Omega_d^e = 0.03$ depicted as dashed-dotted (blue) line. These two models correspond to values of Ω_d^e that are allowed within 1σ and 2σ, respectively. For comparison, the solid (black) line shows the evolution for a cosmological constant with the same Ω_d^0. The straight dashed-double dotted (orange) line at $\Omega_d = 0.01$ indicates the asymptotic limiting value of Ω_d for our model with $\Omega_d^e = 0.01$. In contrast to the cosmological constant which has a negligible contribution at early times, our models have $\Omega_d \geq 0.01$ (0.03) always and contribute a considerable effective fraction $\bar{\Omega}_{\rm sf} \sim 0.06$ (0.1) during structure formation. The dotted (green) line indicates the total equation of state of the universe for our $\Omega_d^e = 0.01$ model. For $w_{total} < -1/3$, the universe is accelerating.

The advantage of a parameterization in terms of only three parameters is a minimal setting that accounts for information beyond a Taylor expansion around $z = 0$ (i.e. beyond the parameters Ω_d^0 and w_0). Nevertheless, it embodies the most crucial potential new feature of a dynamical dark energy, namely the possibility of early dark energy. For supernovae, it seems more suitable than a continuation of the Taylor expansion, which in the next step involves the derivative of the equation of state $w_d' = \partial w/\partial z \,_{|z=0}$. The present bounds on w_d' [43] allow a region of large $|w_d'|$, for which the validity of a Taylor expansion is doubtful even for $z = 1$.

5.2 SNe Ia constraints

Type Ia supernovae can be used as standard candles to measure the luminosity distance-redshift relation $d_L(z)$. One can use this relation to constrain the cosmological parameters by comparing the measured value of $d_L(z)$ with the theoretical prediction. The luminosity distance is defined to be the square root of the ratio between luminosity $\mathcal{L}$ and flux F

$$d_L = \sqrt{\frac{\mathcal{L}}{4\pi F}} = (1+z)\int_0^z \frac{dx}{H(x)}, \tag{5.9}$$

where the present value of the scale factor a_0 is normalized to unity. The Hubble parameter H can be computed using eq. (5.4) and the energy conservation equation. The result is

$$H^2(z) = (H^0)^2\left(\Omega_M(1+z)^3 + (1-\Omega_M)(1+z)^3\exp\left[\frac{3w_0\ln(1+z)}{1+b\ln(1+z)}\right]\right), \tag{5.10}$$

where H^0 and Ω_M are the present value of H and the density parameter of matter, respectively. For a flat universe, $\Omega_M + \Omega_d^0 = 1$. It is clear that $d_L(z)$ is a function of w_0, b, Ω_M, and H^0. To compare the theoretical prediction with observations, the extinction-corrected distance modulus μ_p is computed by using the formula

$$\mu_p(z) = m(z) - M = 25 + 5\log_{10}\left[d_L(z; w_0, b, \Omega_M, H^0)\right], \tag{5.11}$$

where $m(z)$ is the observed SNe magnitude and M is the SNe absolute magnitude. The present Hubble parameter H^0 is a statistical nuisance parameter which is marginalized over to estimate the cosmological parameters, so that $\mu_p(z)$ can be estimated without explicit knowledge of H^0 [103]. The cosmological parameters can be estimated by minimizing

$$\chi^2 = \frac{\sum_i(\mu_o(z_i) - \mu_p(z_i))^2}{\sigma_i^2}, \tag{5.12}$$

where σ_i is the total uncertainty in the SNe Ia observations and $\mu_o(z_i)$ is the observed extinction-corrected distance modulus. We assume that the probability distribution $e^{-\chi^2/2}$ is a Gaussian distribution. Thus, the Hubble parameter H^0 can be marginalized over by choosing its value such that it maximizes this distribution. In practice, we compute H^0 from the equation $\partial\chi^2/\partial H^0 = 0$ and substitute it into the equation for μ_p to obtain the marginalized probability distribution.

	w_0	b	Ω_M
no prior	$-1^{+0.11}$	$2.07^{+0.39}_{-0.96}$	$0^{+0.15}$
with prior	$-1^{+0.16}$	0.48 ± 0.48	0.25 ± 0.05

Table 5.1: SNe Ia constraints on the dark energy parameterization discussed in the previous section. We restrict ourselves to the case when $-1 \leq w_0 \leq +1$ and $b > 0$. We use the prior $\Omega_M = 0.27 \pm 0.06$ in the second row of table.

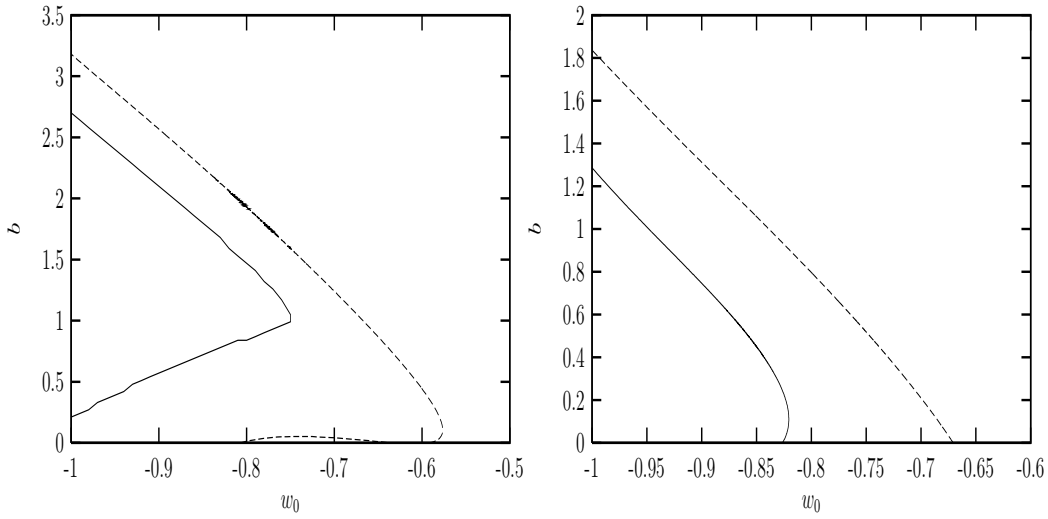

Figure 5.2: Constraints on w_0 and b from SNe Ia data. The left panel shows the case of no prior, while the right panel shows the case with the prior $\Omega_M = 0.27 \pm 0.06$. In both panels, the solid line denotes the 68% confidence contour and the long dashed line denotes the 95% confidence contour.

We use the SNe Ia gold sample compiled by Riess *et al* [43] to constrain our parameterization. The function χ^2 is evaluated on a grid in the multidimensional parameter space. The marginalized likelihood for parameter x_i is obtained by looping over a grid of x_i and choosing the remaining parameters so that they minimize χ^2 in each case. The best fit value and the confidence limit are compute from this marginalized likelihood. The best fit model is shown in table 5.1 and the confidence

contours in the $b - w_0$ plane are shown in figure 5.2. Since there is a degeneracy between b and Ω_M, we have to combine SNe Ia data with the other datasets, or put a prior on Ω_M. One can see from figure 5.2 that the constraint on parameter b is improved when we use the prior $\Omega_M = 0.27 \pm 0.06$. Obviously, the error on parameter b reduces when the error on Ω_M reduces and the upper bound on parameter b decreases when Ω_M increases.

5.3 CMB plus LSS constraints

There are at least two effects of dark energy on the features of temperature anisotropies in the CMB. First, the angular location of the acoustic peaks change when the form of $w_d(z)$ changes. This is because the angular diameter distance to the last scattering surface depends on the averaged amount of dark energy at last scattering. Second, the different evolution of dark energy leads to a different ISW contribution to the low multipoles of the CMB power spectrum.

The evolution of large scale structure (LSS) is influenced by the amount of dark energy after recombination. Since the dark energy fluctuations decay inside the horizon, they give no contribution to the evolution of LSS. In the case of dynamical dark energy the growth rate of the matter fluctuations is reduced compared with ΛCDM because the dark energy starts to dominate earlier in the ΛCDM model. As a result, the shape of the matter power spectrum and the value of σ_8 depend on the dark energy model. Hence, the CMB and LSS datasets can be used to constrain the dark energy model. Moreover, the SNe Ia data and the CMB plus LSS data give orthogonal information, so that the degeneracies between the parameters are reduced when these datasets are combined.

In this section, we fit the dark energy parameterization from section 5.1 to WMAP data [18], as well as the data from CBI [35], VSA [37], SDSS [40] and the Hubble parameter constraint of the Hubble Space Telescope [94] combined. We compute the theoretical angular power spectrum using CMBEASY [78], and compare with observational data using the Markov Chains Monte Carlo (MCMC) package provided by CMBEASY. The mean $\bar{x}_i$ of parameter x_i is computed using $\bar{x}_i = \frac{1}{N}\sum_t^N x_{it}$, where N is the number of points in the merged MCMC chain and x_{it} denotes the value of parameter x_i at the t-th step of the chain. The c% confidence interval of parameter x_i is the interval which encloses c% of the total area under the histogram of this parameter. Roughly speaking, this histogram is the marginalized likelihood for parameter x_i. The mean, 1σ confidence and the best fit value of the cosmological parameters are shown in table 5.2. In this table we use the prior $-1 \leq w_0 \leq 1$ and $b \geq 0$ for the parameters w_0 and b, respectively.

This table shows that the constraints on b and w_0 do not improve much when we combine WMAP data with the other datasets. For the CMB data, the upper

	WMAP		CMB+LSS		CMB+LSS+HST	
	mean$\pm\sigma$	best fit	mean$\pm\sigma$	best fit	mean$\pm\sigma$	best fit
$\Omega_M h^2$	$0.13^{+0.02}_{-0.02}$	0.15	$0.13^{+0.01}_{-0.01}$	0.13	$0.13^{+0.01}_{-0.01}$	0.14
w_0	< -0.82	-0.93	< -0.81	-0.99	< -0.81	-0.96
b	< 0.47	0.57	< 0.4	0.45	< 0.37	0.35
h	< 0.64	0.63	< 0.64	0.61	< 0.65	0.62
$\Omega_B h^2$	$0.026^{+0.002}_{-0.002}$	0.028	$0.024^{+0.002}_{-0.002}$	0.023	$0.024^{0.002}_{0.002}$	0.024
τ	$0.33^{+0.1}_{-0.1}$	0.36	$0.20^{+0.1}_{-0.1}$	0.15	$0.21^{+0.1}_{-0.1}$	0.14
n_s	$1.11^{+0.07}_{-0.07}$	1.15	$1.00^{+0.06}_{-0.06}$	0.98	$1.00^{+0.06}_{-0.06}$	0.98

Table 5.2: Observational constraints on the dark energy parameterization, where CMB + LSS is the combined WMAP+CBI+VSA+SDSS. The prior $h = 0.72 \pm 0.08$ from the Hubble Space Telescope (HST) is added in the third column of the table. For the parameters w_0, b, and h we show only the upper bound (1σ) because we do not have the full marginalized likelihood for these parameters (see figure 5.3 and 5.4).

bound for b is less than the the upper bound from SNe Ia data. Since a large b corresponds to a large value of $\bar{\Omega}_{\rm ls}$, a large value of b is forbidden by the CMB data. The upper bound for w_0 from the CMB data is greater than the upper bound from SNe Ia data because the SNe Ia data seem to prefer $w_0 < -1$. According to section 5.1, one can parameterize the evolution of dark energy in terms of the parameters $w_0, \Omega_d^e, \Omega_d^0$ instead of the parameters w_0, b, Ω_d^0. Thus, we run a MCMC for both parameter sets. The marginalized likelihoods for w_0, b, and Ω_d^e are shown in figures 5.3-5.5 respectively. In these figures, the likelihood functions are computed from the MCMC chains for both CMB+LSS+HST data and SNe Ia data. Comparing the upper bound on b from the SNe Ia data in figure 5.4 with the upper bound in table 5.1, one sees that the upper bound on b from the grid approach is larger than the one that obtained from the MCMC approach. The values of $\Omega_M h^2, \Omega_B h^2$ and n_s are close to the values for the ΛCDM model but the value of τ is slightly larger than the ΛCDM model. The value of h is quite low compared with the value for the ΛCDM model. The value of this parameter does not change much when the prior $h = 0.72 \pm 0.08$ is used. Models of early dark energy typically lead to slightly lower values of h than ΛCDM. The reason is the CMB: dark energy influences the CMB mostly due to projection effects and additional ISW contributions. To match observations, any model must at least provide an acoustic scale l_A that comes close to the one measured by WMAP. With Ω_d^0 fixed, the analytic expression for l_A of [99] yields

$$l_A \propto \int_0^1 da \left(a + \frac{\Omega_d^0}{1-\Omega_d^0} a^{(1-3\bar{w})} + \frac{\Omega_R^0 (1-a)}{1-\Omega_d^0} \right)^{-1/2}, \tag{5.13}$$

where Ω_R is the present energy fraction of radiation and $\bar{w}$ is the weighted average

$$\bar{w} = \int_0^{\eta_0} \Omega_d(\eta) w(\eta) d\eta \times \left(\int_0^{\eta_0} \Omega_d(\eta) d\eta \right)^{-1}. \tag{5.14}$$

The integral (5.13) increases when $\bar{w} \to -1$, i.e. for all other parameters fixed, the acoustic scale l_A becomes larger with more negative $\bar{w}$. Conversely, as our models have $\bar{w} > -1$ by construction, we see that for all other parameters fixed, our models have a smaller acoustic scale compared to ΛCDM. To counterbalance this, a somewhat smaller Hubble parameter h is preferred, because l_A depends on h to a good approximation as [99]

$$l_A \propto 1 + h^{-1} \sqrt{\frac{\Omega^0_{rel.} h^2}{a_{ls}(1 - \Omega^0_d)}} \approx 1 + 0.4 h^{-1}, \tag{5.15}$$

where we have used the estimates $\Omega^0_d \approx 0.7$, $a_{ls} \approx 1100^{-1}$, and $\Omega^0_{rel.} h^2 \approx 4.4 \times 10^{-5}$. Likewise, a sizeable early dark energy $\bar{\Omega}_{\rm ls}$ can increase the acoustic scale according to $l_A \propto 1/\sqrt{1 - \bar{\Omega}_{\rm ls}}$ [99]. Both $\bar{\Omega}_{\rm ls}$ and the somewhat smaller Hubble parameter counterbalance the effect of $\bar{w}$ in our models.

Just as $\bar{\Omega}_{\rm ls}$ determines the main effect of early dark energy on the CMB, the suitable average

$$\bar{\Omega}_{\rm sf} = [\ln a_{tr.} - \ln a_{eq.}]^{-1} \int_{\ln a_{eq.}}^{\ln a_{tr.}} \Omega_d(a) d \ln a, \tag{5.16}$$

with $a_{tr.} = 1/3$ encapsulates the main effects of early dark energy on structure formation [100]. By definition, one has $\bar{\Omega}_{\rm sf}(\Lambda) \sim 0.5\%$ (i.e. non-vanishing) for a cosmological constant model and our choice of $a_{tr.}$. A sizeable $\bar{\Omega}_{\rm sf}$ leads to a decrease in linear structure compared to ΛCDM according to [100] (see also figure 5.6)

$$\frac{\sigma_8(D.E.)}{\sigma_8(\Lambda)} \propto a_{eq.}^{3\bar{\Omega}_{\rm sf}/5}. \tag{5.17}$$

Using $z_{eq.} = 3500$, we obtain for $3\bar{\Omega}_{\rm sf} \ln z_{eq.}/5 \ll 1$, the quick estimate

$$\frac{\sigma_8(D.E.)}{\sigma_8(\Lambda)} \propto (1 - 6\,[\bar{\Omega}_{\rm sf} - \bar{\Omega}_{\rm sf}(\Lambda)]). \tag{5.18}$$

As we leave a free bias for our SDSS analysis, and have no prior on σ_8, one may worry about unphysically low values of σ_8 for our models. It does turn out, however, that this is not necessarily the case. As seen in figure 5.7, our predictions for σ_8 are compatible with observations, given the lower values of σ_8 needed to explain non-linear structure in early dark energy scenarios compared to ΛCDM [104].

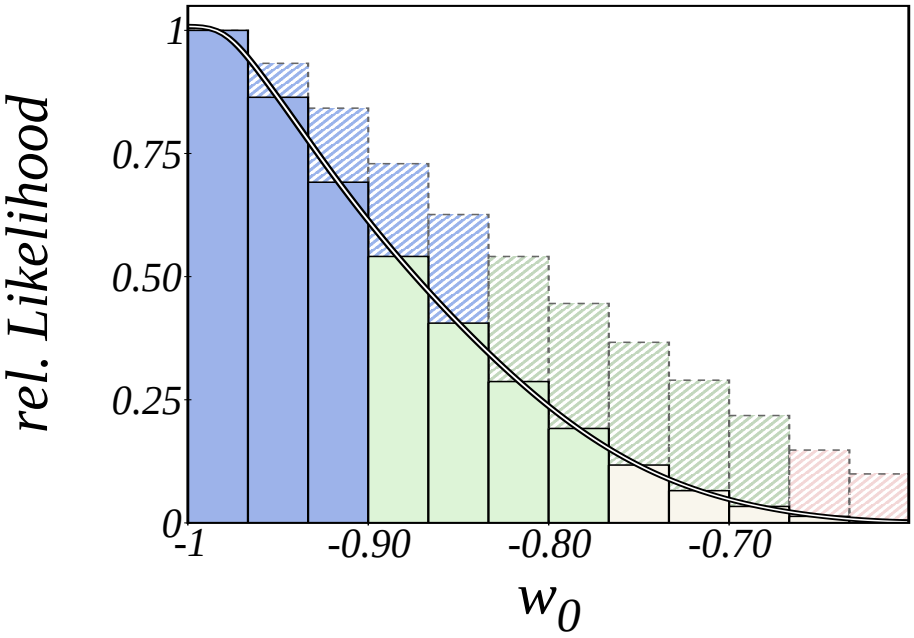

Figure 5.3: Constraints on the equation of state today. The dark (blue), medium (green) and light (red) shaded regions correspond to $1, 2$ and 3σ confidence. The constraint from SNe Ia is displayed in the foreground (solid), while the less tight constraint from WMAP+CBI+VSA+SDSS+HST is depicted in the background.

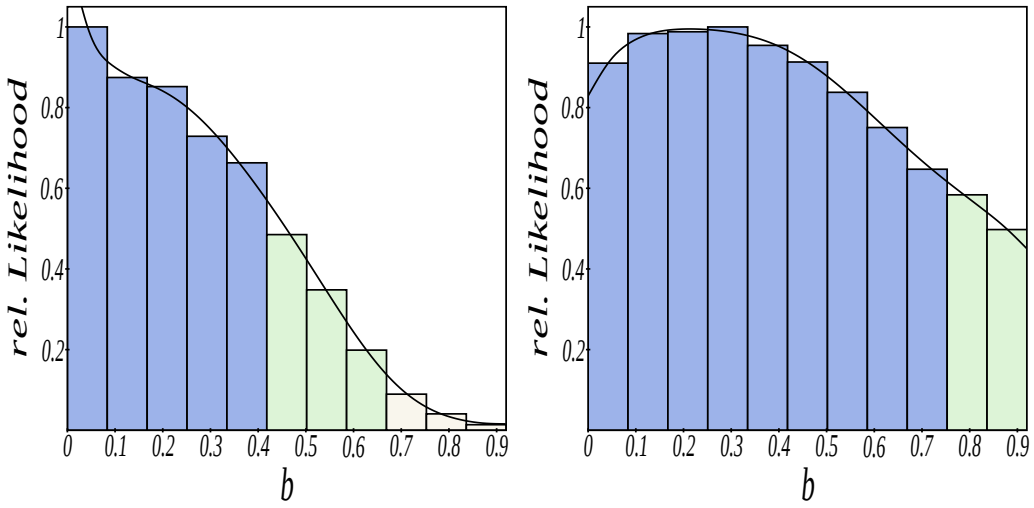

Figure 5.4: Constraints on the parameter b from WMAP+CBI+VSA+SDSS+HST data (left panel) and SNe Ia (right panel).The dark (blue), medium (green) and light (red) shaded regions correspond to $1, 2$ and 3σ confidence.

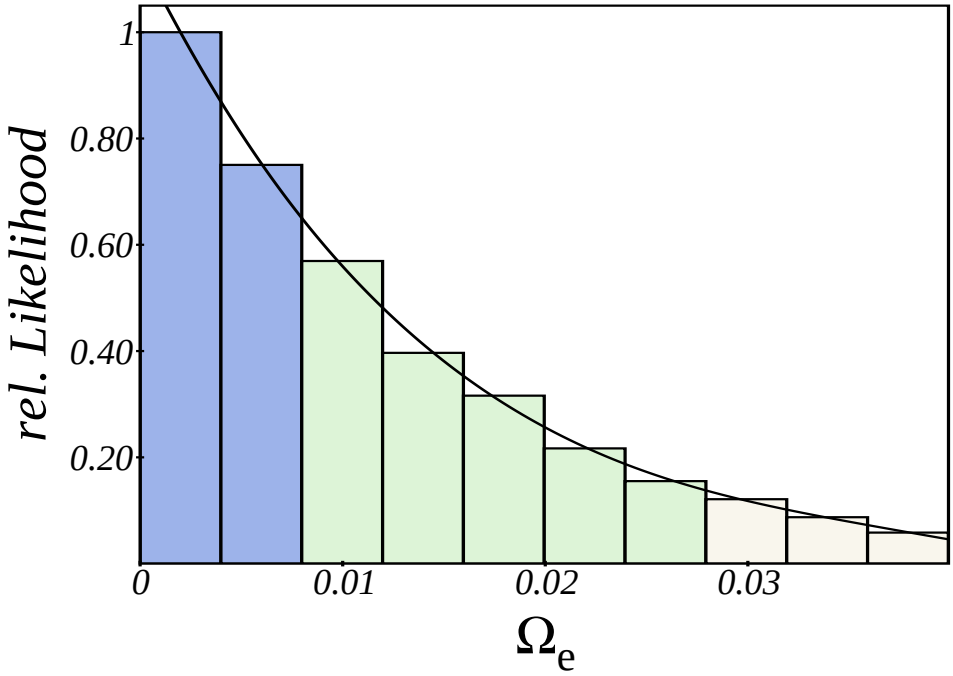

Figure 5.5: Likelihood distribution of the early dark energy parameter Ω_d^e inferred from WMAP+CBI+VSA+SDSS+HST data. The dark (blue), medium (green) and light (red) shaded regions correspond to $1, 2$ and 3σ confidence.

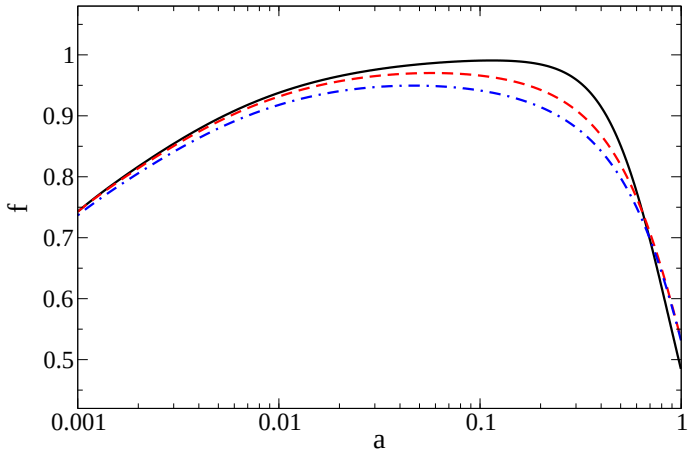

Figure 5.6: Growth exponent $f = \frac{\partial \ln(\delta_M)}{\partial \ln a}$ as a function of a. The black solid line represents a ΛCDM model. The red dashed line represents a dark energy model with $\Omega_d^e = 2 \times 10^{-4}$ (leading to $\bar{\Omega}_{\rm sf} = 0.01$) and the blue dashed-dotted line represents a model with $\Omega_d^e = 5 \times 10^{-3}$ (leading to $\bar{\Omega}_{\rm sf} = 0.05$). The mode depicted is at scale $k = 3.7 {\rm Mpc}^{-1}$ which is well inside the horizon at $a = 10^{-3}$.

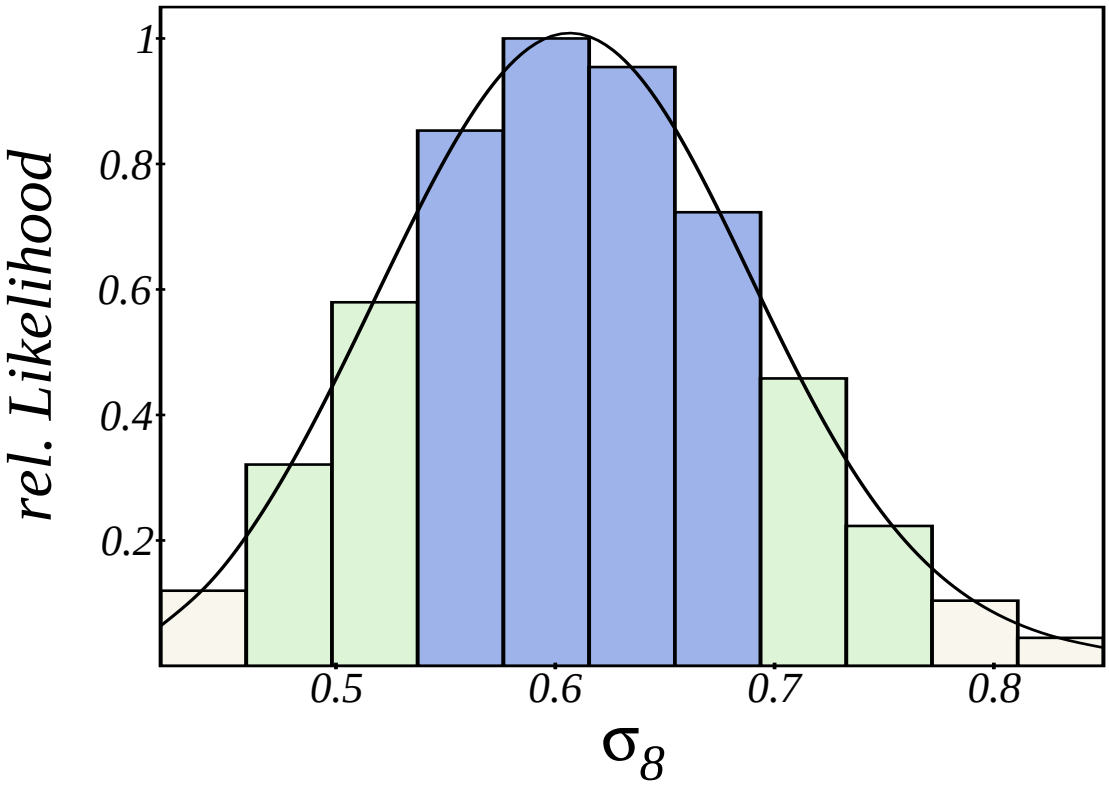

Figure 5.7: The linear rms power of matter fluctuations on $8h^{-1}$Mpc scales, σ_8. As σ_8 is not a monte carlo parameter, we caution the reader that the underlying prior is not flat. With $\sigma_8 = 0.61 \pm 0.08$ the power is rather low compared to a standard Λ CDM model – a direct result of the suppression of growth due to the presence of dark energy during structure formation.

Chapter 6

Conclusions

Observations suggest that the universe is accelerated expanding today. Thus, the dominant component of the universe at the present epoch should have a negative pressure. This component might be the cosmological constant which is a smoothly distributed, time-independent component, or might be dark energy which is a inhomogeneous, time-dependent component. Observations also indicate that the universe is not perfectly homogeneous and isotropic. On small scales, matter is not uniformly distributed. There are galaxies, clusters of galaxies, etc. The small anisotropies in the universe are reflected in the anisotropies of the observed CMB power spectrum. The inhomogeneities of matter in the universe lead to the inhomogeneities in the spacetime, i.e., metric, of the universe.

Dark energy affects those inhomogeneities in two ways. First, dark energy governs the evolution of the universe at the present epoch, i.e., the expansion rate of the universe depends on the evolution of dark energy. Hence, the evolution of the metric and matter fluctuations at the present epoch depend on the evolution of dark energy. The metric perturbations are constant during matter domination, but decrease due to the acceleration of the universe during the present epoch. The decay rate of the metric perturbations increases when the acceleration rate of the universe increases. After matter domination, the growth rate of the matter fluctuations on small scales depends on the amount of dark energy. Second, the fluctuations in dark energy can give significant contributions to the metric perturbations on large scales. On small scales, the fluctuations in dark energy rapidly damp during radiation domination, and do not grow during matter domination. Since the fluctuations in dark matter grow during matter domination, the effects of dark energy fluctuations can be neglected. The dark energy fluctuations cannot grow inside the horizon because of its intrinsic entropy perturbations.

On large scales, quintessence fluctuations can give contributions to the CMB power spectrum via SW and ISW effects if their amplitudes are large enough during the present epoch. Since the quintessence field is an elementary field, it should have

already existed during inflation. Thus, the amplitude of field fluctuation δQ is limited by the observations via the upper bound on the Hubble parameter. However, the magnitude of density contrast of quintessence can be large if the ratio $\delta Q'/Q'$ or $\frac{dV/dQ}{V}$ is large. For the tracking quintessence, the quintessence field may be in the kinetic, tracking or potential regime after inflation. If the quintessence field is in the tracking regime after inflation, its density contrast will decrease and become negligible. Hence, the quintessence fluctuations have no effect on CMB spectrum in this case. The quintessence fluctuations are constant when the quintessence field is in a potential regime after inflation. As discussed in section 3.1, there may be a kinetic regime between inflation and potential regime. However, the kinetic regime is short, and therefore the growth of quintessence fluctuations during this regime can be ignored. The quintessence fluctuations are constant, as long as the quintessence field is in the potential regime, i.e. the field is nearly frozen. Thus, the quintessence fluctuations can affect the CMB spectrum if their magnitude after inflation are large and the quintessence field is frozen until the present epoch. According to section 3.4, the exponential quintessence with non-canonical kinetic term can have a large density contrast after inflation and can be frozen until the present epoch. Assuming that the quintessence fluctuations have a correlation with the curvature perturbation, this quintessence model can lead to the suppression of the CMB spectrum at low multipoles. However, if the density contrast after inflation is too large or the quintessence field leaves the potential regime too late, the ISW effect can dominate SW effect and therefore the CMB spectrum at low multipoles is enhanced.

We then consider whether the quintessence field can be frozen until the present epoch. As shown in section 3.1, the quintessence field will be frozen if the initial value of its energy density is smaller than the tracking value. For simplicity, we assume that the end of inflation is the beginning of the radiation dominated epoch. Thus, one might compute the initial value of the quintessence field at the beginning of the radiation dominated epoch by studying its evolution during inflation. We suppose that the kinetic coefficient of the quintessence field is constant during inflation, and hence the quintessence field behaves like a simple exponential quintessence. In the case when $\frac{dV/dQ}{V} > \bar{M_p}^{-1}$, the energy density of inflaton dominates the energy density of quintessence, as long as the quintessence field is rolls slowly. If the slow-roll condition $\left|\frac{d^2V/dQ^2}{3H^2}\right| \ll 1$ for the quintessence field is violated, the quintessence field will be rapidly driven towards a large value, where the slow roll condition is satisfied. Thus, the evolution of the universe is governed by the inflaton only. As discussed in section 4.2, the value of quintessence field at the end of inflation is strongly dependent on its value at the beginning of inflation and the duration of inflation. The quintessence field can be frozen until the present epoch if its value at the beginning of inflation is large or the duration of inflation is long enough. Thus, one cannot claim that the quintessence field can naturally be frozen until the

present epoch. However, the classical evolution of the quintessence field is influenced by its quantum fluctuations which can be viewed as a classical random noise. The evolution of the classical quintessence field under the random force is described by the Langevin equation. As discussed in section 4.3, the random noise leads to the random evolution of the classical quintessence field around the classical trajectory. This implies that the mean value of the quintessence field may be determined by the classical evolution. Nevertheless, the classical drift dV/dQ dominates the random force when the quintessence field is randomly driven towards a small value by the random force. As a result, the quintessence field is rapidly driven towards a large value by classical drift. Thus, the mean value of the quintessence field is larger than the value determined by the classical evolution, and its value at the end of inflation is large enough to freeze the quintessence field until the present epoch. The mean value of the quintessence field at the end of inflation is weakly dependent on its value at the beginning of inflation, because its evolution is dominated by the random evolution due to its quantum fluctuations.

Finally, we consider the observational constraints on the evolution of dark energy. To describe the evolution of dark energy in a model independent manner, many parameterizations have been proposed. We concentrate on the parameterization proposed by Wetterich. Fitting the parameterization to the SNE Ia data, we get $w_0 < -0.90$ and $b < 0.75$ at 68% confidence level. Here, we use the prior $\Omega_m = 0.27 \pm 0.06$, $w_0 > -1$ and $b \geq 0$. The upper bound on both parameters from the CMB+LSS+HST datasets are $w < -0.81$ and $b < 0.37$ at 68% confidence level. The upper bound on w from CMB+Lss+HST datasets is larger than the upper bound from SNe Ia data because the SNe Ia data favours the dark energy to have $w_0 < -1$. Since large value of b corresponds to the large amount of dark energy in the early epoch, the large value of b is not allowed by CMB data. Thus the upper bound on b from CMB+LSS+HST datasets is smaller than the upper bound from SNe Ia data. Usually, the upper bound on h and σ_8 of the dark energy model is smaller than the ΛCDM model. For our parameterization, the upper bound on both parameters are $h < 0.65$ and $\sigma_8 < 0.7$.

Bibliography

[1] A. G. Riess *et al.*, Astron. J. **116**, 1009 (1998), [astro-ph/9805201].

[2] S. Weinberg, Rev. Mod. Phys. **61**, 1 (1989).

[3] V. Sahni and A. Starobinsky, Int. J. Mod. Phys. D**9**, 373 (2000), [astro-ph/9904398].

[4] C. Wetterich, Nucl. Phys. B**302**, 668 (1988).

[5] B. Ratra and P. J. Peebles, Phys. Rev. D**37**, 3406 (1988).

[6] J. Frieman, C. Hill, A. Stebbins, and I. Waga, Phys. Rev. Lett. **75**, 2077 (1995), [astro-ph/9505060].

[7] R. R. Caldwell, R. Dave and P. J. Steinhardt, Phys. Rev. Lett. **80**, 1582 (1998), [astro-ph/9708069].

[8] P. G. Ferreira and M. Joyce, Phys. Rev. Lett. **79**, 4740 (1997), [astro-ph/9707286].

[9] E. J. Copeland, A. R. Liddle, and D. Wands, Phys. Rev. D**57**, 4686 (1998), [gr-qc/9711068].

[10] P. Brax and J. Martin, Phys. Lett. B**468**, 40 (1999), [astro-ph/9905040].

[11] A. Albrecht and C. Skordis, Phys. Rev. Lett. **84**, 2076 (2000), [astro-ph/9908085].

[12] R. R. Caldwell, Phys. Lett. B**545**, 23 (2002), [astro-ph/9908168].

[13] I. Maor, R. Brustein, and P. J. Steinhardt, Phys. Rev. Lett. **86**, 6 (2001), [astro-ph/0007297].

[14] Y. Wang and M. Tegmark, Phys. Rev. Lett. **92**, 241302 (2004), [astro-ph/0403292].

[15] D. A. Dicus and W. W. Repko, Phys. Rev. D**70**, 083527 (2004), [astro-ph/0407094].

[16] J. P. Ostriker and P. J. Steinhardt, Nature **377**, 600 (1995), [astro-ph/9505066].

[17] J. A. Peacock, *Cosmological Physics* (Cambridge University Press, Cambridge, 1999).

[18] D. N. Spergel *et al.*, Astrophys. J. Suppl. **148**, 175 (2003), [astro-ph/0302209].

[19] S. M. Carroll, *Lecture Notes on General Relativity* (1995), [gr-qc/9712019].

[20] B. F. Schutz, *A First Course in General Relativity* (Cambridge University Press, Cambridge, 1985).

[21] A. D. Linde, *Particle Physics and Inflationary Cosmology* (Harwood Academic, Switzerland, 1990).

[22] A. R. Liddle and D. H. Lyth, *Cosmological Inflation and Large Scale Structure* (Cambridge University Press, Cambridge, 2000).

[23] L. Kofman, A. D. Linde, and A. A. Starobinsky, Phys. Rev. D**56**, 3258 (1997), [hep-ph/9704452].

[24] L. Kofman, (1996), [astro-ph/9605155].

[25] E. W. Kolb and M. S. Turner, *The Early Universe* (Addison-Wesley, 1990).

[26] W. Hu and M. White, Astrophys. J. **471**, 30 (1996), [astro-ph/9602019].

[27] Z. Haiman and L. Knox, Invited Review in "Microwave Foregounds", ASP, San Francisco, 1999, [astro-ph/9902311].

[28] D. H. Lyth and A. Riotto, Phys. Rept. **314**, 1 (1999), [hep-ph/9807278].

[29] D. H. Lyth and D. Wands, Phys. Lett. B**524**, 5 (2002), [hep-ph/0110002].

[30] T. Moroi and T. Takahashi, Phys. Rev. D**66**, 063501 (2002), [hep-ph/0206026].

[31] D. Polarski and A. A. Starobinsky, Quant. Grav. **13**, 377 (1996), [gr-qc/9504030].

[32] G. F. Smoot *et al.*, Astrophys. J. Lett. **396**, L1 (1992).

[33] W. Hu, M. Fukugita, M. Zaldarriaga, and M. Tegmark, Astrophys. J. **549**, 669 (2001), [astro-ph/0006436].

[34] P. de Bernardis *et al.*, Nature **404**, 955 (2000), [astro-ph/0004404].

[35] A. C. S. Readhead *et al.*, Astrophys. J. **609**, 498 (2004), [astro-ph/0402359].

[36] C. L. Kuo *et al.*, Astrophys. J. **600**, 32 (2004), [astro-ph/0212289].

[37] R. Rebolo *et al.*, (2004), [astro-ph/0402466].

[38] A. R. Liddle and D. H. Lyth, Phys. Rept. **231**, 1 (1993), [astro-ph/9303019].

[39] M. Colless *et al.*, (2003), [astro-ph/0306581].

[40] M. Tegmark *et al.*, Phys. Rev. D**69**, 103501 (2004), [astro-ph/0310723].

[41] N. Kaiser and G. Squires, Astrophys. J. **404**, 441 (1993).

[42] R. A. C. Croft *et al.*, Astrophys. J. **581**, 20 (2002), [astro-ph/0012324].

[43] A. G. Riess *et al.*, Astrophys. J. **607**, 665 (2004), [astro-ph/0402512].

[44] J. M. Bardeen, Phys. Rev. D**22**, 1882 (1980).

[45] R. Durrer, Course at the Second Aegean Summerschool on the Early Universe, [astro-ph/0402129].

[46] K. A. Malik, Ph.D thesis, [astro-ph/0101563].

[47] R. H. Brandenberger, Lect. Notes Phys. **646**, 127 (2004), [hep-th/0306071].

[48] R. Durrer, Fund. Cosmic Phys. **15**, 209 (1994), [astro-ph/9311041].

[49] D. H. Lyth, Phys. Rev. D**31**, 1792 (1985).

[50] J. E. Lidsey, A. R. Liddle, E. W. Kolb, E. J. Copeland, T. Barreiro, and M. Abney, Rev. Mod. Phys. **69**, 373 (1997), [astro-ph/9508078].

[51] D. H. Lyth and D. Wands, Phys. Rev. D**68**, 103515 (2003), [astro-ph/0306498].

[52] J. M. Bardeen, P. J. Steinhardt, and M. S. Turner, Phys. Rev. D**28**, 679 (1983).

[53] V. F. Mukhanov, H. A. Feldman, and R. H. Brandenberger, Phys. Rep. **215**, 203 (1992).

[54] H. Kodama and M. Sasaki, Prog. Theor. Phys. Suppl. **78**, 1 (1984).

[55] D. Langlois, Phys. Rev. D**59**, 123512 (1999), [astro-ph/9906080].

[56] D. Langlois and A. Riazuelo, Phys. Rev. D**62**, 043504 (2000), [astro-ph/9912497].

[57] L. Amendola, C. Gordon, D. Wands, and M. Sasaki, Phys. Rev. Lett. **88**, 211302 (2002), [astro-ph/0107089].

[58] U. Seljak and M. Zaldarriaga, Astrophys. J. **469**, 437 (1996), [astro-ph/9603033].

[59] Chung-Pei Ma and E. Bertschinger, Astrophys. J. **455**, 7 (1995), [astro-ph/9506072].

[60] R. Durrer, J. Phys. Stud. **5**, 177 (2001), [astro-ph/0109522].

[61] W. Hu, Astrophys. J. **506**, 485 (1998), [astro-ph/9801234].

[62] C. Gordon and W. Hu, Phys. Rev. D**70**, 083003 (2004), [astro-ph/0406496].

[63] M. Malquarti and A. R. Liddle, Phys. Rev. D**66**, 123506 (2002), [astro-ph/0208562].

[64] L. R. Abramo and F. Finelli, Phys. Rev. D**64**, 083513 (2001), [astro-ph/0101014].

[65] P. J. Steinhardt, L. Wang, and I. Zlatev, Phys. Rev. D**59**, 123504 (1999), [astro-ph/9812313].

[66] P. Brax, J. Martin, and A. Riazuelo, Phys. Rev. D**62**, 103505 (2000), [astro-ph/0005428].

[67] M. Doran, C. M. Müller, G. Schäfer, and C. Wetterich, Phys. Rev. D**68**, 063505 (2003), [astro-ph/0304212].

[68] M. Kawasaki, T. Moroi, and T. Takahashi, Phys. Lett. B**533**, 294 (2002), [astro-ph/0108081].

[69] I. S. Gradshteyn and I. M. Ryzhik, *Table of Integrals, Series, and Products* (Academic Press, 2000).

[70] W. Hu and N. Sugiyama, Phys. Rev. D**51**, 2599 (1995), [astro-ph/9411008].

[71] J. Weller and A. M. Lewis, Mon. Not. Roy. Astron. Soc. **346**, 987 (2003), [astro-ph/0307104].

[72] M. Kawasaki, T. Moroi, and T. Takahashi, Phys. Rev. D**64**, 083009 (2001), [astro-ph/0105161].

[73] T. Moroi and T. Takahashi, Phys. Rev. Lett. **92**, 091301 (2004), [astro-ph/0308208].

[74] H. V. Peiris *et al.*, Astrophys. J. Suppl. **148**, 213 (2003), [astro-ph/0302225].

[75] M. Malquarti and A. R. Liddle, Phys. Rev. D**66**, 023524 (2002), [astro-ph/0203232].

[76] C. Gordon and D. Wands, Phys. Rev. D**71**, 123505 (2005), [astro-ph/0504132].

[77] A. Hebecker and C. Wetterich, Phys. Lett. B**497**, 281 (2001), [hep-ph/0008205].

[78] M. Doran, JCAP **011**, 0510 (2005), [astro-ph/0302138].

[79] J. Martin and M. Musso, Phys. Rev. D**71**, 063514 (2005), [astro-ph/0410190].

[80] A. D. Linde, Phys. Lett. B**175**, 395 (1986).

[81] Y. Nambu and M. Sasaki, Phys. Lett. B**219**, 240 (1989).

[82] Y. Nambu, Prog. Theor. Phys. **81**, 1037 (1989).

[83] M. Sasaki, Y. Nambu, and K. Nakao, Nucl. Phys. B**308**, 868 (1988).

[84] H. E. Kandrup, Phys. Rev. D**39**, 2245 (1989).

[85] H. Casini, R. Montemayor, and P. Sisterna, Phys. Rev. D**59**, 063512 (1999), [gr-qc/9811083].

[86] S. Matarrese, M. A. Musso, and A. Riotto, JCAP **05**, 005 (2004).

[87] M. Liguori, S. Matarrese, M. Musso, and A. Riotto, JCAP **011**, 0408 (2004), [astro-ph/0405544].

[88] S. Winitzki and A. Vilenkin, Phys. Rev. D**61**, 084008 (2000), [gr-qc/9911029].

[89] A. Riotto, Lectures delivered at the "ICTP Summer School on Astroparticle Physics and Cosmology", Trieste, 17 June - 5 July 2002, [hep-ph/0210162].

[90] A. D. Linde, D. A. Linde, and A. Mezhlumian, Phys. Rev. D**49**, 1783 (1994), [gr-qc/9306035].

[91] A. D. Linde and A. Mezhlumian, Phys. Lett. B**307**, 25 (1993), [gr-qc/9304015].

[92] J. H. Goldstein *et al.*, Astrophys. J. **599**, 773 (2003), [astro-ph/0212517].

[93] E. Hawkins *et al.*, Mon. Not. Roy. Astron. Soc. **346**, 78 (2003), [astro-ph/0212375].

[94] W. L. Freedman *et al.*, Astrophys. J. **553**, 47 (2001), [astro-ph/0012376].

[95] P. S. Corasaniti and E. J. Copeland, Phys. Rev. D**67**, 063521 (2003), [astro-ph/0205544].

[96] E. V. Linder, Phys. Rev. Lett. **90**, 091301 (2003), [astro-ph/0208512].

[97] A. Upadhye, M. Ishak, and P. J. Steinhardt, (2004), [astro-ph/0411803].

[98] Y. Wang and M. Tegmark, Phys. Rev. Lett. **92**, 241302 (2004), [astro-ph/0403292].

[99] M. Doran, M. J. Lilley, J. Schwindt, and C. Wetterich, Astrophys. J. **559**, 501 (2001), [astro-ph/0012139].

[100] M. Doran, J. Schwindt, and C. Wetterich, Phys. Rev. D**64**, 123520 (2001), [astro-ph/0107525].

[101] R. R. Caldwell, M. Doran, C. M. Müller, G. Schäfer, and C. Wetterich, Astrophys. J. **591**, L75 (2003), [astro-ph/0302505].

[102] C. Wetterich, Phys. Lett. B**594**, 17 (2004), [astro-ph/0403289].

[103] S. Perlmutter et al., Astrophys. J. **517**, 565 (1999).

[104] M. Bartelmann, M. Doran, and C. Wetterich, (2005), [astro-ph/0507257].

Acknowledgments

I am grateful to my advisor Christof Wetterich, who gave me the very good chance for coming to Heidelberg. He gave me the good advice and gave me the freedom to follow my own interests. He also gave me the help and support, e.g. many letters of recommendation.

I would like to thank Prof. Michael G. Schmidt for his letters for my scholarship extension, Prof. Werner Wetzel for allowing me to connect my private computer to the network of the institute, Prof. Eberhard Freitag for the electronic version of his book, Prof. Matthias Bartelmann for being my thesis referee, and Prof. Hans-Christian Schultz-Coulon for being my thesis committee.

I would like to thank many nice people surrounding me. I often asked for help from Dr. Eduard thommes. Dr. Michael Doran, Dr. Christian M. Müller and Dr. Gregor Schäfer gave me the useful ideas about cosmology. They also help me when I have a problem. Sebastian Diehl helped me to contact Dean office for the thesis examination. Dr. Michael Doran, Mona Frommert, Georg Robbers, Sebastian Diehl, and Hans-Christian Krahl helped me to check some typographical errors and correct english in this thesis. I really would like to thank all people in my work place for their help and their friendship. I would also like to thank some students at student dormitory and thai students in Heidleberg for their help and friendship.

Of course I cannot come to Germany without any financial support. I would like to thank DAAD for the four years scholarship and also thank my DAAD refferee Mrs. Elke Burbach.

Finally, I would like to thank my family and Dr. Ahpisit Ungkitchanukit for their help and support.